Models and inference for population dynamics

Ana Paula Palacios

June 28, 2012

A mis padres

"Essentially, all models are wrong, but some are useful."

George E. P. Box

Agradecimientos

En primer lugar quisiera agradecer a mis directores por su incondicional apoyo y por todo lo que me han enseñado. Mike, gracias por tu increíble lucidez y conocimiento, especialmente en las tardes que compartimos en la *biblioteca*. Juanmi, gracias por ayudarme en mi lucha personal contra los códigos, por tu aporte biológico y *revolucionario*, y fundamentalmente por tu paciencia y por tu comprensión.

En segundo lugar, pero con la misma importancia, quisiera agradecer a mi familia, a mis padres y a mi hermana. Quiero darles las gracias, profundamente, por dejarme vivir mi propio camino, por apoyarme en ésta y en cada cosa que me propongo. Por sufrir (tanto como yo) la distancia, pero a pesar de eso brindarme todo su amor de manera incondicional.

También quisiera agradecer a Peter, quien fue muy importante en una etapa durante este período de tesis. Gracias por ser fundamentalmente mi apoyo emocional en estas tierras lejanas, gracias por nuestras charlas académicas a cualquier hora del día, por tus comentarios y por tu infinita paciencia cuando me explicabas algo.

No quiero olvidarme de nadie, y haré mi mejor intento. Dolo, Lu, Santi y Ale, gracias a ustedes estoy hoy aquí. Ana, Caro y Jona, ustedes fueron como mis hermanos en Madrid, gracias por su amor fraternal. A la banda, Juancho, Diego, Gabi, Huro, gracias por hacerme sentir mas cerca de Córdoba. Eli, Ramón y especialmente Irene, gracias por acompañarme en mi *estancia* en Colmenarejo. Carles, Bernardo y Fabrizio, gracias por su buena predisposición a responder mis preguntas y por sus valiosos comentarios. Emiliano, gracias a tu generosidad pudimos enriquecer esta tesis con las aplicaciones a datos reales de bacterias. Gracias a todos mis compañeros y amigos, que de una manera u otra me han ayudado a cumplir mi objetivo: Audra, Adolfo, Leo, Carlo, Gabriel, Pato, Sofi, y Andrea. A mis amigos de Córdoba, Iván, Malu, Sole, Lu, Caro y Guada, gracias por su amistad a pesar de la distancia. Y como olvidarme de Mari y Visi, de sus mimos y de esas ricas meriendas...

Gracias a todos ustedes, esto fue posible.

Contents

List of Figures

List of Tables

Resumen

En el presente trabajo abordamos el problema de la modelización e inferencia de la dinámica de las poblaciones de bacterias. Dado que las mediciones del crecimiento de bacterias en platillos de Petri, pueden fácilmente replicarse bajo las mismas condiciones experimentales, el estudio se centra en los casos donde los datos presentan una estructura jerárquica.

El crecimiento de bacterias está muy influido por las condiciones ambientales, por ejemplo niveles de sal, temperatura o acidez y la relación de estos factores con el crecimiento es muy compleja. Por ello, en experimentos bajo distintas condiciones, es fundamental buscar modelos flexibles para relacionar el crecimiento con tales condiciones.

En esta tesis, presentamos como objetivo desarrollar modelos predictivos capaces de combinar toda la información disponible, como por ejemplo la repetición de los experimentos, con el fin de lograr predicciones mas precisas. Por otra parte, se propone también desarrollar un modelo mas general para el crecimiento aplicable a una gran variedad de microorganismos y bajo un gran número de combinaciones de las condiciones ambientales y ecológicas.

Con estos objetivos en mente, proponemos el uso de modelos jerárquicos cuando se observan multiples curvas de crecimiento. De esta manera, la estimación de una única curva es mejorada a través de la información que brindan el resto de las curvas de crecimiento observadas. Adicionalmente, proponemos también el uso de técnicas no paramétricas para modelizar los procesos de crecimiento, sin necesidad de asumir que las poblaciones se comportan según cierta función paramétrica. En particular, utilizamos redes neuronales ya que tienen una gran capacidad de describir el comportamiento de modelos complejos y no lineales.

Los procesos de crecimiento pueden presentar ciertas fluctuaciones estocasticás que no se deben a errores de medición. Los modelos que simplemente adicionan un error a una función determinística no son capaces de capturar la variabilidad total de estos procesos. En consecuencia, hemos desarrollado un modelo estocástico que presenta dos características deseables: las trayectorias de crecimiento son no-decrecientes y la función de medias del proceso es proporcional a la función de Gompertz de crecimiento.

Finalmente, en este trabajo también se aborda el problema de la estimación de los modelos, para lo cual hemos preferido utilizar inferencia bayesiana ya que, entre otra cosas, brinda un enfoque unificado al tratar con diversos tipos de modelos, como por ejemplo, jerárquicos y redes neuronales. Por otra parte, la inferencia Bayesiana nos permite diferenciar entre distintas fuentes de incertidumbre a través del uso de distribuciones a priori jerárquicas, . Asi mismo, permite la incorporación de información previa, ampliamante disponible en ciencias como la microbiología.

Introduction and Summary

In this dissertation we study the problem of modeling and inference for the dynamics of bacterial populations. Bacterial growth data taken from Petri-dish experiments is easily replicated. Moreover, external factors such as temperature, salinity or acidity of the environment are known to influence bacterial growth and therefore, experiments are often undertaken under a variety of conditions. This implies that often, bacterial growth data present a multilevel structure.

The first issue that we wish to to address in this thesis is how to analyze data from multiple experiments in this context. The aim of our study is to develop a predictive model able to combine all available information, such as replicated experiments, in order to get more accurate predictions. Additionally, we wish to develop a more general model for microbial growth for a variety of organism types and under a larger number of combinations of environmental and ecological variables.

To accomplish this challenges, we propose the use of hierarchical models when multiple growth curve data are observed. In this way, it is possible to improve the estimation of a single growth curve by incorporating information from the other bacterial growth curves. Additionally, we propose the use of non-parametric techniques to model the growth process, where it is not assumed that the population fits any parameterized model. In particular, we shall introduce models based on neural networks which can be used to fit very complex relationships.

A growth process may display some stochastic fluctuations which are not due to measurement errors. Models which simply add an error to a deterministic function cannot necessarily capture the total variability of the growth process. Therefore, it is also important to consider fully stochastic models. Another objective of this thesis is to provide a new, stochastic growth curve model of this type.

In general, in the literature on growth curve modeling, most work has been carried out using weighted least squares techniques and other classical approaches. However, the Bayesian approach brings a unified approach to the handling of complex models, such as hierarchical models and neural networks and allows us to differentiate, through the use of hierarchical prior distributions, between various sources of variability, which is an important issue in predictive microbiology. Fur-

thermore, the Bayesian approach permits the incorporation of prior information which is abundant in experimental sciences. One of the main difficulties with the Bayesian approach for practical purposes is that often, complex algorithms have to be devised for the implementation of these techniques, which is a disadvantage to non specialists. Therefore, a further objective of this thesis is to show that Bayesian inference can be implemented for many of the models proposed using a relatively simple algorithm based on a generally available free software package which can be used without the need to fine tune special samplers.

In summary, this thesis aims to provide a statistical framework for the analysis of bacterial growth processes. Modeling and prediction play a key role in the field of microbiology as a valuable tool for making recommendations on food safety and human health and hence, improvements in the methods available are of interest.

The rest of the thesis is structured as follows.

In Chapter 1, we present a brief description of the main population growth models, focusing in the advantages and disadvantages of each one. Then we show that, given a single sample of growth curve data from one of these models, it is straightforward to implement both classical and Bayesian inference for these models. We concentrate on the Bayesian approach which is growing in interest because of its capability to incorporate information from a variety of widely available sources such as laboratory experiments, field measurements and expert judgements and for the possibility to distinguish formally between different sources of uncertainty. In particular, we show that the free software package `WinBUGS` can be used to implement Bayesian inference for simple bacterial growth models.

In Chapter 2, we consider the case when various replications of Petri dish experiments under identical conditions are observed. In such cases, we would expect the individual growth curves to be similar and this suggests the use of hierarchical models to capture the relationship between the different growth curves. As in Chapter 1, we illustrate that the hierarchical model we use, based on the well known Gompertz curve, can be fitted using `WinBUGS`.

In Chapter 3, we then consider the case of Petri dish experiments under different environmental conditions. The relationship between the growth curve parameters and the environmental factors is complex, and here we consider the use of neural networks to model this relationship. Two basic models are considered. Firstly, we introduce a neural network based secondary model which is based on a Gompertz curve where the parameters of the growth curve are modeled as a function of the environmental factors. Secondly, we consider the direct modeling of the growth curve using neural networks. As previously, inference is carried out using a Bayesian approach implemented via `WinBUGS`.

These first three chapters demonstrate that `WinBUGS` can be a powerful and flexible tool able to handle very complex models. We show that in practice, it

is relatively straightforward to implement complex models in WinBUGS which allows microbiological researchers to conduct Bayesian inference in a simple way, without the necessity to design complex MCMC algorithms and instead to concentrate on the model building aspects of the problem.

In the first three chapters, we concentrate on models in discrete time which have the restriction that, for example they may be difficult to implement if data are observed at irregular time intervals. In contrast, in Chapter 4 we develop a new, continuous time, stochastic growth curve model. We show by means of simulations that our proposed model has the potential to capture the the variability observed in replications of the same experiment under identical conditions. Also, we illustrate that by modifying the parameter values, different shaped growth curves can be generated. Finally, we introduce two approaches to Bayesian inference for our model. Firstly, in a simple case of the model, we introduce a Gibbs sampling algorithm and secondly, for the full model, we consider the use of an approximate Bayesian computing algorithm.

Chapter 1

Growth models for single populations

1.1 Introduction

Population dynamics is the study of how and why the sizes of one or more populations change over time and space. Therefore, the objective of population dynamics is trying to determine the mechanism that explains the observed patterns of population change, not just in the numbers of individuals in the population but also in the age structure. This mechanism can be influenced by both biological and environmental factors, as well as by interactions among individuals from the same or different species. The use of mathematical models helps us to understand the dynamic processes involved and to predict future population sizes. These are very useful tools for the analysis of endangered species populations, bacterial or viral growth, renewable resource management, maximum harvest levels for farmers, evolution of pesticide resistant strains, control of pests and, in the biomedical sciences, epidemics, infections and cancer.

The development of population models started in the late 18th-century with the work of Malthus (1798) who pointed out that if unchecked, populations can grow geometrically, whereas the food supply grows only at an arithmetic rate

leading to severe problems such as famine and social unrest. Mathematically, the ideas of Malthus imply exponential growth in populations. Later, Verhulst (1838) suggested some adjustment to exponential growth and proposed a logistic model. According to this model, the growth curve takes the shape of a sigmoid curve so that, initially, the population grows exponentially, but then the growth rate decreases until an upper limit determined by the environmental conditions and the *carrying capacity* is reached.

This initial work did not consider the possibility of interaction between populations via e.g. predation. Lotka (1925) and Volterra (1926) independently proposed a system of paired differential equations, the well known *Lotka-Volterra* model, for the interaction of two species, one a prey and the other a predator. Improvements in population modelling have continued over time. For a much fuller review, see e.g. Murray (2003).

1.2 Population models

In this section, we describe some of the most well known models for population growth, pointing out their main characteristics and advantages as well as their problems and limitations.

1.2.1 The Malthusian growth model

The first mathematical model developed for analyzing population dynamics is the simple, exponential growth model known as the Malthusian growth model, see Malthus (1798). The main assumption of this model is that of a constant rate.

The model can be represented by the following differential equation,

$$\frac{dN}{dt} = rN, \tag{1.1}$$

where at time t, $N = N(t)$ is the population size and $r = b - d$ is the constant growth rate, equal to the difference between the constant birth and death rates (b and d respectively).[1] The solution to the differential equation (1.1) is

$$N(t) = N_0 e^{rt} = N_0 e^{(b-d)t}, \tag{1.2}$$

where $N_0 = N(0)$ is the initial population size at time zero. If the birth rate is greater than the death rate, that is if $b > d$, then $r > 0$ and the population grows exponentially while if $b < d$, then $r < 0$ and the population decreases exponentially till it dies out. Finally, if $b = d$, then the population remains constant at its initial level. Figure 1.1 shows how the speed of the population growth depends on the value of r. Notice that at time 10, the size of the population represented by the dashed line is more than twice the population size represented by the solid line while the difference in the value of r is only one tenth.

The kind of growth represented by the Malthusian model is possible only under special conditions. For instance, bacteria grow by simple division, so that in an experiment under ideal conditions for reproduction, with plenty of food and lack of predators, it is possible to observe exponential growth. However, in practice even bacteria do not grow indefinitely as eventually, food supplies grow short and reproduction conditions deteriorate. This is the main disadvantage of this model. Nevertheless, the model is very simple and can be useful for predictions in the very short time.

[1] For this reason this model is also called the pure birth-death process model.

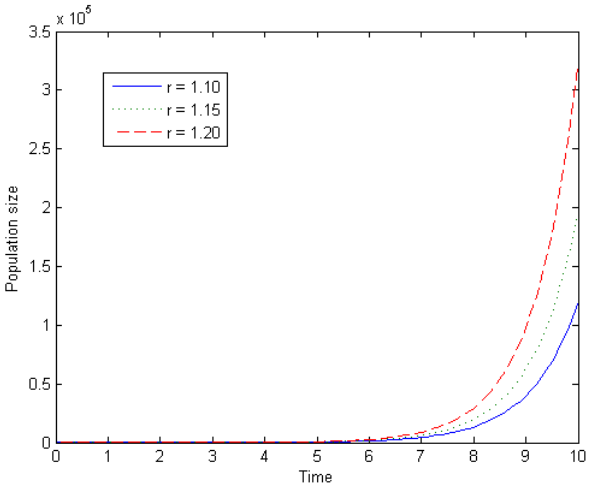

Figure 1.1: Exponential Growth

1.2.2 The logistic growth model

To overcome the problems of the Malthusian model, some adjustments are necessary. Verhulst (1838) proposed a new model where the population has a maximum size. Under this approach, the population growth rate depends not only on the current population size, but also on how far this is from a fixed upper limit. This maximum population size can reach is called the *carrying capacity* of the environment and depends on the availability of resources. Formally, Verhulst's logistic growth model is defined by the following differential equation:

$$\frac{dN}{dt} = rN(1 - \frac{N}{K}), \quad \text{where } r, K > 0, \tag{1.3}$$

where r is the growth rate and K is the *carrying capacity*. This equation is intended to capture two features. Firstly, when the population size is small, then the Verhulst model is close to the Malthusian model so that growth is approximately exponential. Secondly, when the population is large, *starvation* occurs so that the growth rate decreases as the population size gets closer to the *carrying capacity*. Thus, if the population size is far from this maximum, it would grow

quickly, but as it approaches the *carrying capacity* the growth rate slows down. The solution of Equation (1.3) is:

$$N(t) = \frac{KN_0e^{rt}}{K + N_0(e^{rt} - 1)}, \tag{1.4}$$

where N_0 is the initial population size as earlier. Note that for $r > 0$, then $\lim_{t\to\infty} N(t) = K$ so that the population tends to the upper limit as time increases. For $r < 0$ the population eventually dies out and for $r = 0$, the population remains at its initial size as for the Malthusian model.

Figure 1.2 shows the curve produced by the logistic equation. This is an S-shaped or *sigmoidal* curve. Initially the population grows exponentially but, when the population size is closer to the *carrying capacity*, growth decelerates until the stable upper bound is reached.

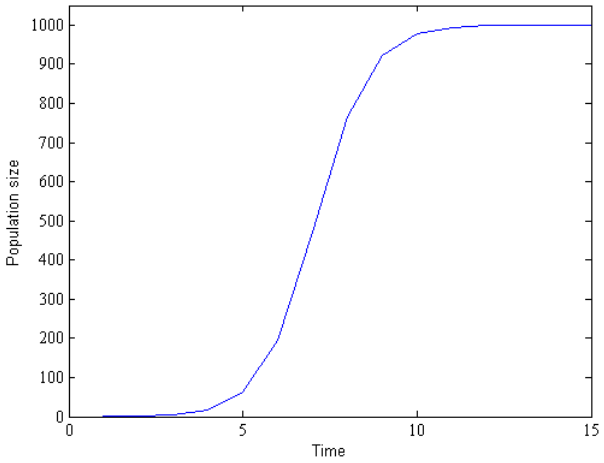

Figure 1.2: Logistic Growth

The logistic growth model describes the self-limiting growth of a population where the growth process depends on the population density. When the population size increases, individuals start to compete with other members of the population for food and other critical resources. This is the so-called *bottleneck*

effect. Nevertheless, the problem with this model is the difficulty of knowing the true value of K in a given habitat. Even when this value is known, at a given moment, it might not be constant and may change over time. Another limitation is that the population dynamics are often more complex than can be captured by this model. For instance, the age of the individuals is not taken into account and this can be an important factor as often, the capacity of reproduction depends on age.

1.2.3 Delay models

The two models considered thus far can be included in a more general class of models, specified by the differential equation

$$\frac{dN}{dt} = f(N)N, \tag{1.5}$$

where $f(N)$ is the specific growth rate. If $f(N)$ is a constant, then differential equation (1.5) leads to Malthusian, pure exponential growth while, if $f(N) = r(1 - N/K)$ we have the Verhulst, logistic growth model. An important problem with these models is that they assume that the reproductive capacity of the population individuals is independent of their age. In particular, many species need to grow to a certain age or undergo a gestation period before they are capable of reproduction. This suggests the incorporation of a time delay. To take into account this feature, the differential equation (1.5) may be modified to become

$$\frac{dN}{dt} = f(N_{-T})N, \tag{1.6}$$

where T is a positive constant and represents the delay parameter and at time t, N_{-T} represents $N(t - T)$. Equation (1.6) shows that the population is now a

function of the current populations and the population T periods before. This new model is a little bit more realistic than the previous ones, but a better model for a delay effect should really be an average over all past populations.

1.2.4 Models for interacting populations

Species are not usually alone in their habitat and on the contrary, usually there are various species interacting in the same habitat so that the population dynamics of each species are affected by the interrelationship among them. From e.g. Murray (2003), there are three main types of interaction:

i) If the density of one population decreases while the other increases, the populations are in a *predator- prey* situation.

ii) If the growth rates of both populations decrease simultaneously, then there is *competition*.

iii) If the growth rates of both populations increase simultaneously then this is called *mutualism* or *symbiosis*.

Here, we will outline a particular model for predator-prey interactions, that is the Lotka-Volterra equations developed in Lotka (1925) and Volterra (1926). Under this model, when the predators population increases, the prey population decreases and as the predator population falls, the prey population increases. These dynamics continue in a cycle of growth and decline. The system of differential equations that model this behaviour is:

$$\frac{dN}{dt} = N(a - bP) \tag{1.7}$$

$$\frac{dP}{dt} = P(cN - d), \tag{1.8}$$

where $N = N(t)$ is the prey population, $P = P(t)$ is the predator population and a, b, c and d are positive constants. This model assumes that the prey has an unlimited food supply so that in the absence of predation the prey population grows exponentially as in the Malthusian model. When predation occurs, this reduces the prey growth rate in proportion to the product of the current prey and predator populations, as can be seen in the last term of Equation (1.7). The change in the prey population is given by its own growth minus the rate at which it is preyed upon. On the other hand, in the absence of any prey for sustenance the predator population decays exponentially. Finally, the prey contribution to the predator growth rate is proportional to the available prey and predator populations, bNP. The change in the predator population is the growth of the predator population minus natural death.

Equilibrium occurs in this model when both population levels are not changing. Setting both differential equations, (1.7) and (1.8), equal to zero and solving, we get two equilibria: first at $N = P = 0$, and second at $N = d/c$ and $P = a/b$. The first solution represents the extinction of both species. If both population levels are at 0, then they will continue to be so indefinitely. The level of the second solution depends on the parameter values. Due to the fact that all the parameters are restricted to be positive, then at this second equilibrium both populations sustain their current non-zero size and do so indefinitely.

Figure 1.3 shows the phase trajectories. As we can see, the trajectories in the in the $N - P$ phase plane are closed lines with elliptical shape. For each possible set of initial conditions, $N_0 = N(0)$ and $P_0 = P(0)$, there is a closed orbit with amplitude determined by the starting point. In order to analyzes the predator-prey phase space is useful divide the graph into four regions by the

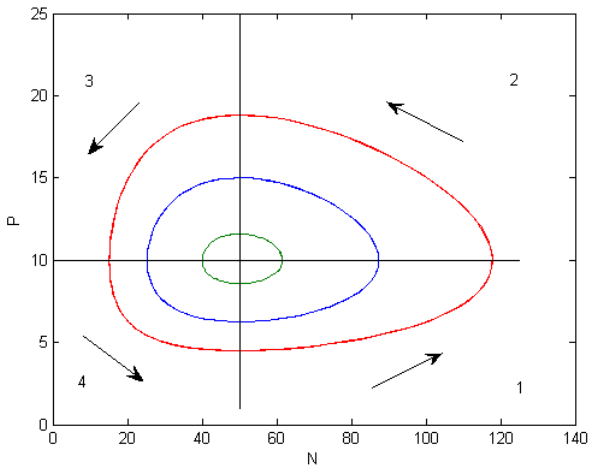

Figure 1.3: Phase plane trajectories of the Lotka-Volterra model

equilibrium ($N = d/c$ and $P = a/b$).[2] In the first region, both populations grow. In the second region, predator population grows and therefore, the number of prey declines. In the third region, both populations decline and in the last region predators still declining while prey population starts to grow. A closed trajectory like this in the phase plane implies periodic solutions in t for N and P in (1.7) and (1.8).

One of the limitations of the Lotka-Volterra model is that it is not very realistic and hence context specific information must be added. The model does not consider any competition for resources among prey or predators and, as a consequence, the prey population may grow infinitely. On the other hand, predators have no saturation, they consumption rate is unlimited and proportional to the prey density. Therefore, the model behaviour shows no asymptotic stability and neither equilibrium point is stable. Instead, the predator and prey populations cycle endlessly. This cyclic behaviour has been observed in nature but it is not very common. The Lotka-Volterra model is insufficient for modelling many

[2]In our example $a = 0.1$, $b = 0.01$, $c = 0.001$ and $d = 0.05$. Then the equilibrium is at $N = 50$ and $P = 10$.

predator-prey systems.

A more general formulation of this model which resolves some of these problems assumes that the growth functions may be non-linear

$$\frac{dN}{dt} = f(N, P)N \tag{1.9}$$

$$\frac{dP}{dt} = g(N, P)P, \tag{1.10}$$

where f and g represent the per capita growth rates of the prey and predator, respectively.

1.2.5 Stochastic models

Population dynamics are complex systems because different factors may affect the populations. Some of these factors can be modelled explicitly but in other cases we cannot model such factors. Nevertheless, it is necessary to include their effects in these population models. One way to do this is to include random variables that account for the collective influence of such factors.

Models in population dynamics include three basic forms of randomness or stochasticity (see Lande et al. (2003)): demographic stochasticity, environmental stochasticity, and sampling error. The first one refers to chance events of individual mortality and reproduction. At a moment of time, an individual can die with a certain probability, and this probability is usually conceived as being independent among individuals. This kind of stochasticity tends to have greater effect in small populations than in large populations. Environmental stochasticity refers to temporal fluctuations in the probability of the mortality and the reproductive rate of all individuals in a population. An extreme example are

the unpredictable catastrophes like fire, flood, hurricane, epidemic, etc. The last source of stochasticity arises from sampling procedure.

Thus, dynamics of populations has both deterministic and stochastic components that operate simultaneously. According to Turchin (2003), there are at least three different ways to include the stochasticity. The most direct approach, when data are observed at regular, discrete time points, say $t = 0, 1, 2, \ldots$, is to add noise to the population rate of change, that is:

$$r_{t+1} = f(\mathbf{Z}_t) + \epsilon_t, \tag{1.11}$$

where $r_{t+1} = \log(N_{t+1}/N_t)$, $\mathbf{Z}_t$ is the vector of state variables and ϵ_t is a random variable with some probability distribution. Noise is included in additive manner because environmental fluctuations are likely to affect per capita death and birth rates, and these rates are combined additively in determining r_{t+1}.

A second approach to including stochasticity in the model is to add a random component directly to N_t. One possible mechanism that supports this approach is the inclusion of random immigration events. Finally, the third approach is to randomly vary the parameters of the model. This approach is useful when researchers know in which part of the population process environmental effects are the most important.

As an example consider the following extension of the Lotka-Volterra model proposed by Gilioli et al. (2008). They initially consider a modified predator-prey system that takes into account the *intra-specific* prey competition as follows:

$$dN = [aN(1 - N) - bNP]dt \tag{1.12}$$

$$dP = [cbNP - dP]dt, \tag{1.13}$$

where $N = N(t)$ and $P = P(t)$ are the biomass of prey and predator at time t per spatial unit normalized with respect to carrying capacity, a is the specific growth rate of the prey, b is a positive constant representing the rate of effective search per predator, c is the maximum specific production rate of the predator and d is the specific loss rate of predator due to natural mortality. The parameters a, c and d are known, as well as the initial values (N_0, P_0). The behavioural parameter b is unknown. A stochastic extension of this model is formulated by including both demographic and environmental stochasticity factors, which are assumed independent. The demographic stochasticity is included by modifying the parameter b:

$$b(t) = b(0) + \sigma\xi(t), \tag{1.14}$$

where $\xi(t)$ is Gaussian white noise, so that b fluctuates around its mean value. [3] Substituting (1.14) in (1.12) and (1.13) the model becomes:

$$dN = [aN(1-N) - b_0NP]dt - \sigma NPdw_1 \tag{1.15}$$

$$dP = [cb_0NP - dP]dt + c\sigma NPdw_1 \tag{1.16}$$

where $b_0 = b(0)$ and w_1 is a Wiener process. Environmental stochasticity is supposed to affect both predator and prey populations because they share the same habitat. The effect of this factor is included by an additive noise depending on each population density. Finally, the proposed stochastic Lotka-Volterra system is

$$dN = [aN(1-N) - b_0NP]dt - \sigma NPdw_1 + \epsilon Ndw_2 \tag{1.17}$$

$$dP = [cb_0NP - dP]dt + c\sigma NPdw_1 + \eta Pdw_2, \tag{1.18}$$

[3] It is assumed that mean and variance fixed are such way that the random variable can rarely take negative values.

where $w_2(t)$ is a Wiener process independent from $w_1(t)$ and ϵ and η are two positive parameters.

1.3 Bacterial growth models

In the field of predictive microbiology the concept of the primary model is fundamental. A primary model describes the kinetics of the growth process by parameters having a biological interpretation. The population size is a function of time and the model aims to describes the different stages of growing.

Bacterial growth is the division of one bacterium into two, identical, daughter cells during a process called *binary fission*. Both daughter cells do not necessarily survive but if the number of surviving cells is, on average, greater than a half, then the bacterial population grows exponentially. Figure 1.4 shows the typical behaviour of bacterial density along the time. Bacterial growth in batch culture experiments where an initial population is planted in a petri dish containing nutrients and then growth is observed over time, can usually be divided in four different phases:

i) In the *lag phase* bacteria adapt themselves to growth conditions. Individual bacteria are not yet able to divide, they are maturing.

ii) The *exponential phase* is the cell doubling period. The number of new bacteria per unit time is proportional to the present population.

iii) During the *stationary phase*, the growth rate slows down as a consequence of nutrient depletion and accumulation of wastes. This phase is reached as the bacteria begin to exhaust the limited resources available to them.

iv) The final phase is the *death phase*. There are no nutrients left and the bacteria die.

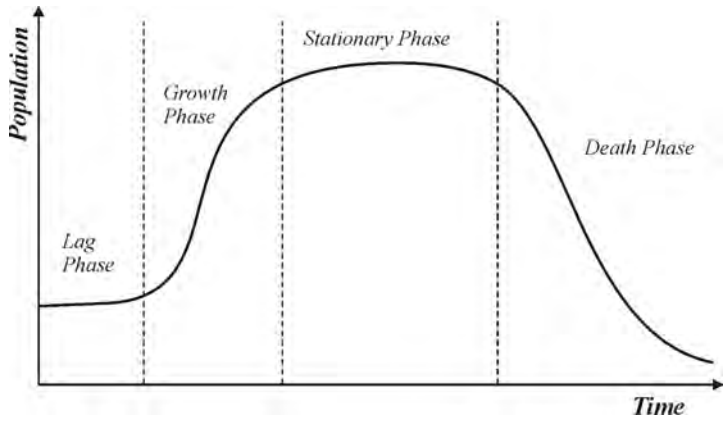

Figure 1.4: Stages of bacterial growth

Given this type of behaviour we can model bacterial growth in the first three phases with a sigmoidal function which represents the different stages of growing. In addition to the logistic model, the most widely used deterministic, parametric bacterial growth models are the Gompertz, (Gompertz (1825)) Baranyi (Baranyi and Roberts (1994), Baranyi and Roberts (1995)) and Buchanan models (Buchanan et al. (1997)) which are outlined below.

1.3.1 Gompertz model

The Gompertz function, introduced in 1825, originated in the field of actuarial science. Gompertz proposed the following equation for the number of survivals of a population at any age t,

$$N(t) = ae^{be^{-ct}} \tag{1.19}$$

where $a > 0$ is the upper asymptote, $b < 0$ is a constant and $c > 0$ is a positive constant related with the growth rate. After some years, the Gompertz equation

caught the attention of other field which used it as a growth curve. The Gompertz growth curve has been useful in applied research like in medicine for tumour growth modelling, in biology for modelling the growth of organism, in marketing for modelling sales of a new product, etc. As a growth curve, it is useful to write the Gompertz curve as follow

$$N(t) = Ke^{\log(\frac{N_0}{K})e^{-rt}} \tag{1.20}$$

where K denote the carrying capacity of the system, $N_0 = N(0)$ is the initial population at time zero, and r is related to the reproduction rate. The dynamics described in (1.20) are governed by the following first order ordinary differential equation for $N(t)$:

$$\frac{dN}{dt} = r \log\left(\frac{K}{N}\right) N, \tag{1.21}$$

This differential equation is a special case of the general formulation of the growth models expressed in (1.5), where $f(N) = r \log\left(\frac{K}{N(t)}\right)$. As was mentioned previously, the Gompertz equation is an S-shaped curve, which means that growth is slowest at the start and end of a time period and there is an inflection point between them. In contrast to the logistic function which has the inflection point mid-way between the asymptotes $(K/2)$, in the Gompertz function the inflection point is reached when approximately 37% of the total growth has been realized (K/e). In other words, in the logistic function, both asymptotes are approached by the curve symmetrically, while in the Gompertz function the upper valued asymptote is approached much more gradually by the curve than the lower asymptote.

It is often more convenient to write Equation 1.20 as the reparametrization suggested by **?** getting new parameters with biological meaning and comparable

with the other models and known as the modified Gompertz equation,

$$N(t) = N_0 + (N_{max} - N_0)\exp(-\exp(\frac{\mu_{max}\exp(\lambda - t)}{(N_{max} - N_0)\log(10)} + 1)) \tag{1.22}$$

where λ is the lag time, μ_{max} is the maximum specific growth rate and N_{max} is the maximum population density.

1.3.2 Baranyi model

The modified Gompertz equation and the logistic function were not originally developed by modelling bacterial growth and therefore are considered as purely empirical models. In a series of papers, see e.g. Baranyi and Roberts (1994), Baranyi and Roberts (1995), Baranyi et al. (1999), Baranyi and co-workers developed a mechanistic model for bacterial growth putting special attention to the lag phase which is attributed to the need to synthesize an unknown substrate q critical for growth. The Baranyi model is different from the previous one because it includes a new term, $g(t)$, called the adjustment function. This function describes the adjustment of the culture to the new environment and it affects the course of growth before the exponential phase. In a typical batch culture experiment the bacterial population is first cultured under more or less optimal conditions and then inoculated and grown in a new environment. The authors argue that the physiological state at $t = 0$ affects the length of the lag period in the new environment. The lag in the post-inoculation environment is longer if the cells are closer to the stationary phase in the pre-inoculation environment. In a general formulation, the new model describes the bacterial batch culture by means of the differential equation

$$\frac{dN}{dt} = g(t)f(N)N, \tag{1.23}$$

with $f(N) = \mu_{max}\left(1 - \frac{N(t)}{N_{max}}\right)$ and $g(t) = \frac{q_0}{q_0+e^t}$, being μ_{max} the maximum specific growth rate, N_{max} the maximum population density and q_0 the physiological state of the inoculum.

The explicit form of the model is the following

$$N(t) = N_0 + \mu_{max}A(t) - \log(1 + \frac{e^{\mu_{max}A(t)} - 1}{e^{(N_{max}-N_0}}) \tag{1.24}$$

$$A(t) = t + \frac{1}{v}\log(\frac{e^{-\mu_{max}t} + q_0}{1 + q_0}) \tag{1.25}$$

with the same parameters as earlier. The more familiar lag time, λ, could be calculated from the values of q_0 and μ_{max} as

$$\lambda = \frac{\log(1 + \frac{1}{q_0})}{\mu_{max}} \tag{1.26}$$

Then, the growth equation was reparametrized by Wilson (1999) in terms of the lag time. The new form is given by:

$$N(t) = N_0 + \frac{N_1}{\log(10)} - \frac{N_2}{\log(10)} \tag{1.27}$$

where

$$N_1 = \mu_{max}t + \log(e^{-\mu_{max}t} - e^{-\mu_{max}(t+\lambda)} + e^{-\mu_{max}\lambda}) \tag{1.28}$$

$$N_2 = \log(1 + 10^{(N_0-N_{max})}(e^{\mu_{max}(t-\lambda)} - e^{-\mu_{max}\lambda})) \tag{1.29}$$

In this form the Baranyi equation is expressed in terms of more familiar quantities with intuitive biological interpretations. Since its introduction, the Baranyi model has been used extensively to model the growth of a wide variety of microorganisms.

1.3.3 Three phase linear model

An alternative model was proposed in Buchanan et al. (1997). This model is a three-phase linear model where each phase describes one of the bacterial growth stages: lag, exponential and stationary, see Figure 1.5. As, during the lag phase bacteria are adapting to the new environment the model assumes that the growth rate is equal to zero. Once the bacteria are adapted, they begin to divide and in the exponential growth phase the model assumes a constant growth rate, with the log of the density population increasing linearly with time. Finally, when the stationary phase is reached, the growth rate returns to zero. The model can be formalized as:

$$N(t) = N_0 \quad \text{for} \quad t \leq t_{lag} \tag{1.30}$$

$$N(t) = N_0 + \mu(t - t_{lag}) \quad \text{for} \quad t_{lag} < t < t_{max} \tag{1.31}$$

$$N(t) = N_{max} \quad \text{for} \quad t \geq t_{max} \tag{1.32}$$

where $N(t)$ is the log of the population density at time t, N_0 the log of the initial population density, N_{max} the log of the maximum population density supported by the environment, t the elapsed time, t_{lag} the time when the lag phase ends, t_{max} the time when the maximum population density is reached and μ the specific growth rate. Despite its simplicity, this model has not been as widely used for fitting growth data as the Gompertz and Baranyi models introduced earlier.

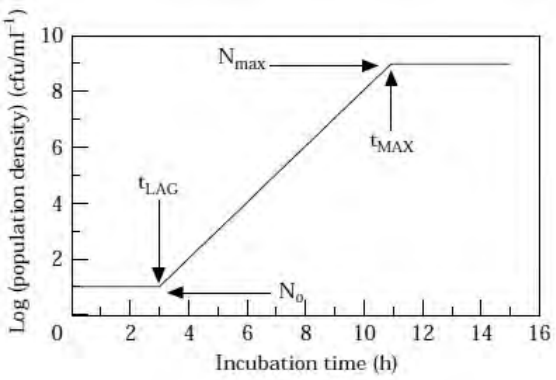

Figure 1.5: Graphical representation of the Buchanan model

1.3.4 Secondary models

Traditionally, primary growth models are developed for static environmental conditions, however reality is characterized by changing environmental conditions. Secondary models are developed to describe the effect of environmental conditions such as, temperature, pH, salinity, water activity, on the values of the growth parameters of a primary model. Most of the secondary models can be divided into one of three categories, that is square root, polynomial and cardinal models. Firstly, square root models describe the effect of suboptimal temperature on growth rate of microorganisms see e.g. Ratkowsky et al. (1982). Secondly, polynomial models allow any of the environmental factors and their interactions to be taken into account and were extensively used in the 1990s. However, these models include an excessive number of parameters with lack biological interpretability. Rosso et al. (1993) introduced a model that described the influence of temperature, acidity level and water activity on the growth rate based on the gamma concept and using only parameters that were biologically significant. This model then became widely known as the cardinal model. In Chapter 3, secondary models will be presented in more detail.

1.4 Model fitting

Most of the growth models presented previously, and, in particular, the logistic function, the Baranyi and the Gompertz equations, are nonlinear growth models. These were presented as deterministic parametric models, where the parameters have meaningful biological interpretations and the functional form represents the underlying behaviour in the growth system. Assuming that data are observed at a set of equally spaced time points, then by adding an error term, the deterministic model is replaced by a statistical model. In general notation, these models can be expressed as

$$y_i = f(\boldsymbol{x}_i, \boldsymbol{\theta}) + \epsilon_i \quad \text{(i=1,2,...,n)}, \tag{1.33}$$

where y_i is the i^{th} observation of the dependent variable, f is a (nonlinear) function, $\boldsymbol{x}_i$ are the i^{th} observations of the independent variables, $\boldsymbol{\theta}$ is the vector of parameters and the error terms, ϵ_i, have zero mean.

To fit the curve, sometimes it is possible to transform the nonlinear model in a linear one. This kind of models are called transformably linear or "intrinsically linear". The advantage to apply this transformation relies on that with a linearized model we can apply standard linear regression methods. Additionally, depending on the structure of the errors, transformation to linearity could also achieve errors approximately normally distributed and with constant variance. Nevertheless, parameters of the transformed model are not as interesting or as important as the original parameters and usually they are difficult to interpret.

1.4.1 Nonlinear Least Squares

As in linear regression, parameters of interest can be estimated by the method of least squares. The least squares estimate of $\boldsymbol{\theta}$, denoted by $\hat{\boldsymbol{\theta}}$, it is obtained

minimizing the error sum of squares,

$$S(\boldsymbol{\theta}) = \sum_{i=1}^{n} [y_i - f(\boldsymbol{x}, \boldsymbol{\theta})]^2. \tag{1.34}$$

Assuming that errors are independent and identically distributed with zero mean and constant variance, $\hat{\boldsymbol{\theta}}$ is an asymptotically unbiased estimate of the parameter vector $\boldsymbol{\theta}$. Under certain regularity assumptions $\hat{\boldsymbol{\theta}}$ is also asymptotically normally distributed as $n \to \infty$. Additionally, if it is assumed that the errors are normally distributed, then $\hat{\boldsymbol{\theta}}$ is also the maximum-likelihood estimator. For more details see Seber and Wild (1989).

This minimization problem yields normal equations that are nonlinear in the parameters and therefore they can not be solved analytically for most of the models. Therefore, in order to provide approximate, analytic solutions it is necessary to employ iterative methods.

Approximating the model by the first-order Taylor series expansion, yields the vector of parameter estimates: $\mathbf{b} = (\mathbf{J}'\mathbf{J})^{-1}\mathbf{J}'y$; being $\mathbf{J}$ the Jacobian matrix which contains the derivatives of the model with respect to the parameters and evaluated in the n points. An estimate of the covariance matrix V of the parameter estimates can be computed as $\hat{V} = (\mathbf{J}'\mathbf{J})^{-1}\sigma^2$, where σ^2 is the error variance. This method will converge fast provided the neighbourhood of the true parameter values has been reached. However, if the initial parameter values are too faraway, the convergence would never be reached. Alternative iterative procedures could be applied such as the steepest descent method and the Levenberg-Marquardt's method. The former method is able to converge even though initial values are far removed from the true parameter values, but the asymptotic rate of convergence is very slow. The Levenberg-Marquardt (Levenberg (1944),Marquardt (1963)) method is the most widely used method of computing nonlinear least squares es-

timators and most standard statistical packages contain computer routines to fit nonlinear regression models using this algorithm. This method is a compromise between the linearization and the gradient methods. It almost always converges and the convergence rate does not slow down at the later stages of the iterative procedure.

A number of software packages are available for fitting the various bacterial growth models previously described using these techniques. In particular, the `grofit` package for `R` available from

`http://cran.r-project.org/web/packages/grofit/index.html`

can be used to fit the logistic, Gompertz and modified Gompertz models among others. In the case of the Baranyi model, software includes `DMFit`, for `Microsoft Excel`, available from

`http://www.combase.cc/index.php/en/downloads/category/11-dmfit`

and `MicroFit`, a stand alone package distributed by the Institute of Food Research in the U.K which can be obtained from

`http://www.ifr.ac.uk/microfit/`.

1.4.2 Bayesian estimation

As we have seen, classical statistical methods for nonlinear regression are based on linearization of the nonlinear models around the unknown parameter. Typically, the distribution of the least squares parameter estimators is known only asymptotically and these asymptotic approximations may be inadequate in practice for small-sample problems. Assuming that the error distribution of the nonlinear model is known, an alternative procedure which does not rely on the linearization of the model is to use a Bayesian approach where asymptotic theory is not involved. The Bayesian approach assumes that the parameters are random

variables instead of unknown constants, that is the parameters themselves have some unknown probability distribution. The approach relies on the idea that researches have some prior beliefs or knowledge about the system under study and this knowledge is updated once the data are observed. The inclusion of readily accepted prior information is particularly useful when the sample size is small.

Consider the nonlinear model (1.33) in vector form,

$$\boldsymbol{y} = \boldsymbol{f}(\boldsymbol{\theta}) + \boldsymbol{\epsilon} \tag{1.35}$$

Bayesian models are constructed by specifying the conditional distribution of the observable variable $\boldsymbol{y}$ (data) given the model parameters $\boldsymbol{\theta}$, that is $p(\boldsymbol{y}|\boldsymbol{\theta})$, and a prior distribution for these parameters, $p(\boldsymbol{\theta})$ which expresses the current level of uncertainty before any data are observed. Once data are observed, inference about the parameters is based on the posterior distribution $p(\boldsymbol{\theta}|\boldsymbol{y})$. Using Bayes Theorem, this is calculated as:

$$\begin{aligned} p(\boldsymbol{\theta}|\boldsymbol{y}) &= \frac{p(\boldsymbol{y}|\boldsymbol{\theta})p(\boldsymbol{\theta})}{p(\boldsymbol{y})} \\ &\propto p(\boldsymbol{y}|\boldsymbol{\theta})p(\boldsymbol{\theta}) \end{aligned}$$

so that the posterior parameter distribution, $p(\boldsymbol{\theta}|\boldsymbol{y})$, is proportional to the product of the likelihood function, $p(\boldsymbol{y}|\boldsymbol{\theta})$ and the prior distribution of the parameters $p(\boldsymbol{\theta})$. The posterior distribution is a joint probability distribution of all model parameters and point estimates or uncertainty intervals can be obtained from it. For good general reviews of the Bayesian approach in ecological modeling see e.g. McCarthy (2007), King et al. (2009).

The computation of the exact conditional posterior distributions is most often impossible. In such cases, Markov-Chain Monte-Carlo (MCMC) techniques can

be applied to generate samples from the posterior distributions. This method generates chains of simulated values for parameters, with the sampling distribution converging to the relevant posterior distribution. The freeware computer package `WinBUGS`, see Lunn et al. (2000) is a powerful and flexible tools able to implement these chains for a wide range of possible models. In the next section, we show how a Bayesian approach can be implemented to make inference for the growth models using `WinBUGS`.

1.5 Growth curve modeling using `WinBUGS`

In Section 1.4.1 we commented on a number of packages for fitting growth models using non-linear least squares approaches. However, to the best of our knowledge, thus far, no general computational package has been developed for the implementation of Bayesian inference in bacterial growth models. For that reason, in this section we describe the use of `WinBUGS`, in the context of bacterial growth. For a full review of `WinBUGS` in the context of ecological modeling, see e.g. Kéry (2010).

1.5.1 Model specification

Assume that population density data $N_t = N(t)$, are observed at a set of regular time points, say $t = 0, 1, \ldots, T$. Then, a model specification must be assumed. For illustration, consider the modified Gompertz equation, where $N_t = g(N_0, N_{max}, \mu_{max}, \lambda, t)$ where g is the function defined in (1.22) with four parameters: N_0 is the initial population density, N_{max} the maximum population size, μ_{max} is the maximum growth rate and λ is the lag period. Then, a sample distribution for the error term must be assumed. Suppose that the errors are independent and identically normally distributed with variance σ^2, so that we

have:

$$N_t \sim \mathcal{N}(g(N_0, N_{max}, \mu_{max}, \lambda, t), \sigma^2). \tag{1.36}$$

The model specification is completed by assigning prior distributions for the model parameters. A possible structure of prior distributions is:

$$\begin{aligned} \log N_0 &\sim \mathcal{N}(\mu_{N_0}, \sigma_{N_0}) \\ \log N_{max} &\sim \mathcal{N}(\mu_{N_m}, \sigma_{N_m}) \\ \log \mu_{max} &\sim \mathcal{N}(\mu_\mu, \sigma_\mu) \\ \log \lambda &\sim \mathcal{N}(\mu_\lambda, \sigma_\lambda) \end{aligned}$$

where μ_i and σ_i are the mean and the standard deviation of the natural logarithm of the parameter i. The parameters of the prior distributions are chosen in such a way that they reflect the prior knowledge about the model parameters. The source of information could come from the opinion of an expert and / or the results of previous studies. If there is no reliable previous information, it is better to used non-informative prior distributions, that is priors with high variance which reflect the uncertainty about model parameters. We follow this approach and set the means of the prior distributions equal to zero and the variances equal to 100. Finally, the prior distribution of the error variance is an inverse gamma distribution, $1/\sigma^2 \sim \mathcal{G}(a, b)$.

The dependence structure represented by this model and prior is represented in Figure 1.6. In the figure, called a doodle in WinBUGS, random and logical nodes are represented by ellipses and fixed nodes (independent variables) are represented by rectangles. The arrows represent dependence relationships with the single arrows showing stochastic dependence and the double arrows representing logical dependence.

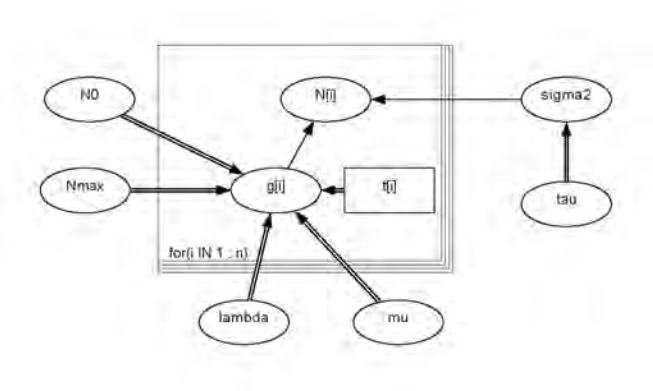

Figure 1.6: The dependence structure of the modified Gompertz model

The following `WinBUGS` code to represent the model specification can be generated from the doodle or programmed directly:

```
model{
for(i in 1:n) {
   g[i] <- N0 + (Nmax-N0)* exp(-exp(((mu*exp(1)*(lambda-t[i]))/
            ((Nmax-N0)*log(10)))+1))
   N[i] ~ dnorm(g[i], tau)
}
N0  ~ dlnorm(0, 0.01)
Nmax  ~ dlnorm(0, 0.01)
lambda  ~ dlnorm(0, 0.01)
mu  ~ dlnorm(0, 0.01)
tau  ~ dgamma(0.01,0.01)
}
```

where n is the number of observations. As the population size, the growth rate and the lag period are non-negative quantities, we used lognormal prior distributions, but alternative distributions can be used, such as the truncated normal distribution

```
mu ~ djl.dnorm.trunc((0,0.01,0,1000)
```

or the gamma distribution

```
mu ~ dgamma(0.01, 0.01).
```

Note that WinBUGS requires the specification of the precision ($\tau = 1/\sigma^2$) instead of the variance. This is not a problem however as a helpful feature of WinBUGS is the use of logical relationships to define functions of the parameters in the model. For example, to calculate the variance, it is enough to define

```
sigma2 <- 1 / tau
```

which allows inference for the variance parameter to be undertaken.

In the field of microbiology, a very useful quantity of interest in is the doubling time, also called generation time. Doubling time is the time it takes a bacterium to do one binary fission starting from having just divided. That is looking at the all population, it is the period of time required for the population to double in size. Then, generation time is can be computed as the natural logarithm of 2 divided by the growth rate. Calling gt the generation time, the code for compute it in WinBUGS in our example is

```
gt <- log(2) / mu
```

After the model code has been checked, the data must be loaded in S-Plus format or, for data in arrays, in rectangular format. For instance, in our Gompertz example, we need to specify the sample size, n, the vector with the observations of the population size N and the vector of the corresponding observations times t, both of length n. This is achieved as follows:

```
list(
n = 16,
t = c( 0, 1, 2, 3, 4, 5, 6, 7, 8, 9, 10, 11, 12, 13, 14, 15),
N = c( 0.07, 0.07, 0.08, 0.09, 0.14, 0.31, 0.52, 0.74, 0.85, 0.88, 0.90, 0.92,
        0.94, 0.95, 0.96, 0.96)
 )
```

Finally, we need to specify the initial values for the variables to be estimated. The format for introducing this information is the same as for the data. In our example,

```
list(N0 = 0.07, Nmax = 1, lambda = 4, mu = 0.25, tau = 1)
```

Alternatively, it is possible to use the `WinBUGS` generator of initial values, which are drawn from the prior distributions (or from an approximation to the prior). Nevertheless, when vague prior distributions are used, it is not appropriate to use this generator as the values generated could be very improbable.

After that, the model is run until convergence is reached. Convergence can be checked in `WinBUGS` by looking at the trace of the sample values generated at each iterations to see if the chain seems to be stabilized. Additionally, the Gelman-Rubin statistic (Gelman and Rubin (1992), Brooks and Gelman (1998)) can be computed for what run several chains is needed. Finally, it is important to check the autocorrelation of the MCMC sampled data which, for example, can be done using simple autocorrelation plots. If there is autocorrelation up to lag 5 say, the data can be *thinned* by taking just every fifth datum to produce an approximately independent sample.

A standard session in `WinBUGS` can be resumed as follows. Firstly, the model is specified in the form of the likelihood and prior distributions for all the unknown

model parameters. Secondly, data and initial values are loaded. Finally the model is run and assuming convergence, the generated MCMC simulations are a sample from the posterior distributions of interest.

1.5.2 Data analysis

Useful summary statistics and graphical representations of the posterior distributions can easily be obtained in WinBUGS trough the *Sample Monitor Tool*. The posterior mean, standard devitation and quantiles, as well as plots of smooth kernel density estimate or trace for the parameters are outputs that WinBUGS provides to summarize the posterior distribution.

1.5.3 Model comparison

A widely used statistic for comparing models in a Bayesian framework is the Deviance Information Criterion (DIC) of Spiegelhalter et al. (2002). This criterion penalizes actions for departure from the corresponding observed value as well as for the number of parameters in the model. In this way, the approach is a compromise between goodness of fit and model complexity. The DIC is easily calculated from the samples generated by a Markov chain Monte Carlo simulation and is implemented automatically in WinBUGS. Formally, for a model with data $\mathbf{y}$ and parameters $\boldsymbol{\theta}$, the DIC is equal to

$$DIC = p_D + \overline{D(\boldsymbol{\theta})} \tag{1.37}$$

where $D(\boldsymbol{\theta}) = -2\log(p(\mathbf{y}|\boldsymbol{\theta}))$ is the deviance and $\overline{D(\boldsymbol{\theta})}$ is the posterior mean of the deviance, approximated by $\sum_{i=1}^{m} = \boldsymbol{\theta}^i$ (m is the number of iterations). The expected deviation measures how well the model fits the data. The lower is, the

better the fit. The effective number of parameters, p_D, computed as the difference between the measure of fit and the deviance at the estimates $\overline{D(\boldsymbol{\theta})} - D(\overline{\boldsymbol{\theta}})$ is a measure of model complexity, roughly speaking the number of parameters in the model. Lower values of the criterion indicate better fitting models. More details about the DIC can be found in Spiegelhalter et al. (2002).

1.6 Application: *Listeria monocytongenes*

Listeria is a bacterial genus containing six species. These species are Gram-positive bacilli and are typified by *listeria monocytogenes*. This bacteria is a well-known food-borne pathogen (rarely but fatally infectious as listeriosis) and is commonly found in soil, stream water, sewage, plants, and food. The serious health and economic consequences of listeriosis have lead to a wide amount of studies of this bacteria, see e.g. Augustin and Carlier (2000), Delignette-Muller et al. (2006), Pouillot et al. (2003) and Powell et al. (2006) among others. In our application the models are fitted to listeria growth curves. The data come from an experiment in broth monoculture. The environmental conditions remained the same for the curve, which was generated at 42 °, pH=7,4 and 2,5% NaCl (salt concentration). The data set consists of 16 observations.

Classical inference

Figure 1.7 shows the growth data and the fitted curves for two general growth models discussed previously, that is the Malthusian model and the logistic model. The Malthusian model was fitting taking into account only the data corresponding to the exponential phase of growth and the logistic model was fitting to all the observations. The Malthusian model fits the first part of the data well, but cannot

explain the stationary phase of the bacterial growth.

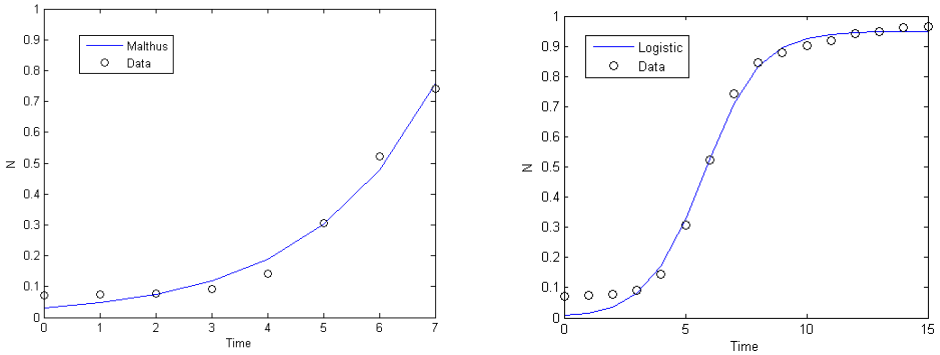

(a) Malthusian model (b) Logistic model

Figure 1.7: Growth models fitted to the Listeria growth data

In contrast, the logistic model fits the data on the exponential and stationary phases, but fails to explain the lag phase. To overcome these problems, we also fitted the Baranyi and Gompertz models to these data.[4] Figure 1.8 shows the new fitted curves and Table 1.1 summarizes the results of the estimation.

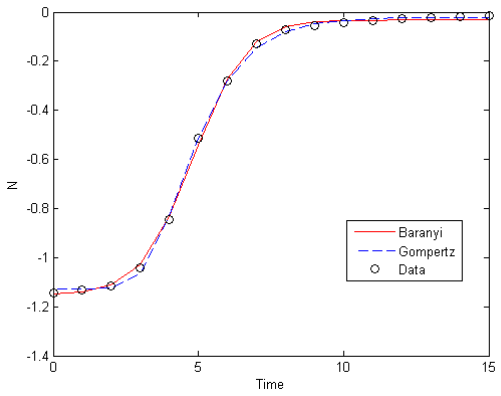

Figure 1.8: Baranyi and Gompertz models fitted to the Listeria growth curve

[4]These models were fitted to the data using the `nlstools` package of `R`. Note that we consider the log to base ten of the cell concentration

Table 1.1: Baranyi and Gompertz Parameters

	Estimate	Std. Error	2.50%	97.50%	P-value	
Baranyi's model:						
λ	3.804	0.063	3.666	3.943	3.05E-16	***
μ_{max}	1.246	0.044	1.150	1.342	2.35E-12	***
N_0	-1.149	0.009	-1.169	-1.129	2.00E-16	***
N_{max}	-0.032	0.005	-0.044	-0.021	4.93E-05	***
RSE	0.014					
Gompertz's model:						
λ	3.087	0.058	2.960	3.214	1.34E-15	***
μ_{max}	0.747	0.021	0.702	0.792	1.29E-13	***
N_0	-1.126	0.007	-1.142	-1.111	2.00E-16	***
N_{max}	-0.022	0.005	-0.033	-0.011	0.00109	**
RSE	0.013					
*** : $\alpha = 0.01$ and ** : $\alpha = 0.05$						

We can observe that both models fit the experimental data well, with the greatest differences being observed during the transition periods, from lag to exponential phase and from the last one and the stationary phase. Analyzing the residual standard errors, we can see that Gompertz model fits a little bit better than Baranyi model. Regarding the parameter estimates, both models yields statistically significant estimates, but the standard errors of the Gompertz model are lower than in Baranyi model. Finally, the initial and the maximum population density predicted for both models are similar. However, there are some differences in the lag and the maximum specific growth rate. In the Gompertz model, the estimated lag parameter is lower than in the Baranyi model. Also, since the maximum population density is almost the same, the specific growth rate in the Gompertz model is greater, as we can see in Table 1.1. Comparing the estimation among the four parameters, the estimated error indicates that lag parameter has larger uncertainty. [5]

To asses the validity of the fitted models it is necessary to study the residuals. Figure 1.9 shows the fitted values versus the standardized residuals, autocorre-

[5]Baranyi and Roberts (1994), Wijtzes et al. (1995) and Grijspeerdt and Vanrolleghem (1999) have reported on this phenomenon previously.

lations and histograms of the residuals for each model. In both cases, there are neither signals of heteroscedasticity nor autocorrelation of the residuals, so that the assumptions of the models seem to hold. Nevertheless, looking at the histograms, in the case of the Baranyi model the residuals do not seem to be normal as in the Gompertz case. Two tests were performed to complement the previous residual analyses: the Shapiro-Wilk test to evaluate the normality of the residuals and the runs test to asses the randomness of the residuals. The results of the first test give p-values equal to 0.1033 for the Baranyi model and 0.9241 for the Gompertz model respectively. Hence, the null hypothesis that the residuals are normally distributed is not rejected at a 5% significance level. The results of the runs test are p-values equal to 0.04139 and 0.6451 for the Baranyi and Gompertz models respectively; therefore, in the first case the null hypothesis of randomness is rejected at a 5% significance level.

For finite samples, in nonlinear estimation, even when the dependent variable y_t is normally distributed (so that the least squares estimator is also the maximum likelihood estimator of β), $\hat{\beta}$ is not a linear combination of the y_t and hence in general is not normally distributed. For this reason we computed bootstrap confidence intervals based on percentiles of the bootstrap distribution of the statistics. These confidence intervals are more accurate when the distribution of the statistic is not normal and, moreover, they have good theoretical coverage properties, see Efron and Tibshirani (1993). Table 1.2 shows the parameter estimates and their confidence intervals using least square method and bootstrap techniques. Note that the parameter estimates are almost the same but the length of the confidence intervals are narrower in the bootstrap case. This suggests that the bootstrap distribution of the parameter estimates are more leptokurtic than the asymptotic normal distribution.

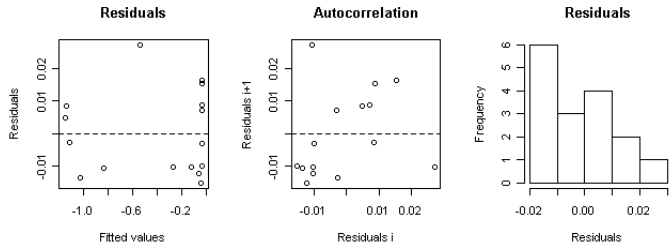

(a) Baranyi model

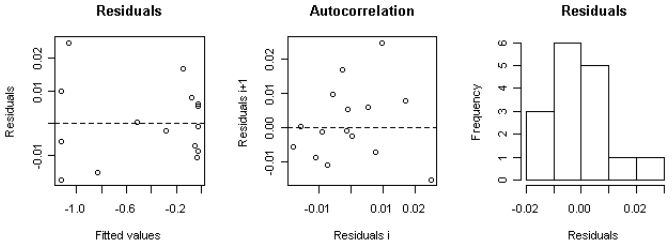

(b) Gompertz model

Figure 1.9: Residual analysis

Table 1.2: Confidence Interval for Baranyi and Gompertz Parameters

	Least square estimate	Bootstrap estimate	Asymptotic CI 2.50%	Asymptotic CI 97.50%	Bootstrap CI 2.50%	Bootstrap CI 97.50%
Baranyi's model:						
λ	3.804	3.808	3.666	3.943	3.689	3.903
μ_{max}	1.246	1.244	1.150	1.342	1.171	1.322
N_0	-1.149	-1.149	-1.169	-1.129	-1.163	-1.134
N_{max}	-0.032	-0.032	-0.044	-0.021	-0.040	-0.022
Gompertz's model:						
λ	3.087	3.089	2.960	3.214	2.988	3.178
μ_{max}	0.747	0.748	0.702	0.792	0.710	0.784
N_0	-1.126	-1.127	-1.142	-1.111	-1.138	-1.114
N_{max}	-0.022	-0.022	-0.033	-0.011	-0.030	-0.013

1.6.1 Bayesian inference

This will be our basic approach to define prior distributions for the parameters of our models, N_0 the initial size population, μ_{max} the maximum specific growth rate, λ the lag parameter and τ the precision parameter (the reciprocal of the variance). Prior variances were chosen so as to be high enough to give relatively diffuse priors.

The model specification and the prior distributions for the unknown model parameters are

$$\begin{aligned} N_t &\sim \mathcal{N}(f(\mathbf{t}, N_0, N_{max}, \mu_{max}, \lambda), \sigma^2) \\ N_0 &\sim \mathcal{N}(0, 100) && (1.38) \\ N_{max} &\sim \mathcal{N}(0, 100) && (1.39) \\ \mu_{max} &\sim \mathcal{NT}(0, 100, 0, 10) && (1.40) \\ \lambda &\sim \mathcal{NT}(0, 100, 0, 16) && (1.41) \\ \tau = \frac{1}{\sigma^2} &\sim \mathcal{G}(0.01, 0.01) && (1.42) \end{aligned}$$

where $f(\mathbf{t}, N_0, N_{max}, \mu_{max}, \lambda)$ is the growth model. For the parameters that cannot assume negative values we choose truncated normal distributions for μ_{max} and λ, and a gamma distributions for the precision parameter, $G(a, b)$ where a is shape parameter and b is the rate parameter (the inverse of the scale parameter).

Bayesian inference was carried out using `WinBUGS` as outlined previously. After a burn-in phase, 6 x 10^4 sample values were generated. Convergence of the MCMC algorithm was checked by visually analyzing three independent MCMC chains using three different initial values.

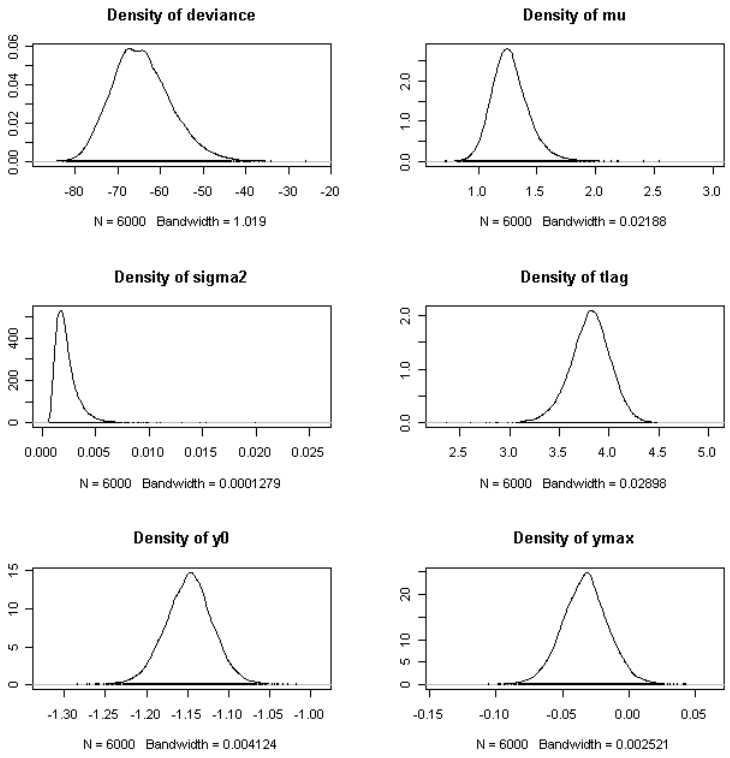

Figure 1.10: Baranyi Model

Following the suggestions of Cowles and Carlin (1996) about to combine a set of strategies to asses convergence, we also compute the Geweke (1992) and Gelman and Rubin's test to complement and formalize the previous conclusions. Geweke's test compute the z-score calculated as the difference between the two sample means of the first and last part of each Markov chain[6] divided by its estimated standard error. If the samples are drawn from the stationary distribution of the chain, then the two means are equal and Geweke's statistic has an asymptotically standard normal distribution.

Table 1.3 shows that at a 0.05 significance level, the null hypothesis of equality of the means is rejected only in the third chain of the Baranyi model for the lag parameter, λ, and the estimated variance. In the rest of the cases we can-

[6]The first 10% and the last 50% part.

Table 1.3: Geweke's test

	lag	mu	N0	Nmax	sigma2
Baranyi model:					
Chain 1	-0.494	-0.401	-0.794	1.180	-1.567
Chain 2	0.052	0.115	-1.150	0.610	-1.857
Chain 3	2.225	1.743	0.916	-0.588	1.973
Gompertz model:					
Chain 1	0.519	-0.500	-0.077	-1.862	-1.494
Chain 2	-0.647	-0.918	-0.072	0.236	0.318
Chain 3	0.387	0.363	0.128	0.226	-1.879

not reject the null hypothesis, which indicates convergence of the Markov chain. Convergence is also supported by the Gelman and Rubin test. For almost all the parameters in both models, the scalar factor is equal to one, which indicates convergence (only for the case of the maximum specific growth rate, μ_{max}, in the Gompertz model, the scalar factor is different to one and is equal to 1.27, which is not too far from one).

Table 1.4: Descriptive statistics of Bayesian inference

	Mean	Median	Std. Error	2.50%	97.50%
Baranyi's model:					
λ	3.807	3.816	0.207	3.370	4.193
μ_{max}	1.272	1.258	0.162	0.996	0.005
N_0	-1.149	-1.148	0.029	-1.211	-1.091
N_{max}	-0.033	-0.033	0.018	-0.068	0.002
σ^2	0.002	0.002	0.001	0.001	0.005
Gompertz's model:					
λ	3.098	3.102	0.232	2.630	3.538
μ_{max}	0.765	0.754	0.180	0.620	0.951
N_0	-1.127	-1.126	0.027	-1.182	-1.074
N_{max}	-0.022	-0.022	0.019	-0.059	0.016
σ^2	0.002	0.002	0.001	0.001	0.005

The empirical posterior distributions of the model parameters are represented in Figure 1.10 for the Baranyi model and in Figure 1.11 for the Gompertz model. Several descriptive statistics are shown in Table 1.4. In both models, posterior distributions of the parameters are reasonably symmetric except for σ^2 that is slightly skewed to the right. Posterior means of the parameters are relatively

close to the least squares estimates. As in the least squares method, the greater difference between the two models is found in the lag parameter. The estimated standard error is always greater in Bayesian inference than in the case of least square method. Table 1.4 also shows the estimated high posterior density intervals. Note that in Bayesian inference we deals with *credible intervals* which are different from the classical concept of confidence intervals.

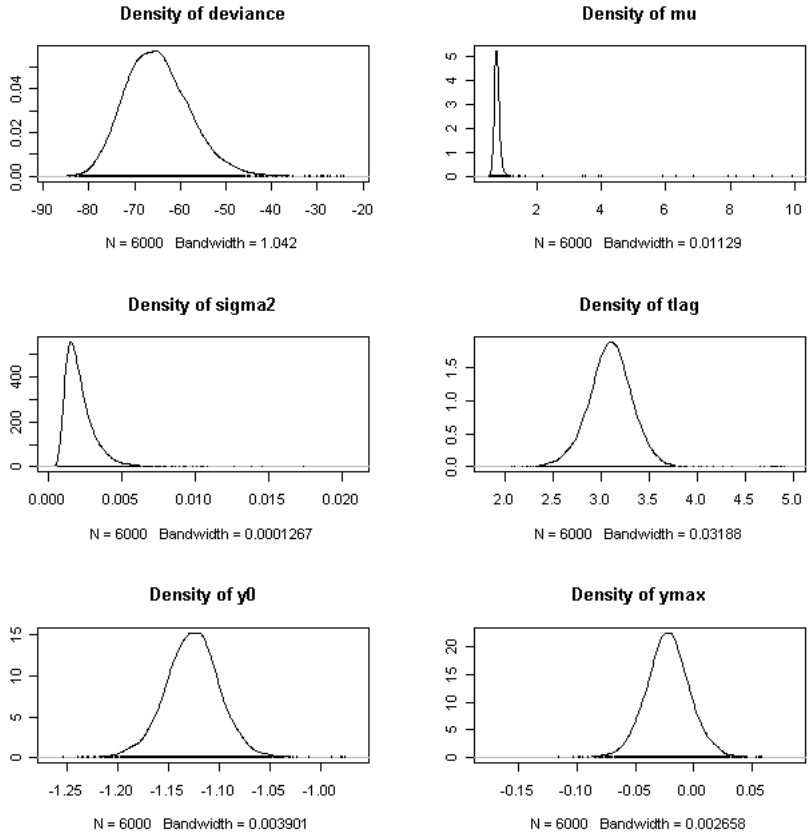

Figure 1.11: Gompertz Model

1.7 Conclusions

In this chapter, we have presented a brief description of the main population growth models, focusing in the advantages and disadvantages of each one. Then

we have shown that given a single sample of data from one of these models, it is straightforward to implement both classical and Bayesian inference for these models. In the following chapter, we shall consider how to extend the basic approach outlined here to the case when various replications of a Petri dish experiment are carried out under identical conditions and we would expect that the information learned from one set of growth curve data is relevant to the prediction of a new growth curve, motivating the use of hierarchical models.

Chapter 2

Hierarchical models for multiple populations

One of the main characteristics of microbiological experiments is that typically, researchers can replicate the same experiment several times under equal conditions. For example, in Petri dish experiments, bacteria are collected and grown in Petri dishes prepared with certain levels of nutrients and it is possible to repeat the same experiment under similar conditions many times. However, up to now, there has been little research on incorporating multiple experimental results into the prediction of bacterial growth under fixed conditions. In this chapter, we shall examine the situation when we observe the growth of $r > 1$ bacteria populations under identical environmental conditions and we shall develop a Bayesian, hierarchical modeling approach for systems of this type.

2.1 Introduction

Growth or longitudinal data consist of repeated observations of a growth process or of a given characteristic over time among a population of individuals. For instance, in medicine, height and weight may be measured for children at consecutive ages to control their development. Other examples are measurements of blood pressure, cholesterol or tumour volume at different moments of time for different patients. In ecology, the mean size of fin fish or shellfish, for instance, are measured at different ages; in biology, animal populations are measured over time, etc. Finally, in microbiological experiments, bacterial growth is observed over time for several experiments undertaken under equal environmental conditions.

In contrast to generalized linear models where the response variable can be assumed to be independent, in the presence of this kind of data, with repeated measurements for each subject, independence is unlikely. These dependencies must be taken into account to correctly model the underlying processes and to this end, various statistical procedures might be considered.

To illustrate in a simple way the different approaches that can be followed, consider the case that repeated measures of a continuous response variable are observed over time for each of m subjects. Let y_{ij} be the measurement of the characteristic observed of individual i at time t_{ij}, for $i = 1, \ldots, m$ and $j = 1, \ldots, n_i$ and n_i be the total number of observations of individual i. For this data we consider three kinds of model.

The first approach assumes a common or pooled mean effect, μ. Assuming a

normal distribution the model can be expressed as:

$$Y_{ij}|\mu,\sigma \sim \mathcal{N}(\mu,\sigma^2) \quad \text{for } i = 1,\ldots,m \text{ and } j = 1,\ldots,n_i. \tag{2.1}$$

Under this model, all observations are assumed to come from a common distribution. However, the assumption that the mean and variance are the same for all individuals may be unrealistic in cases where the population is heterogeneous for example.

A second approach assumes different, independent mean effects, μ_i, for each individual i. The model is:

$$Y_{ij}|\mu_i,\sigma \sim \mathcal{N}(\mu_i,\sigma^2) \quad \text{for } i = 1,\ldots,m \text{ and } j = 1,\ldots,n_i. \tag{2.2}$$

This model estimates the expected performance of each individual. However, each mean effect is independent of the other individuals which does not seem a realistic assumption when the behaviour of one individual is expected to be similar to that of the others.

Finally, a third approach assumes that each mean effect μ_i is a sample from a common population distribution with mean μ, called the population mean effect. A new level of hierarchy is added to the model of (2.2) to give:

$$\mu_i|\mu,w \sim \mathcal{N}(\mu,w^2). \tag{2.3}$$

In this model, the *random effects*, μ_i, are related and we can learn something about one individual observing the others. Therefore, it is possible to obtain more accurate estimations due to *borrowing strength* among individuals and this effect is specially important when we deal with few number of observations for

some of the subjects.

Note also that models with further levels of hierarchy could easily be considered. For example where the mean effect, say μ_{it}, is dependent on time and then we might assume that the mean of μ_{it}, say μ_i, just depends on the individual i, and finally that the individual effects μ_i are distributed around some common mean μ.

2.1.1 Bayesian Hierarchical Modeling

Various approaches to inference for random effects or longitudinal models can be considered. Firstly, classical methods are well reviewed in e.g. Fitzmaurice et al. (2008). A second approach is to consider empirical Bayes methods whereby the so called *hyperparameters*, μ, w of the distribution of μ_i in (2.3) are estimated from the data via e.g. maximum likelihood or method of moments techniques and then the analysis proceeds in a Bayesian way. See e.g. Cassella (1985) for a good introduction to this approach.

In contrast to the empirical Bayes approach, fully *hierarchical Bayesian analyses* can be carried out by specifying *hyperprior* distributions for these hyperparameters.

In our example, the model of (2.2) and (2.3) is completed by adding a *hyperprior* distribution for the *hyperparameters*, μ, w. For example,

$$\mu|w \sim \mathcal{N}\left(0, \frac{w^2}{c}\right) \quad \frac{1}{w^2} \sim \mathcal{G}(a, b). \tag{2.4}$$

Given these prior distributions, inference for the parameters of interest, e.g. μ_i, σ^2

can be carried out by simply integrating out the hyperparameters, for example

$$p(\mu_1, \ldots, \mu_m, \sigma^2|\mathbf{y}) \propto p(\mathbf{y}|\mu_1, \ldots, \mu_m, \sigma^2) \int \int p(\mu_1, \ldots, \mu_m|\mu, w)p(\mu, w)\, d\mu\, dw. \tag{2.5}$$

As is typical in hierarchical models, the distribution in (2.5) does not have a simple form. However, it is easy to see that the conditional distributions, $p(\mu|\mathbf{y}, \ldots, \mu_m, w)$, $p(w|\mathbf{y}, \mu_1 \ldots, \mu_m, \mu)$ and $p(\mu_1, \ldots, \mu_m|\mathbf{y}, \mu, w)$ can all be easily evaluated which implies that inference can be carried out using e.g. a Gibbs sampling type algorithm. Algorithms of this type are now the standard tool for the practical analysis of Bayesian hierarchical models. For a good recent review of Bayesian hierarchical modeling, see e.g. Congdon (2010).

2.2 A hierarchical Gompertz model for bacterial growth

As was presented in the previous chapter, the modified Gompertz equation is a well known model for bacterial growth over time. This model has a sigmoidal shape which reflects the three stages that characterize the bacterial growth process: the lag stage, the exponential stage and the stationary stage. If N_t represents the population size of bacteria cultivated in a Petri dish experiment at time $t \geq 0$, then the modified Gompertz model can be expressed as

$$\begin{aligned} E[N_t|N_0, D, \mu, \lambda] &= N_0 + D \exp\left(-\exp\left(1 + \frac{\mu e(\lambda - t)}{D}\right)\right) \\ &\equiv g(t, N_0, D, \mu, \lambda) \quad \text{say.} \end{aligned} \tag{2.6}$$

where e is the Euler's number, N_0 is the initial bacterial density, D is the maximum possible growth and is equal to the difference between the maximum bacterial density and the initial population density, μ is the maximum growth rate and λ is the time lag.

Now, assume that r bacterial growth experiments under fixed conditions were measured over time. Let N_{ij} be the population density of replication i at time t_{ij}, where $i = 1, \ldots, r$, $j = 0, \ldots, n_i$ and n_i is the total number of observations of replication i.

As was explained previously in Section 2.1, one possible approach to model this kind of process is to assume that the growth curve has the same nature for every experiment or replica. We can represent this by assuming a common model for each growth curve. We call this a pooled model and express this in the following form:

$$E[N_{ij}|N_0, D, \mu, \lambda] = g(t, D, N_0, \mu, \lambda). \tag{2.7}$$

Often it is not possible to fully control all the circumstances under which the experiment of bacteria are carried out and could be appreciable variation among different Petri dishes. Therefore, a disadvantage of this approach is that it does not take into account any specific, unobserved, characteristics of the growth process. A second possibility is to estimate each growth curve independently, following the approach of Section 1.6.1, but this does not take into account the fact that we should expect the different subjects to grow in a similar way under the same conditions. Therefore we propose a a hierarchical modeling approach. Under this approach each population follows its own growth process that is characterized by its own growth parameters but these parameters are considered as a sample from

a common distribution.

Hence, we extend (2.6) to the case of hierarchical Gompertz model. This can be expressed as

$$\begin{aligned} E[N_{ij}|N_{i0}, D_i, \mu_i, \lambda_i] &= N_{i0} + D_i \exp\left(-\exp\left(1 + \frac{\mu_i e(\lambda_i - t_{ij})}{D_i}\right)\right) \\ &\equiv g(t_{ij}, N_{i0}, D_i, \mu_i, \lambda_i). \end{aligned} \tag{2.8}$$

Here, instead of a sampling process that comes from a unique density function, now the growth data of each experiment is produced by a distinct but related mechanism because of the common population density. In other words, each particular experiment grows according to its own Gompertz curve with growth parameters drawn from the common population density. This is a hierarchical model structure as described in the previous section.

In order to complete the basic model, we shall assume that the observations can be expressed as

$$N_{ij} = g(t_{ij}, N_{i0}, D_i, \mu_i, \lambda_i) + \epsilon_{tij}.$$

and will define a normal distribution for the errors.

One possiblility would be to consider independent, identically distributed errors. However, Figure 2.1 illustrates different bacterial growth curves from petri dish experiments under the same conditions (T=42°, pH=7.4 and NaCI=2.5%). It can be seen that the curves are closer together initially when the population density is lower and then diverge over time as the population density grows which suggests that the error variance should increase with population density.

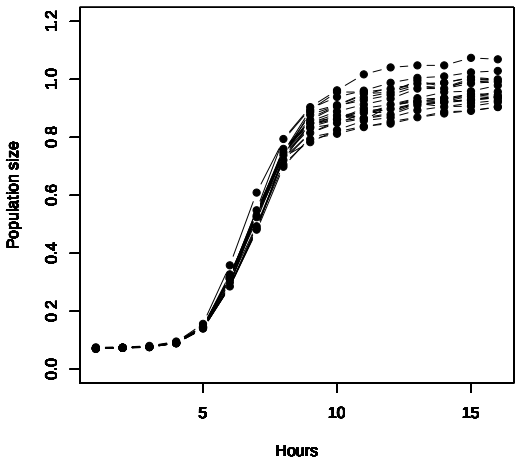

Figure 2.1: Growth curves under fixed environmental conditions: T=42°, pH=7.4 and NaCI=2.5%

Therefore, we shall assume the following model:

$$\epsilon_{tij}|g(t_{ij}), \sigma, p \sim \mathcal{N}\left(0, \sigma^2 g(t_{ij})^p\right) \tag{2.9}$$

where $g(.)$ is the Gompertz function, $\sigma^2 \geq 0$ and $p \geq 0.5$ so that the possibility that the error variance increases with the population size is allowed for.

2.3 Bayesian inference

In order to fit the hierarchical model described in the previous section, one possibility would be to use classical, random effects techniques, but here, we prefer to use a fully Bayesian approach. In microbiology risk assessment is important to distinguish two sources of risk, variability and uncertainty. Uncertainty is defined as the lack of perfect knowledge of some particular value. It may be reduced by additional measurements. Variability represents the true heterogeneity of a population and it can not be reduced by further information or studies. The

bacterial growth process is intrinsically variable: the growth curve observed in a Petri dish may not be equal as that of another experiment even when all growth conditions are the same. The growth process is also uncertain mainly due to that the microbial measurements are imperfect. In a Bayesian approach variability and uncertainty for the growth parameters can be modelled by means of a hierarchical structure and the hyperparameters. Moreover, the Bayesian approach makes it possible to incorporate various sources of previous information such as expert knowledge, or previous empirical results which are typically plentiful in the field of microbiology.

In order to implement Bayesian inference, we must also define distributions for the unknown growth parameters and the hyperparameters. Firstly, we assume the following priors for the growth parameters:

$$\begin{aligned} N_{ij}|N_{i0}, D_i, \mu_i, \lambda_i, \sigma &\sim \mathcal{N}\left(g(t_{ij}, N_{i0}, D_i, \mu_i, \lambda_i), \sigma^2\right) \\ N_{i0}|m_0, s_0 &\sim \mathcal{N}\left(m_0, s_0^2\right) \\ \log D_i|\alpha_D, \tau_D &\sim \mathcal{N}\left(\alpha_N, \tau_N^2\right) \\ \log \mu_i|\alpha_\mu, \tau_\mu &\sim \mathcal{N}\left(\alpha_\mu, \tau_\mu^2\right) \\ \log \lambda_i|\alpha_\lambda, \tau_\lambda &\sim \mathcal{N}\left(\alpha_\lambda, \tau_\lambda^2\right) \end{aligned}$$

where σ^2 is an unknown variance assumed to be common for each growth curve and α_D, τ_D, m_0, s_0, α_μ, τ_μ, α_λ, τ_λ are unknown hyperparameters. We will typically have very good prior knowledge concerning the initial population densities N_{i0}, as the Petri dishes are typically seeded to some theoretical level.

Secondly, we consider an inverse gamma distribution for the model variance σ^2, that is

$$\frac{1}{\sigma^2} \sim \mathcal{G}\left(a, b\right).$$

Small values can be fixed for the parameters a, b to reflect an absence of prior information.

Finally, the prior specification is completed by setting vague, but proper prior distributions for the remaining hyperparameters:

$$\begin{aligned} \alpha_D &\sim \mathcal{N}(m_D, s_D) & \frac{1}{\tau_D^2} &\sim \mathcal{G}(r_D, v_D) \\ \alpha_\lambda &\sim \mathcal{N}(m_\lambda, s_\lambda) & \frac{1}{\tau_\lambda^2} &\sim \mathcal{G}(r_\lambda, v_\lambda) \\ \alpha_\mu &\sim \mathcal{N}(m_\mu, s_\mu) & \frac{1}{\tau_\mu^2} &\sim \mathcal{G}(r_\mu, v_\mu) \end{aligned}$$

where m_D, m_λ, m_μ, s_D, s_λ, s_μ, r_D, r_λ, r_μ, v_D, v_λ and v_μ are assumed known and fixed.

Given the observed data, the likelihood function can be easily derived from (2.9) as:

$$\begin{aligned} f(N_{ij}|N_{i0}, D_i, \mu_i, \lambda_i, \sigma^2) &= \prod_{i=1}^{r}\prod_{j=1}^{n} \frac{1}{\sqrt{2\pi\sigma^2}} \exp\left(-\frac{(N_{ij} - g(t_{ij}))^2}{2\sigma^2}\right) \\ &\propto \exp\left(-\frac{1}{2\sigma^2}\sum_{i=1}^{r}\sum_{t=1}^{n}(N_{it} - g(t_{ij}))^2\right) \end{aligned}$$

where $g(t_{ij})$ is the modified Gompertz equation.

Unfortunately, given the nonlinearity of this model, the joint posterior parameter distribution does not have a simple form and, even the conditional posterior distributions of most of the growth parameters cannot be obtained in a simple closed form. Therefore, Markov-Chain Monte-Carlo (MCMC) techniques must be employed to allow us to generate an approximate Monte Carlo sample from the posterior parameter distributions. As in the previous Chapter, we propose to

use WinBUGS to implement the MCMC sampler. In this case, implementation is carried out in using WinBUGS in combination with R, via the R2WinBUGS package available from

http://cran.r-project.org/web/packages/R2WinBUGS/.

In a similar way to Figure 1.6 in the previous chapter, Figure 2.2 illustrates the dependence structure of the model in WinBUGS style. WinBUGS code can be constructed based on the doodle.

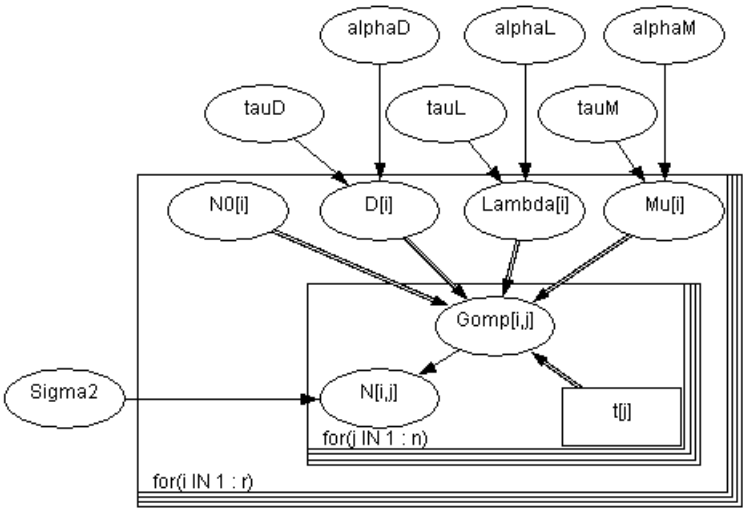

Figure 2.2: Doodle showing the dependence structure of the hierarchical Gompertz model

As WinBUGS is a generic approach to MCMC sampling, it is important to check on the convergence of the sampler. Various tools can be used to check the convergence. In particular, as well as standard graphical techniques such as looking at the trace, the evolution of the mean and the autocorrelations of the sampled output, we also use formal diagnostic techniques such as the modified Gelman-Rubin statistic, discussed in the previous chapter.

For the pooled and the independent models we follow the same approach as before, assuming relatively uninformative log-normal prior distributions for the non-negative Gompertz parameters D, λ and μ, and a vague inverse-gamma prior distribution for σ^2. Inference for these models is also implemented via `WinBUGS`.

2.4 Application: Listeria monocytogenes

In our application the models are fitted to listeria growth curves. Data come from an experiment in broth monoculture where bacteria growth curves were generated at fixed temperature, (42 °), acidity (pH = 7.4) and salt concentration ($2,5\%$ NaCl) levels and measured as optical density. Observations were equally spaced and measurement times were common across replications. The data set consists of 20 curves, each observed at 16 fixed time intervals of one hour are those that we have seen previously in Figure 2.1.

We assume that bacteria grows according to the Gompertz equation of (2.6) and compare the hierarchical, independent and pooled models described earlier in Section 2.2. In order to fit the models, in each case we generated two parallel chains using different initial values with 350000 iterations each, including 250000 iterations of burn-in. To diminish the autocorrelation between the generated values we also used a thinning rate of 10. Trace plots and autocorrelation functions were used to check convergence and in all cases it was found that the burn-in period was reasonable. Furthermore, the Gelman-Rubin statistic was equal o very close to 1, giving a good indicator of convergence.

Table 2.1: Posterior mean parameter estimates and standard deviations in the independent model

Replicate	N_0	sd	D	sd	μ	sd	λ	sd
1	0.07	0.04	0.91	0.10	0.25	0.09	4.98	0.69
2	0.07	0.04	0.95	0.09	0.26	0.09	4.74	0.65
3	0.08	0.04	0.92	0.09	0.25	0.09	4.88	0.67
4	0.07	0.04	0.86	0.09	0.25	0.10	4.87	0.73
5	0.07	0.04	0.93	0.10	0.24	0.09	4.87	0.69
6	0.07	0.04	0.86	0.09	0.25	0.10	4.88	0.71
7	0.07	0.04	0.87	0.09	0.24	0.09	4.80	0.71
8	0.07	0.04	0.87	0.09	0.24	0.09	4.86	0.72
9	0.08	0.04	0.92	0.10	0.24	0.08	4.84	0.69
10	0.07	0.04	1.00	0.10	0.26	0.08	4.93	0.63
11	0.07	0.04	0.91	0.10	0.25	0.09	4.93	0.70
12	0.07	0.04	0.86	0.10	0.23	0.08	4.82	0.76
13	0.07	0.04	0.82	0.10	0.23	0.09	4.88	0.80
14	0.07	0.04	0.84	0.10	0.23	0.09	4.89	0.77
15	0.07	0.04	0.82	0.10	0.23	0.10	4.87	0.80
16	0.07	0.04	0.86	0.10	0.24	0.10	4.95	0.75
17	0.07	0.04	0.86	0.10	0.23	0.09	4.90	0.75
18	0.07	0.04	0.93	0.09	0.26	0.09	4.92	0.65
19	0.07	0.04	0.85	0.09	0.25	0.10	4.91	0.72
20	0.07	0.04	0.89	0.10	0.23	0.08	4.80	0.71
Mean			0.89		0.24		4.88	

Independent model

Table 2.1 summarizes the estimated growth parameters for the independent model. The posterior mean and the standard deviation for each parameter are shown. Comparing the values of the estimated parameters for each curve, we can see the range of variation which indicates that there are significant differences among curves even when the environmental conditions are the same for all the cases. The maximum specific growth rate ranges from 0.23 to 0.26, the lag parameter ranges from 4.74 to 4.98 and the maximum population size ranges from 0.82 to 1.00. The differences between the initial population size are very small, while the maximum observed differences are observed in the maximum population size.

Figure 2.3 shows the fit and the 95 % credible interval for three of the curves (replications 10, 13 and 20).

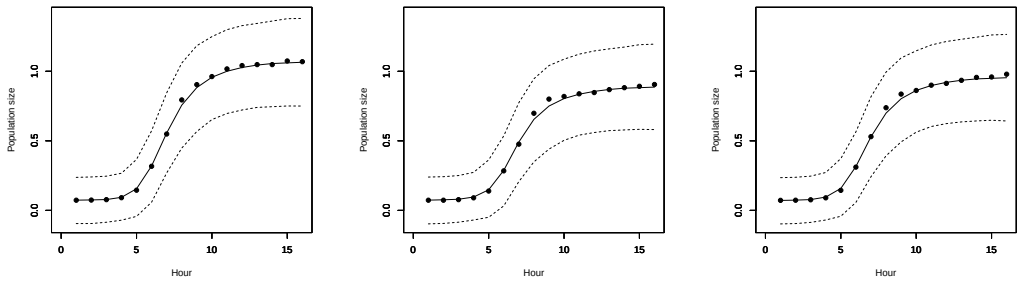

(a) Curve 10 (b) Curve 13 (c) Curve 20

Figure 2.3: Fitted growth curves under the independent model

The fitted mean growth curves are very close to the observed data as we would expect. Nevertheless, the credible intervals for the estimations are not very accurate.

Pooled model

One problem with the independent model is that usually, microbiologists are interested in a predictive curve for a bacterial population under certain environmental conditions. Unfortunately, under the independent model, it is assumed that each for the growth curves is independent of the others, and therefore there is no information from the data to enable us to predict an unobserved growth curve. However, the pooled model does enable us to generate a predictive mean curve.

Table 2.2 shows a summary of the estimated parameters under this model. As we can see, the standard errors of the estimations for all the parameters are

lower with the pooled model compared with the independent one. The reason is that to estimate this growth parameters we use the information from all of the replications in the group because each observed growth curve is assumed to be a sample from a unique growth curve implying that we have a larger sample and therefore reduced uncertainty, leading to increased precision when estimating the unknown parameters. The estimated curve can be interpreted as the mean bacterial growth curve under given environmental conditions.

Table 2.2: Posterior mean parameter estimates and standard deviations in the pooled model

	N_0	D	μ	λ
mean	0.08	0.87	0.23	5.00
sd	0.00	0.01	0.01	0.04

Figure 2.4 shows the fit of the pooled model. The solid line represents the posterior mean and the dashed lines are the 95% credible intervals. Dotted lines are 3 of the replications, curve 10, curve 13 and curve 20. Some observations from curve 10 fall outside of the credible interval. As expected, the posterior mean curve can be seen as the mean of the observed curves, but fails to describe the exact behaviour of each individual curve.

Hierarchical model

The summary of the estimated parameters with the hierarchical model are presented in Table 2.3. The posterior mean and standard deviation of the estimated parameters of each curve are shown and also for the population parameters. The estimated parameter values for each curve are very similar to those obtained

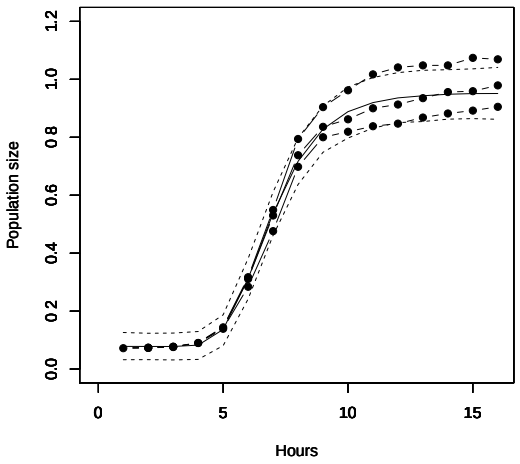

Figure 2.4: Fit of the Pooled model

with the independent model. However, the standard errors are significantly lower for the hierarchical model. To summarize the behaviour of the bacterial growth with the given environmental growth we can use the estimated population growth parameters.

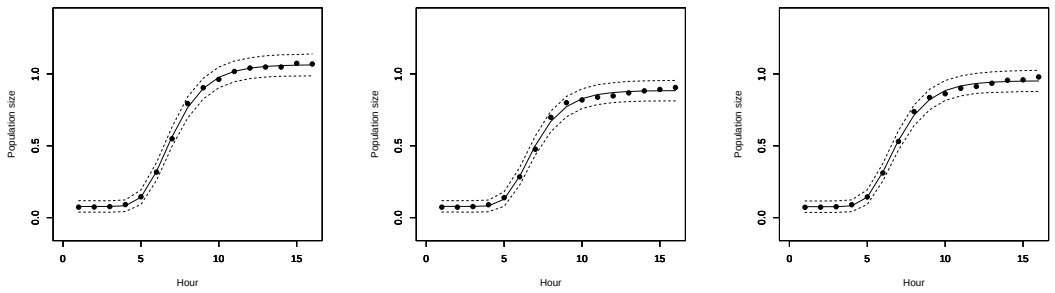

(a) Curve 10 (b) Curve 13 (c) Curve 20

Figure 2.5: Fitted Growth curves under the hierarchical model

To compare the parameter estimations of the different models, the main results for the parameters modeled with hierarchical structure are included in Table

Table 2.3: Posterior mean parameter estimates and standard deviations in the hierarchical model

Replicate	N_0	sd	D	sd	μ	sd	λ	sd
1	0.08	0.01	0.90	0.02	0.24	0.02	5.08	0.14
2	0.08	0.01	0.94	0.02	0.25	0.02	4.83	0.14
5	0.08	0.01	0.92	0.02	0.23	0.02	4.97	0.15
6	0.08	0.01	0.85	0.02	0.24	0.02	4.99	0.14
7	0.08	0.01	0.86	0.02	0.23	0.02	4.92	0.15
8	0.08	0.01	0.86	0.02	0.23	0.02	4.98	0.15
9	0.08	0.01	0.91	0.02	0.23	0.02	4.95	0.15
10	0.08	0.01	0.99	0.02	0.25	0.02	5.01	0.14
11	0.08	0.01	0.89	0.02	0.24	0.02	5.05	0.14
12	0.08	0.01	0.85	0.02	0.22	0.02	4.97	0.15
13	0.08	0.01	0.81	0.02	0.22	0.02	5.03	0.16
14	0.08	0.01	0.82	0.02	0.22	0.02	5.04	0.16
15	0.08	0.01	0.80	0.02	0.22	0.02	5.03	0.16
16	0.08	0.01	0.85	0.02	0.23	0.02	5.07	0.15
17	0.08	0.01	0.84	0.02	0.22	0.02	5.05	0.15
18	0.08	0.01	0.92	0.02	0.24	0.02	4.99	0.14
19	0.08	0.01	0.84	0.02	0.24	0.02	5.03	0.15
20	0.08	0.01	0.88	0.02	0.23	0.02	4.93	0.15
Population mean (α_i)			0.92	0.07	0.25	0.02	5.23	0.39
Population sd (τ_i)			0.32	0.05	0.09	0.00	1.78	1.48

2.4. The posterior mean and the 95% credible interval for the population growth parameters are shown for the full hierarchical model, the mixed model and the pooled model. Moreover, for the first two models and for the independent one, individual parameters are shown for curves 10, 13 and 20 - the same curves represented graphically before. When comparing among the individual parameter estimations between the independent model and the hierarchical models, it can be seen that there are small differences. However, if we look at the credible intervals it is possible to see that in hierarchical models the estimations are more precise. Regarding the population parameters, we observe some differences between the estimated parameters values between the pooled model and the hierarchical models. But, the credible intervals of the hierarchical models include the estimated

Table 2.4: Parameter estimations

	D		**Mu**		**Lambda**	
	mean	95%	mean	95%	mean	95%
Independent model						
Curve 10	1.00	(0.83 1.22)	0.26	(0.14 0.50)	4.93	(3.53 6.10)
Curve 13	0.82	(0.66 1.05)	0.23	(0.10 0.49)	4.88	(2.97 6.27)
Curve 20	0.89	(0.73 1.12)	0.23	(0.11 0.47)	4.80	(3.15 6.08)
Hierarchical model						
Curva 10	0.99	(0.95 1.03)	0.25	(0.22 0.28)	5.01	(4.74 5.28)
Curva 13	0.81	(0.77 0.84)	0.22	(0.18 0.26)	5.03	(4.70 5.35)
Curva 20	0.88	(0.84 0.91)	0.23	(0.19 0.26)	4.93	(4.63 5.22)
Population	0.92	(0.80 1.08)	0.25	(0.21 0.29)	5.23	(4.53 6.08)
Pooled model						
Population	0.87	(0.86 0.88)	0.23	(0.22 0.24)	5.00	(4.90 5.08)

values with the former model.

Prediction

To asses the predictive capacity of the models, we consider two types of predictions: one and various step ahead predictions for a given curve, and the prediction of a new curve. Firstly, consider the case where the first 19 curves are fully observed and where only the first 6 values of the 20th curve are observed, so that we can try to predict the trajectory of the rest of the growth curve. Figure 2.6 shows the predictive curves for the hierarchical and pooled models respectively. The predictive curve for the hierarchical model is more accurate than the one for the pooled model. Moreover, when computing the mean squared error between the predictive curve and the real curve, the value for the former model is equal to 0.0020 while for the later is equal to 0.0042. In general, the more the growth process differs from the mean, the better the hierarchical model performs in comparison with the pooled model.

Now, we will consider the case of prediction for a new curve, $\widetilde{J}$ which at the beginning has not been observed at all. The procedure is as follows. First, having observed the previous 19 curves, we will predict the cell density of the new curve at $t = 0$. Then, given the true value of the bacteria density at that time, we predict the following value, that is the cell density at $t = 1$. After that, we observed the first two points and predictive the population density at $t = 3$ and so on. Figure 2.7 shows the predictive curves for a new experiment for the hierarchical model and the pooled model, respectively.

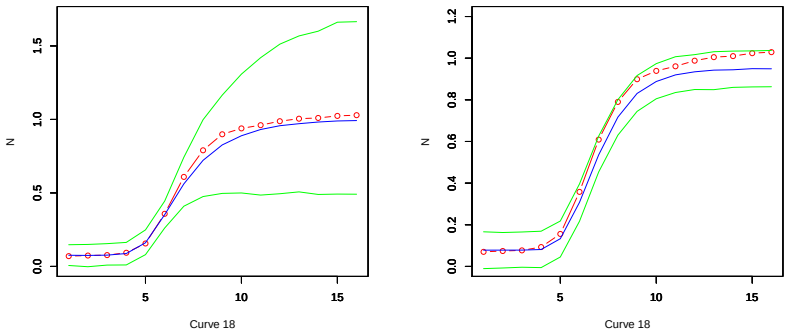

(a) Hierarchical model (b) Pooled model

Figure 2.6: The predictive mean curve for future observations

Once again, the hierarchical model outperforms the pooled model with the predicted curve being very close to the true curve. The mean square error of the predictions are equal to 0.0006 and 0.0040, for the hierarchical and the pooled model respectively, being significantly lower for the hierarchical model.

Finally, if we want to answer the previously mentioned questions of the microbiologists with the models presented here we have two possibilities. The first one is to use the posterior predictive distribution of the pooled model. The mean curve was represented in Figure 2.4. The second possibility is to use the hierarchical model: with the posterior distribution of the population parameters (learned from the observed curves) in combination with the prior distribution of the in-

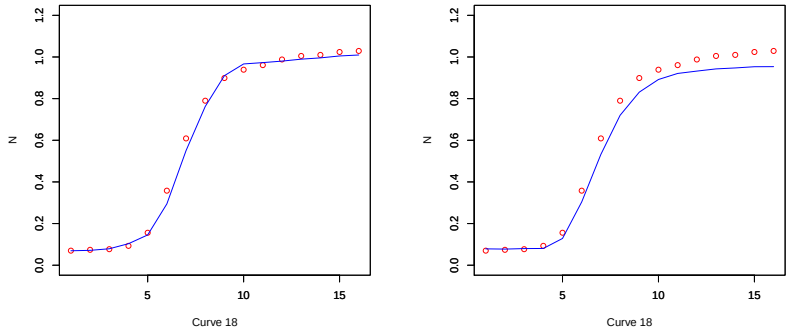

(a) Hierarchical model (b) Pooled model

Figure 2.7: Predictive Future Experiment

dividual parameters it is possible to derive a posterior predictive distribution for the new curve. Calling $\boldsymbol{\theta}$ the vector of individual growth parameters and $\boldsymbol{\phi}$ the vector of population parameters, the predictive distribution is equal to

$$p(\boldsymbol{y}_{new}|\boldsymbol{y}_{obs}) = \int_{\boldsymbol{\theta}} \int_{\boldsymbol{\phi}} p(\boldsymbol{y}_{new}|\boldsymbol{\theta}) p(\boldsymbol{\theta}|\boldsymbol{\phi}) p(\boldsymbol{\phi}|\boldsymbol{y}_{obs}) d\boldsymbol{\theta} d\boldsymbol{\phi}$$

A sample from that distribution can be easily obtained from the MCMC previously generated.

Table 2.5: Predictive mean values at each time.

Hour	1	2	3	4	5	6	7	8
HM	0.07	0.07	0.07	0.09	0.16	0.33	0.53	0.70
PM	0.08	0.08	0.08	0.08	0.14	0.31	0.54	0.72
Hour	9	10	11	12	13	14	15	16
HM	0.81	0.87	0.91	0.93	0.94	0.95	0.95	0.95
PM	0.83	0.89	0.92	0.94	0.94	0.95	0.95	0.95

Figure 2.8 shows the predictive mean curve and the 95% credible interval. Dotted points represent the various curves observed under the given fixed envi-

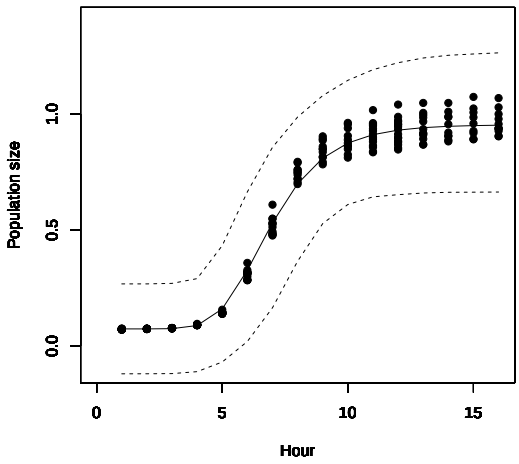

Figure 2.8: Predictive mean curve of a new replication

ronmental conditions. The estimated predictive curve is a good representation of the mean behaviour of the bacterial growth process. The mean curve is very similar to the mean curve of the pooled model (Table 2.5 shows the estimated mean values of the curve for each time). Nevertheless, in contrast with the former model, here all the curves lie inside the credible intervals. Finally, the posterior mean of the growth parameters are very closed to those estimated with the pooled model (see Table 2.6).

Table 2.6: Posterior mean of the growth parameters.

	N_0	D_{max}	μ	λ
Pooled	0.08 (0.00)	0.87 (0.01)	0.23 (0.01)	5.00 (0.04)
Hierarchical	0.07 (0.10)	0.88 (0.12)	0.24 (0.03)	4.99 (0.67)

The better performance of the hierarchical model with respect to the pooled and the independent model regarding both, fitting and prediction, is also supported by the DIC and the MSE values. Table 2.4 shows that the hierarchical model has a lower MSE indicating the goodness of fit but also a lower DIC which

also penalizes for model complexity.

	DIC	MSE
IM	-646.23	1.98
HM	-1489.62	0.02
PM	-1326.01	0.05

2.5 Conclusions

In this chapter, we have illustrated that hierarchical models can be used to model bacterial growth functions when several replications of the same experiment under equal environmental conditions such as temperature, acidity level and salt concentration are available. Various simpler models, keeping some of the growth parameters fixed, are also suitable.

A number of extensions to this approach are possible. Firstly, in this chapter we have extended the modified Gompertz equation to the case of a hierarchical model, but the approach is equally applicable to other bacterial growth models such as the logistic or Baranyi models. Furthermore, it can also be applied to the cases where we assume no parametric growth model and instead use a nonparametric approach. Finally, in the present study we have considered experiments under fixed environmental conditions. A natural extension of this work is to consider modeling what happens at different levels of the environmental conditions. These last two situations will be considered in the following chapters of this thesis.

Chapter 3

Neural networks models

3.1 Introduction

In the previous chapter we have seen how to model and the predict the bacteria growth process when environmental conditions are fixed. Nevertheless, in reality, these external factors are not fixed. For instance, food products are affected by different factors depending on environmental conditions in the production, distribution, storage and consumption stage. Shelf life is determined by the evolution and growth of the micro-organisms which can spoil the product and cause pathogenic effects. The aim of predictive microbiology is to know which environmental factors most influence the growth processes of micro-organisms in food. The relationships between these factors are complex, interactive and dynamic and therefore, it is important to develop secondary bacterial growth models to predict the shelf life of perishable foods or the behaviour of food borne pathogens.

In this chapter, we shall start by briefly summarizing the most popular secondary models and then propose two different approaches based on the use of

neural network techniques. The first model is based on the Gompertz function where the dependence of the growth parameters on the environmental factors is modeled by a neural network. Secondly, we shall consider a direct, non-parametric approach based on the use of neural networks as a primary growth model. An important feature of our approaches is that in cases where we observe bacterial growth in various colonies under possible different environmental conditions, we use hierarchical modeling, as in Chapter 2, to improve the estimation of a single growth curve by incorporating information from the various different bacterial populations.

As in the previous chapter, inference for our models is undertaken throughout using a Bayesian approach. One of the main problems with inference for neural networks models was that typically, complicated inference algorithms need to be designed and a great deal of tuning often needs to be carried out for these to work efficiently, see e.g. Lee (2004). Here, however, we show that inference can be still be carried out using WinBUGS.

3.2 Secondary models

Primary models for growth curve typically assume some parametric form, e.g. the Gompertz curve for the growth model under specific environmental conditions. It is natural however to suppose that growth will typically be different under different environmental conditions and this can be done by allowing the model parameters to vary depending on these conditions. Models for this variation in parameters are called secondary models and some of the most important of these are are outlined below.

3.2.1 The square-root model

Ratkowsky et al. (1982) suggested a simple empirical model that describe the effect of suboptimal temperature on growth rates of micro-organisms. Before fitting the model to experimental growth rates, data is transformed taking the square root in order to stabilize the variance and for this reason this model and their future extensions are called square-root models. Suppose that μ_{max} is the maximum growth rate of a bacterium under optimal temperature conditions. Then the basic square root model supposes that:

$$\sqrt{\mu_{max}} = b(T - T_{min}) \tag{3.1}$$

where b is a constant and T_{min} is a parameter which indicates the minimum temperature at which growth can occur. From growth curve observed at different temperature levels, the parameters b and T_{min} can be estimated by classical model fitting techniques. This first equation was expanded to include the effect of other factors besides temperatures, such as water activity, acidity level, salinity level, etc. The extended version which describes the combined effect of temperature and other factors can be expressed as

$$\sqrt{\mu_{max}} = b(T - T_{min})\sqrt{X - X_{min}} \tag{3.2}$$

where b and T_{min} are as previously defined, X is another factor different from T such as water activity or level of acidity (pH) and X_{min} is the minimum level of the that factor below which growth is not possible. These models are simple, easy to interpret and use few parameters. Each term expresses how an environmental factor changes the growth rate of a micro-organism. However, as pointed out in McKellar and Lu (2004), in these models, the expected multidimensional growth

space is not influenced by the levels of the different environmental parameters. Thus, for instance, the level of acidity influences the range of pH values for which growth is theoretically observed.

3.2.2 Cardinal parameter models

Cardinal parameter models (CPMs) rely on the assumption that the inhibitory effect of the environmental factors is multiplicative. This idea was formalized in the gamma concept introduced in Zwietering et al. (1992). Under optimal conditions a micro-organism has a maximum growth rate, but when any environmental factor becomes suboptimal the growth rate declines and the extent of that inhibition depends on the rate between the test condition compared to that at the optimum. Thus, a CPM consists of a discrete term for each environmental factor, where each term is the growth rate relative to that when that factor is optimal. An extensive CPM developed for growth of Listeria monocytogenes, includes the effect of temperature (T), water activity (a_w), acidity level (pH), inhibitory substances (c_i), and qualitative factors (k_j) on μ_{max} and can be expressed as:

$$\mu_{max} = \mu_{opt}\tau(T)\rho(a_w)\alpha(pH)\prod_{i=1}^{I}\gamma(c_i)\prod_{j=1}^{J}k_j \tag{3.3}$$

where $\tau = CM_2$, $\rho = CM_1$ and $\alpha = CM_2$ with

$$CM_n = \begin{cases} 0 & \text{if } X \leq X_{min} \\ \frac{X_{opt}-X_{min})^{1-n}(X-X_{max})(X-X_{min})^n}{([(X_{opt}-X_{min})(X-X_{opt})-(X_{opt}-X_{max})((n-1)X_{opt}+X_{min}-nX)]} & \text{if } X_{min} < X < X_{max} \\ 0 & X \geq X_{max} \end{cases}$$

$$\gamma(c_i) = \begin{cases} (1 - c_i/MIC_i)^2 & \text{if } c_i < MIC_i \\ 0 & \text{otherwise} \end{cases}$$

where X is the temperature, water activity or pH, X_{min} and X_{max} are the values of the factor X below and above which growth impossible, X_{opt} is the value at which μ_{max} is equal to its optimal value μ_{opt} and MIC_i the minimal inhibitory concentration of specific compounds above which no growth occurs.

Cardinal models assume that different environmental factors have independent and multiplicative effects on μ_{max}. The assumption of independence might not be reasonable in all cases. As is pointed out in McKellar and Lu (2004) numerous studies have shown that the growth range of a micro-organism in one environmental condition is affected by other environmental conditions.

3.2.3 Polynomial models

Polynomial models, also called response surface models, are probably the most common secondary model. These kinds of models are relatively easy to fit by using multiple linear regression techniques. Polynomial models are able to incorporate different environmental factors and their interactive effects in a simple way. The model can be expressed as:

$$\theta = \beta_0 + \sum_{j=1}^{k} \beta_j X_j + \sum_{j=1}^{k} \beta_{jj} X_j^2 + \sum_{j<l} \sum_{l=2}^{k} \beta_{jl} X_j X_l \tag{3.4}$$

where θ is the response variable, for instance a parameter of the primary growth rate model, β_j, β_{jj} and β_{jl} are the parameters of the model and the X_i are the environmental factors such as temperature, salinity level, acidity level, etc. One of the main criticisms of the polynomial models is that they have a high number of parameters without biological interpretation that make difficult to compare this kind of model with other secondary models.

3.2.4 Artificial neural network models

Square-root models, cardinal parameter models and polynomial models all have several versions depending on the micro-organisms, the environmental factors included, the quantity of factors, the growth parameters which we want to explain (growth rate, lag parameter, the maximum population size), etc. Due to the long list of parametric models, it is possible to talk about model uncertainty. Which model is the best? More recently artificial neural networks (ANNs) have been proposed as a way to model complex non-linear systems (see e.g. Hajmeer et al. (1997), Geeraerd et al. (1998) and García-Gimeno et al. (2002)). Neural networks, in statistical terms, are non-parametric models, as opposed to the parametric models we have used earlier, which are characterized by a small number of parameters, which often have a meaningful interpretation. Although neural network models lose this easy interpretation, the advantages of neural networks are their capability to describe very complex non-linear relationships and that they do not impose any structure on the relationship between the interacting effects.

3.3 Neural network based growth curve models

In this section we give a brief presentation of artificial neural networks. We will focus on feed forward neural networks, which are the most popular and widely used network in many applications. Then we shall present two neural network based models for bacteria growth, the first of which is a secondary model where the parameters of the Gompertz curve are related to environmental factors using ANNs and the second of which is a primary neural network model where no specific form for the basic growth curve is presupposed.

3.3.1 Feed forward neural networks

Assume that there are q dependent variables, $(Y_1, \ldots, Y_q) = \mathbf{Y}$, and a set of explanatory variables, $(x_1, \ldots, x_p) = \mathbf{x}$. Often, the relationship between $\mathbf{Y}$ and $\mathbf{x}$ is modeled by assuming a simple relationship such as e.g. multivariate regression. However, such a relationship may not always be appropriate and often, a more general functional relation between the dependent and independent variables must be assumed, say

$$E[\mathbf{Y}|\mathbf{x}] = \mathbf{g}(\mathbf{x})$$

where the functional form, $(g_1, \ldots, g_q) = \mathbf{g} : \mathbb{R}^p \to \mathbb{R}^q$, is unknown.

One of the most popular methods of modeling the function $\mathbf{g}$ is via neural networks, see e.g. Stern (1996). In particular, a *feed forward neural network* takes a set of inputs $\mathbf{x}$, and from them computes the vector of output values as follows

$$\mathbf{g}(\mathbf{x}) = \boldsymbol{B} \cdot \boldsymbol{\Psi}^T(\mathbf{x}^T\boldsymbol{\Gamma}) \tag{3.5}$$

where $\boldsymbol{B}$ is a $q \times M$ matrix with $q \in \mathbb{N}$ the number of output variables and $M \in \mathbb{N}$ the number of nodes and $\boldsymbol{\Gamma}$ is a $p \times M$ matrix with $p \in \mathbb{N}$ being the number of explicative variables. The element $\gamma_{rk} \in \mathbb{R}$ is the weight of the connection from input r to hidden unit k and the element $\beta_{sk} \in \mathbb{R}$ is the weight connection from hidden unit k to output unit s. Finally, $\boldsymbol{\Psi}(a_1, \ldots, a_M) = (\Psi(a_1), \ldots, \Psi(a_M))$ where Ψ is a sigmoidal function such as the logistic function

$$\Psi(x) = \frac{exp(x)}{1 + exp(x)}, \tag{3.6}$$

which we will use here. Equations (3.5) and (3.6) define a feed forward neural network with a logistic activation function, p explanatory variables (inputs), one

hidden layer with M nodes and q dependent variables (outputs) that is illustrated in Figure 3.1. Note that each output in the neural network combines the node values in a different way.

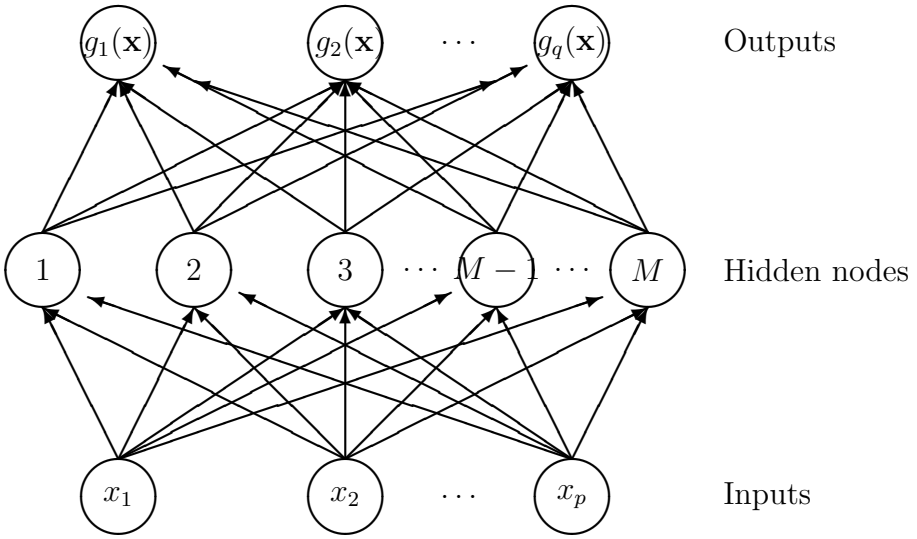

Figure 3.1: Neural network representation

Several features of neural networks make them valuable and attractive for predictive microbiology, where the environmental conditions that affect growth are complex and poorly understood. First, ANNs have few prior assumptions about the models for the problem studied. The network can learn from data and capture subtle functional relationships even if the underlying relationships are unknown or very complex to describe. Thus, ANNs are particularly useful when there is little knowledge about the underlying laws governing the systems from which data is generated but for which there are enough data or observations. ANNs can also be used for prediction. After learning from data, an ANN can often give good inferences about the unseen part of a population, such as prediction of the future behaviour from knowing the past. Finally, ANNs are universal functional approximators, meaning that a network can approximate any continuous function

to any desired accuracy. ANNs have more general and flexible functional forms which make possible to model very complex nonlinear systems. ANNs can deal with nonlinear modeling without a priori assumptions about the relationships between input and output variables.

Standard secondary growth curve models commented previously may not capture the complex relationships and interactions between growth and external factors such as temperature, pH or salt levels. Therefore, here we propose to use neural networks to model the complex system of interactions between environmental factors. In particular, we shall consider two neural network based models, the first of which is a secondary model based on the Gompertz equation and the second of which is a primary neural network model.

3.3.2 A neural network based Gompertz model

As we have commented previously, the Gompertz equation, has been used extensively by researchers to fit a wide variety of growth curves from different microorganisms. However, the primary growth model described in Equation (2.6) does not allow for the case where we wish to study bacterial populations under a variety of controlled environmental conditions. Therefore, suppose that we observe the growth of I bacterial populations under similar initial conditions and that we have J different environments determined by temperature, level of acidity (pH) and salt concentration (NaCI). Now, because we want to know how the growth process is affected by different external conditions, it may be reasonable to assume that all replications have the same growth curve parameters under fixed environmental conditions. However, growth rates will vary under different conditions and therefore, assuming a Gompertz model, we propose the use of neural networks to reflect the parameter dependence on the environmental factors. If

N_{tij} is the concentration in population i under environmental conditions j at time t the Gompertz function is

$$E[N_{tij}|N_{0j}, D_j, \mu_j, \lambda_j] = g(t_{ij}, N_{0j}, D_j, \mu_j, \lambda_j), \tag{3.7}$$

where $g(\cdot)$ is as in (2.7), for $i = 1, \ldots, I$ and $j = 1, \ldots, J$. Now, we model the growth parameters μ, λ and D as a function of the temperature, the level of acidity and the salt concentration by a feed forward neural network, that is

$$\boldsymbol{\theta}_s = \sum_{k=1}^{M} \beta_{sk} \cdot \Psi(\mathbf{x}'\boldsymbol{\gamma}_k), \quad \text{for } s = 1, 2, 3. \tag{3.8}$$

where $\boldsymbol{\theta}_s$ represents the parameters (D, μ, λ) and $\mathbf{x} = (T, pH, NaCI)$ is the vector of explanatory variables representing the environmental conditions and Ψ is the logistic function, so that

$$\Psi(x) = \frac{1}{1 + \exp(-x)}.$$

From now on, the model defined by (3.7) and (3.8) will be referred to as the GNN model.

3.3.3 A hierarchical neural network model

Here, we generalize the previous model to a new one which does not assume any underlying parametric growth function. Instead, we propose the use of a neural network as a primary model. The output of the network is the instantaneous reproduction rate per member of the population and the inputs are the current population size and the experimental conditions. Formally, we can write this

model as

$$E[N_{tij}|N_{(t-1)ij}, f_j, T_j, pH_j, NaCl_j] =$$
$$N_{(t-1)ij} + N_{(t-1)ij} f_j(N_{(t-1)ij}, T_j, pH_j, NaCI_j) \tag{3.9}$$

$$f_j(N_{(t-1)ij}, T_j, pH_j, NaCI_j) =$$
$$\sum_{k=1}^{M} \beta_{jk}(\Psi(\gamma_{1k} N_{(t-1)ij} + \gamma_{2k} T_j + \gamma_{3k} pH_j + \gamma_{4k} NaCI_j)$$
$$-\Psi(\gamma_{2k} T_j + \gamma_{3k} pH_j + \gamma_{4k} NaCI_j)), \tag{3.10}$$

for $i = 1, \ldots, I$ and $j = 1, \ldots, J$, $f_j(\cdot)$ is the growth rate for populations with environmental condition j. From now on, the model defined by (3.9) will be referred to as the NN model.

3.3.4 Error modeling

In the previous subsections, two approaches to modeling the expected population density have been provided. These models are completed by including an error term. We might consider using independent, identically distributed errors, but, in a similar way to (2.9) in the previous chapter it would appear more reasonable to assume that the error variance increases with population size.

Therefore, in the case of the GNN model, we assume that the error term is

$$\epsilon_{tij}|gt_{ij}, \sigma, p \sim \mathcal{N}\left(0, \sigma^2 g(t_{ij})^p\right) \tag{3.11}$$

where $g(.)$ is the Gompertz function as in (2.9).

In the case of the NN model, we assume that

$$N_{tij} = N_{(t-1)ij} + N_{(t-1)ij} f_j(N_{(t-1)ij}, T_j, pH_j, NaCI_j) + \epsilon_{tij} \tag{3.12}$$

where we assume that the error term is

$$\epsilon_{tij} | N_{(t-1)ij}, \sigma, p \sim \mathcal{N}\left(0, \sigma^2 N_{t-1}^p\right). \tag{3.13}$$

Note in particular that for $p > 0$, this error structure implies that if $N_{(t-1)ij} = 0$, then $N_{tij} = 0$, so that once the population has died out, then it remains extinct.

3.4 Bayesian inference for the neural network models

Typically, when fitting secondary models using classical statistical procedures, a two-stage procedure is carried out. In the first stage, a primary model is fitted to the observed data in order to get the estimated growth parameter values under each set of environmental conditions. The second stage then involves fitting a secondary model to these using the sets of estimated parameters as data. These two steps are usually not linked, which means that the uncertainty of the first step is not taken into account in the second step. However, in a Bayesian context, inference can be carried out directly using a one-step procedure.

Regarding fitting of neural networks, given a set of observed inputs and outputs, say $D = (x_1, y_1), \ldots, (x_N, y_N)$, inference can be carried out using a variety of approaches, see e.g. Neal (1996) and Fine (1999) for reviews. Here, we shall consider a Bayesian approach which allow an overall fitting of the primary and

the secondary models.

In order to implement such an approach, we must first define suitable prior distributions for the neural network parameters β and γ and for the uncertainty. Firstly, we suppose little prior knowledge concerning the variance and hence we propose a vague, inverse-gamma, prior distribution for it $\sigma^{-2} \sim \mathcal{G}(a/2, b/2)$. In neural network models is common to use relative uninformative prior distributions due to the scarcity of prior information about the parameters. For simplicity we choose hierarchical prior structures, as follows:

$$\begin{aligned} \beta_{ik}|m_{i\beta}, \sigma_\beta^2 &\sim \mathcal{N}\left(m_{i\beta}, \sigma_\beta^2\right) \\ \boldsymbol{\gamma}_k|m_\gamma, \sigma_\gamma^2 &\sim \mathcal{N}\left(\boldsymbol{m}_\gamma, \sigma_\gamma^2 I\right), \end{aligned}$$

where the subscript i in the GNN model accounts for the growth parameters and, in the NN model for the groups defined by the environmental conditions. The Bayesian approach is completed by vague, but proper prior distributions for the remaining hyperparameters as follows:

$$\begin{aligned} m_{i\beta}|\sigma_\beta^2 &\sim \mathcal{N}\left(m_{0\beta}, \frac{\sigma_\beta^2}{c_\beta}\right) \\ m_{0\beta}|\sigma_\beta^2 &\sim \mathcal{N}\left(0, \frac{\sigma_\beta^2}{e_\beta}\right) \\ \frac{1}{\sigma_\beta^2} &\sim \mathcal{G}\left(\frac{d_{\beta 1}}{2}, \frac{d_{\beta 2}}{2}\right) \\ \boldsymbol{m}_\gamma|\sigma_\gamma^2 &\sim \mathcal{N}\left(\mathbf{0}, \frac{\sigma_\gamma^2}{c_\gamma} I\right) \\ \frac{1}{\sigma_\gamma^2} &\sim \mathcal{G}\left(\frac{d_{\gamma 1}}{2}, \frac{d_{\gamma 2}}{2}\right), \end{aligned}$$

where $c_\beta, e_\beta,\ d_{\beta 1},\ d_{\beta 2},\ c_\gamma,\ d_{\gamma 1}$ and $d_{\gamma 2}$ are assume known and fixed. Similar hierarchical prior distributions are typically used in Bayesian inference for neural network models, see e.g. Lavine and West (1992), Müller and Insua (1998) and

Andrieu et al. (2001). For alternatives, see e.g. Lee (2004), Robert and Mengersen (1999) and Roeder and Wasserman (1997).

Given the above prior structure, a closed form for the posterior parameter distributions is not available. However, Markov-Chain Monte-Carlo (MCMC) techniques can be employed to allow us to generate an approximate Monte Carlo sample from the posterior parameter distributions, see e.g. Gilks et al. (1996) for a full review. Various different MCMC algorithms have been proposed in the neural networks literature, but in general the efficiency of such samplers depends on the model, see e.g. Lee (2004). MacKay (1995b) uses a Gaussian approximation for the posterior distribution of the networks parameters and single values estimates for the hyperparameters. This method was useful in some practical applications but Neal states that not always these approximations are close to the true result implied by the model. Neal (1996) introduces a hybrid Monte Carlo method combining ideas from simulated annealing and Metropolis algorithm. Muller and Rios Insua (1998) introduce an efficient MCMC algorithm based on partial marginalization over the weights of the network and blocking (all weights are jointly resampled). As an alternative, we propose using `WinBUGS` in conjunction with `R2WinBugs`.

Figure 3.2 illustrates the dependence structure of the NN model in `WinBugs` style (although code cannot be constructed directly from this diagram).

As we have noted previously, `WinBugs` is a generic approach to MCMC sampling. Therefore, it is important to check on the convergence of the sampler and to do this we use both informal trace plots and diagnostics as commented in the previous chapters.

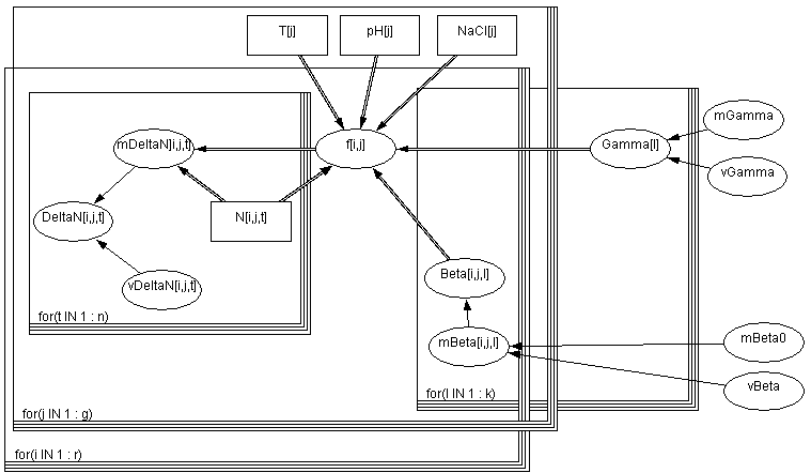

Figure 3.2: Dependence structure of the NN model

3.4.1 Model selection

Thus far, inference is conditional on the number of hidden nodes, M, being unknown. Various approaches to estimating M may be considered. One possibility is to treat M as a variable and given a prior distribution for M, use variable dimensional MCMC approaches to carry out inference, see e.g. Müller and Insua (1998) or Neal (1996). An alternative which we shall employ here, is to use an appropriate model selection technique to choose the value of M.

A number of criteria have been proposed for model selection in Bayesian inference. A standard, Bayesian selection criterion which is particularly appropriate when inference is carried out using MCMC methods is the deviance information criterion (DIC), as proposed in Spiegelhalter et al. (2002). However, in the context of neural networks, the possible lack of identifiability of the model or multimodality of the posterior densities make this criterium unstable. Many variants of the DIC have also been considered and here, we prefer to apply the DIC_3 criterion of Celeux et al. (2006). For a model $\mathcal{M}$ with parameters $\boldsymbol{\theta}$ and observed

data $\mathbf{y}$ the DIC_3 is defined as follows:

$$DIC_3 = -4E_{\boldsymbol{\theta}}[\log f(\mathbf{y}|\boldsymbol{\theta})|\mathbf{y}] + 2\log \prod_{i=1}^{n} E_{\boldsymbol{\theta}}[f(y_i|\boldsymbol{\theta}, \mathbf{y})].$$

In Celeux et al. (2006) this criterion is recommended in the context of latent variable models.

An alternative approach which we also consider when comparing different models is the posterior predictive loss performance (PPLP) proposed by Gelfand and Ghosh (1998). Based on the posterior predictive distribution, this criterion consists in defining a weight loss function which penalizes actions for departure from the corresponding observed value as well as for departure from what we expect the replication to be. In this way, the approach is a compromise between the two types of departures: fit and smoothness. Under squared error loss, the criterion becomes

$$PPLP = \frac{k}{k+1} \sum_{i=1}^{n} (m_i - y_i)^2 + \sum_{i=1}^{n} s_i^2$$

, where $m_i = E[y_i^{rep}|\mathbf{y}]$ and $s_i^2 = Var[y_i^{rep}|\mathbf{y}]$ are, respectively, the mean and the variance of the predictive distribution of y_i^{rep} given the observed data $\mathbf{y}$ and k is the weight we assign to departures from the observed data. The first term of the $PPLP$ is a plain goodness-of-fit term and the second term penalizes complexity and rewards parsimony.

3.5 Application: Listeria monocytogenes

In this section we analyze the same data set studied in the previous chapter, but now we incorporate new curves observed under several experimental conditions.

The environmental factors taken into account are temperature, level of acidity and salinity. Temperatures range between 22°C and 42°C, pH between 4.5 and 7.4 and NaCI between 2.5% and 5.5%. In order to facilitate the fitting of the neural network models, temperature, pH and NaCI were all scaled to take values in $[0.1, 0.9]$.

There are 96 different combinations of environmental factors (which we shall call groups) and for each group there are several replications (between 15 and 20, depending on the group). The number of observations per curve varies between 16 and 24, depending on the curve. We retained 74 groups for the analysis (excluding cases with extreme values of the environmental factors which inhibit growth) and randomly choose 10 replications for each one.

Using the DIC_3 criterion as outlined earlier, the optimum number of nodes for both models is 2. In the implementation of the GNN model we keep the hyperparameters $m_{i\beta}$, σ_β, m_γ and σ_γ fixed at $m_{i\beta} = 0$, $\sigma_\beta = 10$, $\boldsymbol{m}_\gamma = (0, \ldots, 0)'$ and $\sigma_\gamma = 10$. Regarding the error variance we choose $a = 0.2$ and $b = 0.2$. In the NN model the highest level of hyperparameters were set to $c_\beta = 10$, $e_\beta = 10$, $d_{\beta 1} = 0.1$, $d_{\beta 2} = 0.01$, $c_\gamma = 10$, $d_{\gamma 1}$ and $d_{\gamma 2} = 0.01$.

In order to fit the models, in each case we generated chains with random initial values and 200000 iterations each, including 100000 iterations of burn-in. To diminish autocorrelation between the generated values we also used a thinning rate of 1000. Trace plots and autocorrelation functions were used to check convergence in the predictions and in all cases it was found that the burn-in period of 100000 iterations was reasonable. Furthermore, the Gelman-Rubin statistic was equal o very close to 1 for predictions, being a good indicator of convergence.

In order to have a benchmark for the comparison of models we also fit two dif-

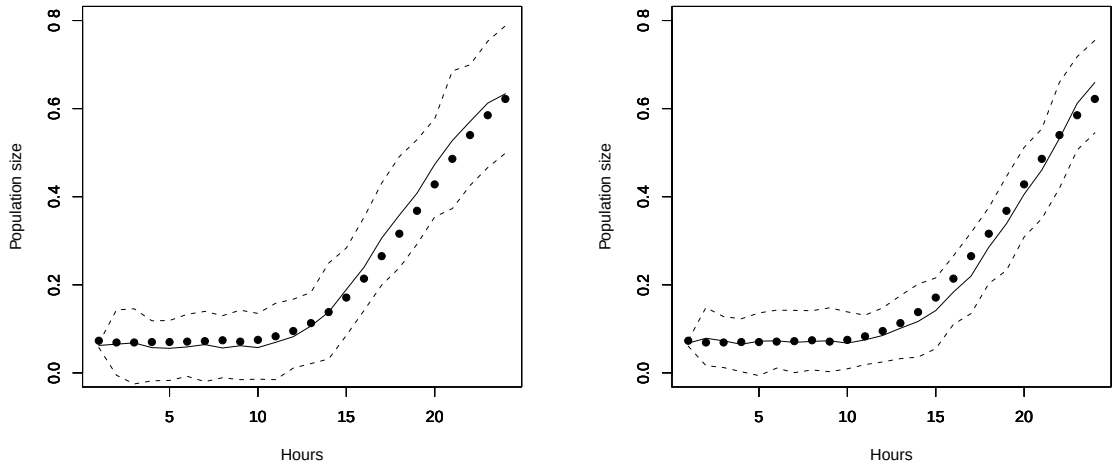

Figure 3.3: Fitting bacterial growth curves

ferent simple models, the independent Gompertz model and the pooled Gompertz model. The first of these implies that each observed curve, including the replications, is independent and therefore has its own Gompertz growth parameters. Independent, relatively diffuse normal $N(0, 100)$ prior distributions are assumed for these parameters. In contrast, the pooled model assumes that the replications under a fixed set of environmental conditions are samples from a unique, underlying growth curve for that set of conditions. Normal priors are then placed on the parameters of this growth curve as for the independent model. For both benchmark models the errors are the same as in the GNN case with a $\mathcal{G}(0.1, 0.1)$ prior distribution for the error variance.

The $DIC3$ and the $PPLP$ criteria were computed in order to compare the different models under consideration and Table 3.1 shows the estimated values for all of these models. As is expected, the pooled model performs better than de independent one since the assumption of independence for all the curves is somewhat extreme. Therefore, it seems reasonable to assume different curves under different environmental conditions but under equal conditions we assume a

common curve. And this is the approach we choose for the proposed models. But the problem of this model is that it does not explain the effect of the environmental factors and it is needed to estimate one model for each group of conditions. Then, regarding our proposed models which incorporate the environmental factors as explicative variables the results show that hierarchical neural network model outperforms the Gompertz model with neural networks for the parameters. The $DIC3$ and the $PPLP$ values are lowest for the former model.

Figure 3.3 shows for a particular curve ($T = 34°C$, $pH = 6.5$ and $NaCI = 5.5\%$) the fitting of both models. On the left, the Gompertz model with neural networks explaining the dependence of the growth parameter on the environmental factor and on the right the fitting of the hierarchical neural network model. The observed values are represented by points, the estimated growth curves are represented by the solid line, and the dashed lines represents the 95% credible interval computed from the posterior distributions. It can be observed that the fit is good in both cases and the credible intervals included all the true observations. In the remaining curves (replications and different group conditions), we also found good fits for both models. Similar results are observed in the fitted plots for all the groups.

Table 3.1: Model comparison

Model	DIC3	PPLP
Independet Gompertz	-19136	781
Pooled Gompertz	-39420	211
Gomp & NN	-40099	41
Neural Networks	-58492	28

Now, we consider one-step ahead predictions. That is, for a particular curve

we observe data until observation t and predict the population size at $t+1$. In the next step, we observe data until $t+1$ and predict the population size at $t+2$ and so on, until the completion of the predictive curve. Figure 3.4 shows the one-step-ahead predictive curves for both models for a particular growth curve ($T = 42°\text{C}$, $pH = 5.5$ and $NaCI = 2.5\%$). The fit, the Gompertz model shows a better predictive performance. The mean square error of the prediction in the Gompertz model is equal to 0.001, while for the NN model, this is 0.008. In the second model higher accuracy is reached as can be seen from the narrower credible interval.

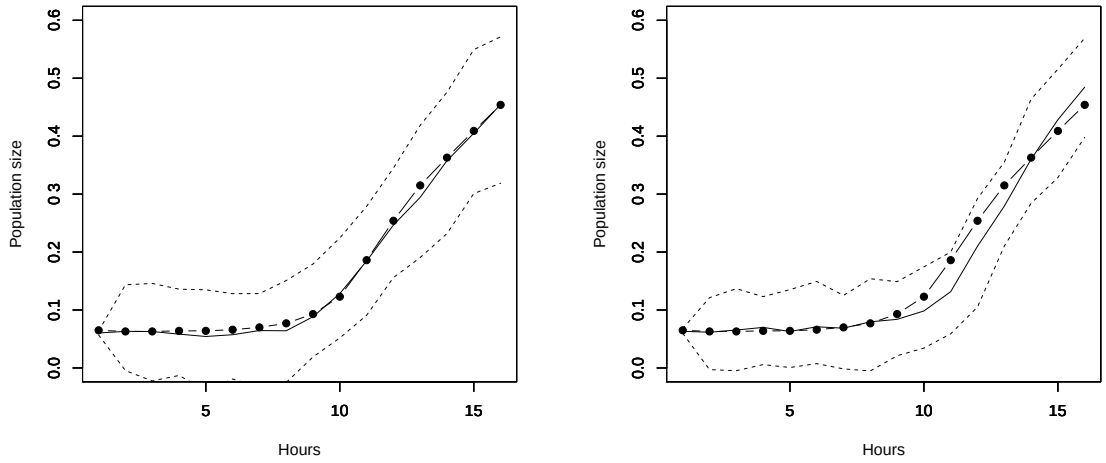

Figure 3.4: One-step ahead predictions

In the context of model checking, several authors, e.g. Gelfand (1996) and Vehtari and Lampinen (2003) have proposed the use of cross-validatory predictive densities. Following this approach, the data is divided in two subsets $(\mathbf{y_1}, \mathbf{y_2})$. The first of these is used to fit the model and to estimate the posterior distribution of the parameters, while the second set is used to compute the cross-validatory predictive density: $f(\mathbf{y_1}|\mathbf{y_2}) = \int f(\mathbf{y_2}|\boldsymbol{\theta}) f(\boldsymbol{\theta}|\mathbf{y_1}) d\boldsymbol{\theta}$. In our case, we computed the predictive density for one of the groups which was not used in the model

fitting. The environmental conditions for this new group are $T = 26°C$, $pH = 6.5$ and $NaCI = 5.5\%$. Figure 3.5 shows the mean prediction (solide line) and the 95% credible interval (dashed line) for both models, GNN on the left and NN on the right. As there are many replications for this group, we plot only the mean curve and shade the area between the minimum value and the maximum value observed for each time t among replications. As an input of the neural network for the NN model we used the mean curve of the replications.

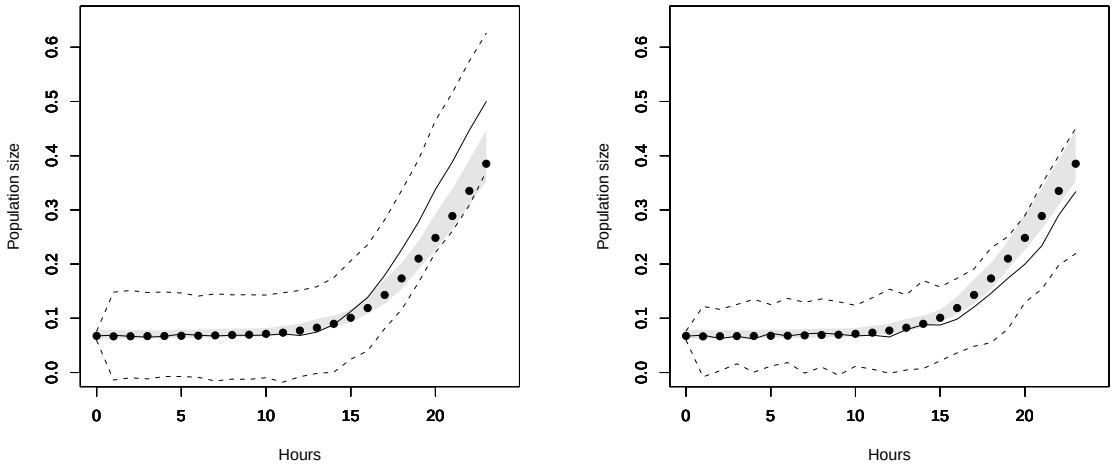

Figure 3.5: Cross-validation

Although both cross-validation predictions are fairly good, in the case of the GNN model some observations lie outside the credible interval. Moreover, comparing the mean prediction with the mean observed curve, the NN model yields more accurate predictions.

3.6 Conclusions

In this chapter, we have illustrated that neural networks can be used to model bacterial growth for multiple populations. Neural networks were used as a sec-

ondary model that explains the dependence on environmental factors and also as a primary model which, besides time, includes experimental conditions as explicative variables. Inference was carried on in a Bayesian approach that avoids the problems for doing inference in two steps. Both models yield accurate estimations and good predictions which show that NNs can be used to model bacterial growth describing accurately the complex interacting effects of environmental factors without imposing any simplifying assumption.

Estimations were implemented in `WinBUGS` via `R2WinBUGS` showing that `WinBUGS` can be a powerful and flexible tool able to handle very complex models such as neural networks with great ease. As MacKay (1995a) pointed out, Gibbs sampling method is not the most efficient of MCMC methods, but there may be problems of interest where the convenience of this tool outweighs this drawback.

Chapter 4

Stochastic models

4.1 Introduction

Up to now, we have presented a number of parametric growth curve models to describe the behaviour of bacterial populations over time. In particular, the models analyzed in Chapters 2 and 3 have all been discrete time models where the mean function is deterministic conditional on the model parameters and where a stochastic element is introduced via an additive random noise component. An alternative approach, which we shall pursue in this chapter is to consider a continuous time modeling approach. One advantage of such an approach is being able to easily deal with data that are irregularly spaced in time or different curves that are observed at different moments of time.

There are several applications of the use of continuous time stochastic process models such as birth-and-death processes, branching process and diffusion processes in biology. In some recent papers, inter individual variability is added as a stochastic factor to the general growth curve of the population or modelled by stochastic differential equations (Russo et al. (2009) and (Donnet et al., 2010)).

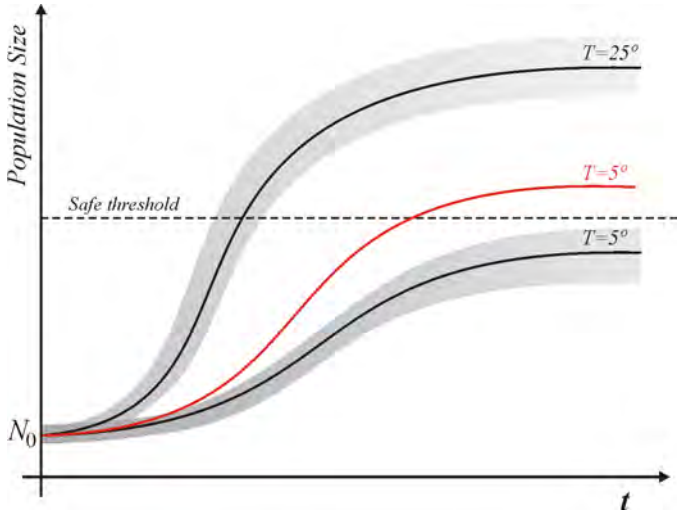

Figure 4.1: Effect of temperature

For a complete review see Renshaw (2011). Nevertheless, thus far, relatively little work has addressed the stochastic nature of the bacterial growth in terms of modeling and data analysis.

It is important to account for the randomness of the process in order to make good predictions and good recommendations in predictive microbiology. For example, imagine a situation where bacteria grow in a perishable food, such as yoghurt. After some threshold, the level of bacterial contamination can become dangerous to human health. Figure 4.1 illustrates bacterial growth under two different temperature levels and the corresponding fitted curves and credible intervals. If we do not take into account stochasticity, we can make the suggestion that stocking yoghurt at a temperature below 5° is enough to ensure that bacterial will not cross the safety limit. However, because of the random behaviour of bacterial growth we could observe a population of bacteria growing beyond that limit even when the temperature is below the 5°, in our case the red line.

Some stochastic models have been proposed in the field of predictive microbiology. In Baranyi (1998) a stochastic birth process model, where individual cell

lag time follows a common distribution is introduced. Later, McKellar (2001) proposed a model which is dynamic in the lag phase and able to describe the adaptation of homogeneous populations of cells. In the context of interacting populations, Gilioli et al. (2008) consider a stochastic predator-prey system where the noise term summarizes both demographic and environmental stochasticity.

In this chapter we shall propose an alternative stochastic growth model, monotonically non-decreasing with mean trajectory that follows the classic Gompertz equation. The approach is illustrated with real bacterial growth experiment and simulated data. Bayesian computation methods are used.

4.2 The model

Consider a birth-death process (BDP), $\{U_t : t \geq 0\}$, that is a continuous, time homogeneous, Markov process with finite state space such that if, at time t, the process is in state i, after an exponential amount of time, then it moves to either of the neighbouring states $i \to i+1$ or $i \to i-1$. The process U_t is uniquely determined by the generator matrix, $\mathbf{Q}$, and the initial distribution of the process, $\boldsymbol{\nu}_0$. Consider the following generator matrix:

$$\mathbf{Q} = \begin{pmatrix} -\alpha & \alpha & 0 & 0 & 0 & \dots \\ \beta & -(\alpha+\beta) & \alpha & 0 & 0 & \dots \\ 0 & \beta & -(\alpha+\beta) & \alpha & 0 & \dots \\ \vdots & \vdots & \vdots & \vdots & \vdots & \\ 0 & 0 & 0 & 0 & \beta & -\beta \end{pmatrix}$$

which is a tri-diagonal matrix, where the parameters $\alpha, \beta > 0$ are, respectively, the instantaneous birth and death rates. Let $\mathcal{S} = \{a + ib; i = 0, \dots, k\}$ be the

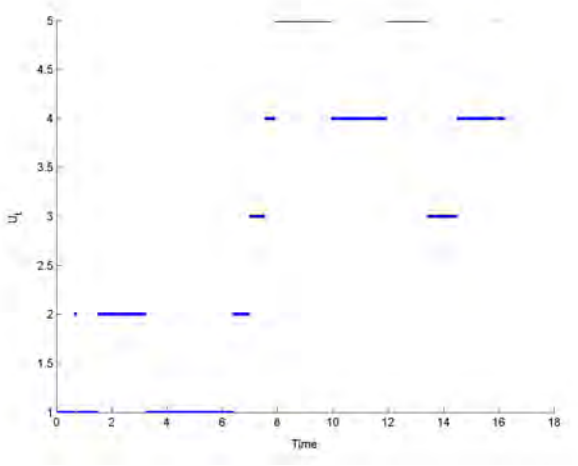

Figure 4.2: One possible realization of the U_t process

state space, where $a \geq 0$ is the minimum state value, b is a jump size and $k+1$ is the number of states.

Figure 4.2 shows one realization of the BDP with $\alpha = \beta = 1$ and $k = 4$ and $a = b = 1$ so that $\mathcal{S} = \{1, 2, \ldots, 5\}$.

Each time the process enters state i the amount of time it spends before making a transition to a different state is exponentially distributed with parameter $\lambda = (\alpha + \beta)$ and when it leaves state i, it next enters state $i+1$ with probability $\frac{\alpha}{(\alpha+\beta)}$, or enters state $i-1$ with probability $\frac{\beta}{(\alpha+\beta)}$. Obviously, in the edge states, when $i = a$ $(i = a + kb)$, the only chain transition possible is to state $a + b$ $(a + (k-1)b)$.

Let $\mathbf{P}(t) = (p_{ij}(t) : i, j \in \mathcal{S}, t \geq 0)$ be the transition matrix function of the Markov process. Then, solving the Kolmogorov forward and backward equations, it is shown that $\mathbf{P}(t) = e^{\mathbf{Q}t}$, where $e^{\mathbf{Q}t} = \sum_{k=0}^{\inf} \frac{\mathbf{Q}^k t^k}{k!}$ (for more details see Taylor and Karlin (1998).

If all states of the BDP communicate (for each pair (i, j), starting in state i there is a positive probability of ever being in state j) and the process is positive

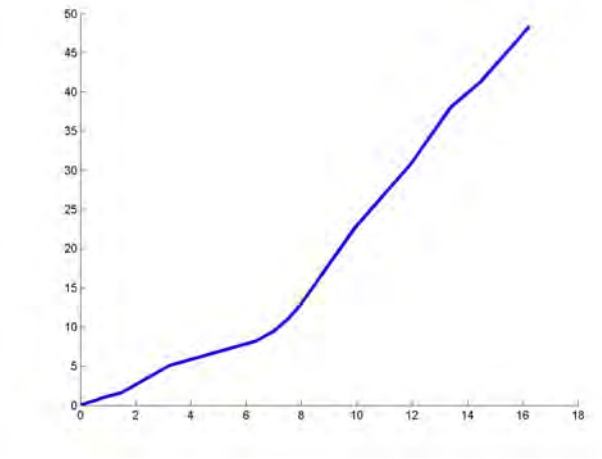

Figure 4.3: One possible realization of the V_t process

recurrent (starting in any state, the expected time to return to that state is finite), then the limiting probabilities exist, $p_j = \lim_{t\to\inf} p_{ij}(t)$, and are independent of the initial state i. Any distribution, $\boldsymbol{\pi}$, of a continuous time Markov process with transition matrix function $(\mathbf{P}(t), t \geq 0)$ which satisfies $\boldsymbol{\pi}\mathbf{Q} = 0$ is called the invariant distribution, also known as equilibrium or stationary distribution.

Now, we define a continuous state process, $\{V_t : t \geq 0\}$ such that

$$V_t = \int_0^t U_s ds. \tag{4.1}$$

This is a non-decreasing, continuous time process. The following graph (Figure 4.3)shows the trajectory of the V_t process corresponding to the U_t process plotted in Figure 4.2.

The stochastic process $\{V_t\}$ defined in (4.1) is the basis for our growth curve model. However, realizations of this process, which is the integration of a step function, do not present a standard sigmoidal shape which is typical in bacterial growth curves. Thus the process is not directly applicable to modeling bacterial growth. In order to do this, we apply a deterministic time change to the V_t process

which incorporates the different growth phases. We need first to delay the growth in the acclimatization phase, then accelerate growth in the exponential phase and finally decelerate growth when the maximum population level is reached. This can be done by transforming time using any sigmoidal function, for example a Gompertz curve, to get the desirable shape.

Therefore, finally, we define our stochastic growth process, $\{Y_t : t \geq 0\}$ be the continuous time, continuous state space stochastic process with continuous state space, defined as

$$Y_t = V_{G(t)}, \tag{4.2}$$

where V_t as defined in (4.1) is a *subordinator* and $G(t)$ is the Gompertz equation of (2.6).

In Figure 4.4 we have represented how the time change works. All the quadrants measure positive quantities. In quadrant IV, the Gompertz function is represented. The Gompertz value function increases in a negative direction, starting from the origin. In the third quadrant the identity function is plotted and in the second quadrant there is a realization of the V_t process. In quadrant II, time increases from the origin to the left. Finally, in quadrant I, a realization of the process Y_t is represented, which is equal to $V_{G(t)}$, that is the process V_t after the transformation of time.

What is the value of the trajectory of Y_t at t_1? To answer that question we start by evaluating the Gompertz function at that point. When the time is t_1, the Gompertz value is $G(t_1) = g_1$. We translate this to the time axis of quadrant II using the identity function. Then the process V_t is evaluated at that point producing the value $V_{g_1} = v_1$ which is exactly the value of Y_{t_1}. At t_2 the Gompertz function has the same value as before, g_1, which means that time in process V_t is stopped until the Gompertz function starts to increase. Then the

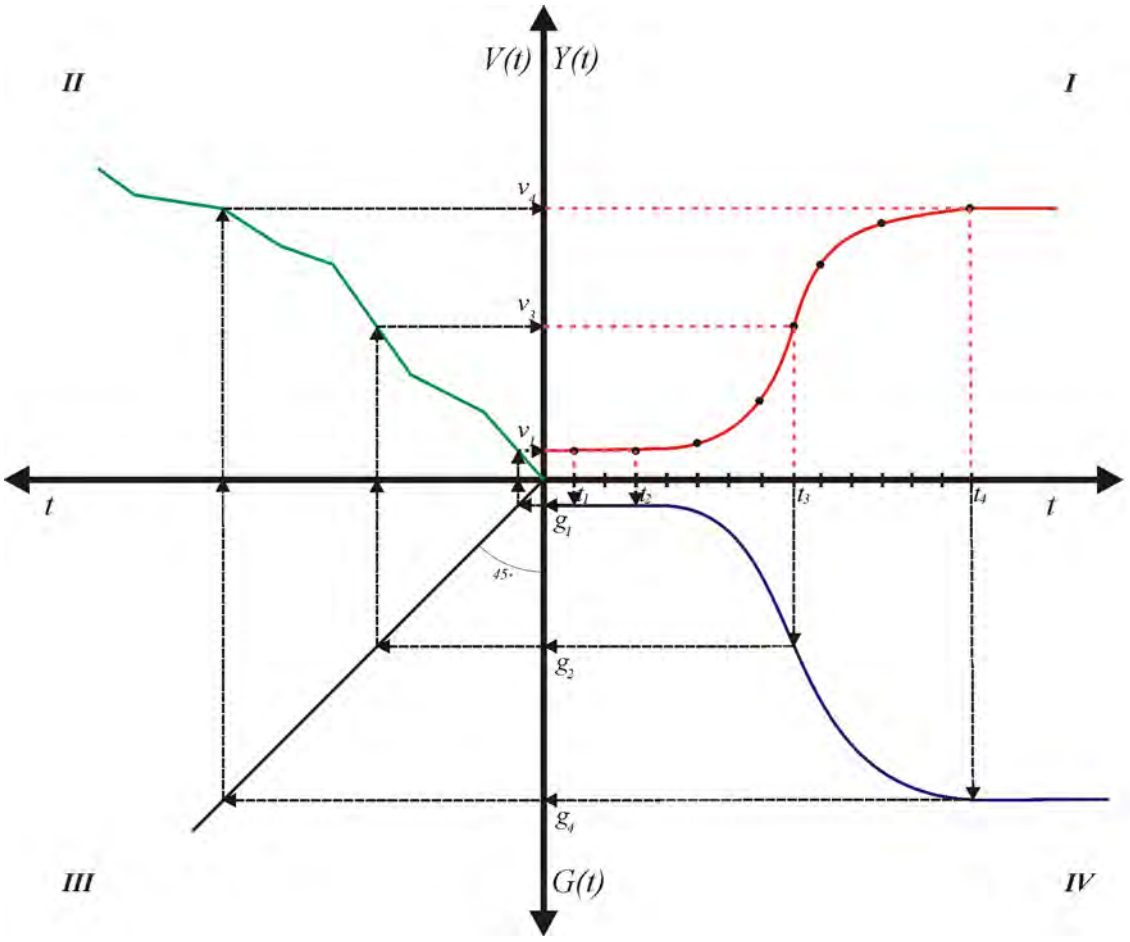

Figure 4.4: Deterministic time change

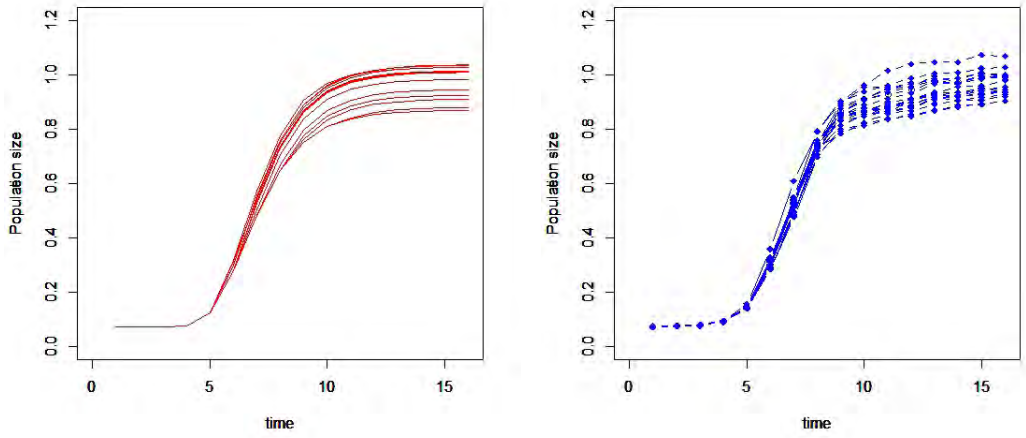

(a) Several realizations (b) Replications

Figure 4.5: Simulated realizations and real growth curves

time is accelerated when we are in the exponential part of the Gompertz function and at the end the time is slowed down. The resulting transformed curve is plotted in red. Obviously, with a different realization of V_t we will get a different transformed curve but still with a sigmoidal shape.

In Figure 4.5 the plot on the left shows several realizations of the same process, while the plot on the right shows different replications of the real bacterial (listeria) growth experiment under a given set of environmental conditions which has been used to illustrate the previous chapters. It can be seen that the simulated and real growth curves show similar characteristics.

To see the abilities of the proposed model to describe different growth scenarios, we show realizations of this model with different parameter values. Each plot shows 100 realizations of the process.

We can see that when the jump sizes are lower, the realizations show smoother trajectories. Secondly, the greater the intensity rate of the jumps, the lower the variability between curves. Additionally, we can get more variability when we

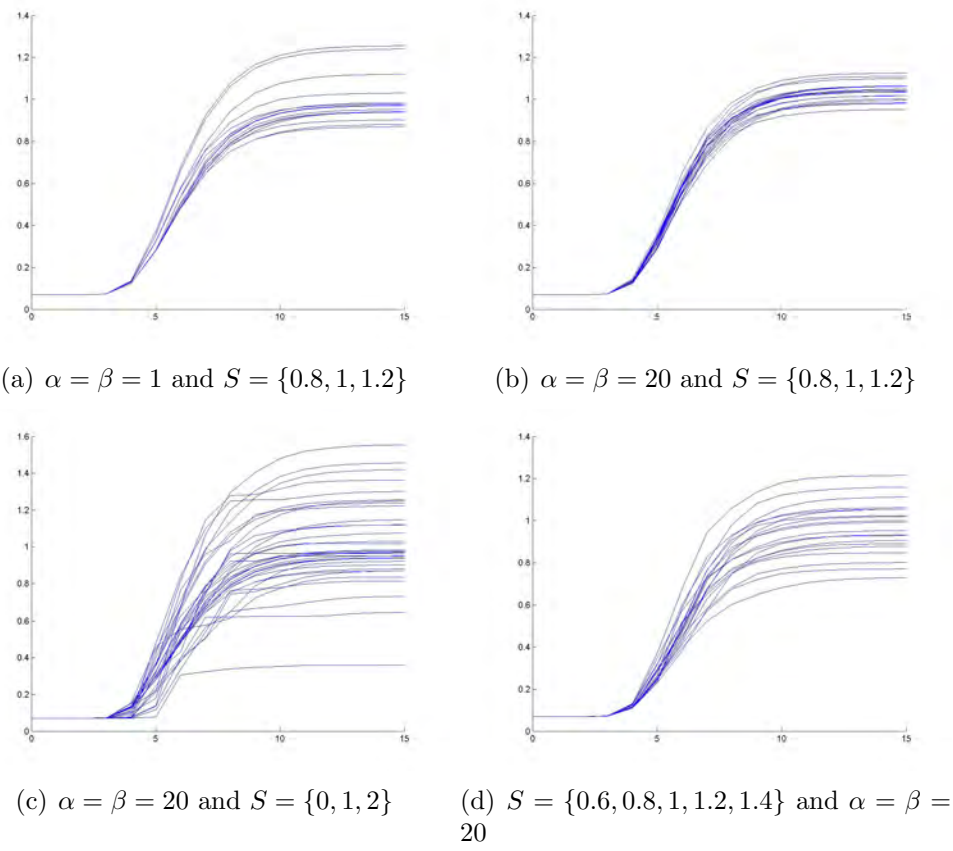

(a) $\alpha = \beta = 1$ and $S = \{0.8, 1, 1.2\}$

(b) $\alpha = \beta = 20$ and $S = \{0.8, 1, 1.2\}$

(c) $\alpha = \beta = 20$ and $S = \{0, 1, 2\}$

(d) $S = \{0.6, 0.8, 1, 1.2, 1.4\}$ and $\alpha = \beta = 20$

Figure 4.6: Simulations of Y_t. Gompertz parameters: $\lambda = 4$, $\mu = 0.26$ and $D = 1$

consider more states in the Markov process. Finally, note that we can change the shape of the curves by changing the parameters of the Gompertz curve as Figure 4.7 shows.

4.3 The mean function of the growth process

In this section we compute the mean function of the process $\{Y_t\}$. As we use a deterministic time change, it is sufficient to compute the expected trajectory of the subordinator, $m_V(t) = E[V_t]$, and then to apply the deterministic time transformation to it. The expected trajectory can be computed as

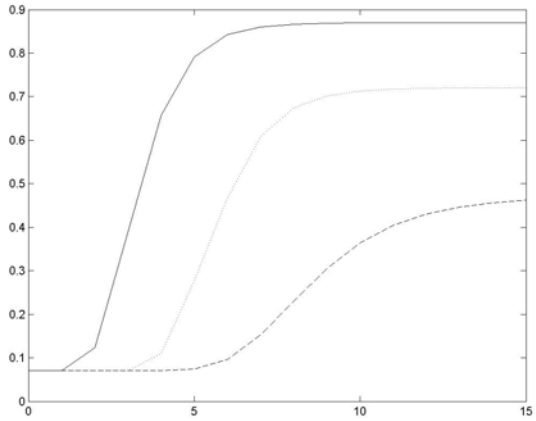

Figure 4.7: Solid line: $\mu = 0.40$, $D = 1$ and lag= 2; dotted line:$\mu = 0.26$, $D = 0.75$ and lag= 4 and dashed line $\mu = 0.10$, $D = 0.5$ and lag= 6

$$\begin{aligned} E[V_t] &= E\left[\int_0^t U_s(\omega)\, ds\right] \\ &= \int_\Omega \int_0^t U_s(\omega) ds\, dP(\omega) \\ &= \int_0^t \int_\Omega U_s(\omega) dP(\omega)\, ds \\ &= \int_0^t E[U_s] ds. \end{aligned} \tag{4.3}$$

By Fubini's theorem it is possible to change the order of the integration. To compute the expected trajectory of the U_t it is necessary to distinguish to cases: i)U_t is in transient state; ii) U_t is in steady state.

4.3.1 Transient state

The process U_t is an homogeneous, continuous-time Markov chain with finite number of states and transition matrix $\mathbf{P}_t = e^{\mathbf{Q}t}$. Let $\boldsymbol{\nu}_0$ be the initial distribution of the process and $\mathbf{s} = (s)_{s\in\mathcal{S}}$ be the vector containing all the elements of the state

space. Then:

$$E[U_t] = \boldsymbol{\nu}_0' \, e^{\mathbf{Q}t}\mathbf{s}. \tag{4.4}$$

In the case where all the eigenvalues of $\mathbf{Q}$ are different, the generator matrix can be diagonalized as $\mathbf{Q} = \mathbf{B}\mathbf{D}\mathbf{B}^{-1}$, where $\mathbf{D}$ is a diagonal matrix with diagonal entries equal to the eigenvalues of $\mathbf{Q}$ and $\mathbf{B}$ is an invertible matrix with the corresponding eigenvectors as columns. In that case, we have:

$$e^{\mathbf{Q}t} = \sum_{n=0}^{\inf} \frac{t^n(\mathbf{B}\mathbf{D}\mathbf{B}^{-1})^n}{n!} = \mathbf{B}(\sum_{n=0}^{\inf} \frac{t^n\mathbf{D}^n}{n!})\mathbf{B}^{-1} = \mathbf{B}e^{\mathbf{D}t}\mathbf{B}^{-1}. \tag{4.5}$$

Then, the exponential matrix can be obtained by just exponentiating every entry on the main diagonal. Replacing this result in (4.4) gives

$$E[U_t] = \boldsymbol{\nu}_0' \, \mathbf{B}e^{\mathbf{D}t}\mathbf{B}^{-1}\mathbf{s}$$

and substituting this result in (4.3), we find

$$\begin{aligned} E[V_t] &= \int_0^t \boldsymbol{\nu}_0' \, \mathbf{B}e^{\mathbf{D}s}\mathbf{B}^{-1}\mathbf{s} \, ds \\ E[V_t] &= \boldsymbol{\nu}_0' \, \mathbf{B} \int_0^t e^{\mathbf{D}s} \, ds\mathbf{B}^{-1}\mathbf{s}. \end{aligned}$$

To integrate the matrix $e^{\mathbf{D}s}$ we simply take the integral of each individual component of the matrix. The mean trajectory will be a function of t, and we can apply the deterministic time change transforming t by $G(t)$, the Gompertz function. When the matrix is not diagonalizable, it is still possible to work with the Jordan form or to solve the exponential matrix using the Laplace transform.

Example with two states

Consider the case that $\mathcal{S}$ has just two sates, $\mathcal{S} = \{s_1, s_2\}$. The generator matrix of the Markov process is:

$$\mathbf{Q} = \begin{pmatrix} -\alpha & \alpha \\ \beta & -\beta \end{pmatrix}.$$

Then the eigenvalues of $\mathbf{Q}$ are 0 and $-\alpha-\beta$ and the corresponding eigenvectors $(1 \quad 1)'$ and $(\alpha \quad -\beta)'$. Hence, $\mathbf{Q}$ can be diagonalized as

$$\mathbf{Q} = \mathbf{B} \begin{pmatrix} 0 & 0 \\ 0 & -\alpha-\beta \end{pmatrix} \mathbf{B}^{-1}$$

where $\mathbf{B} = \begin{pmatrix} 1 & \alpha \\ 1 & -\beta \end{pmatrix}$, $\mathbf{B}^{-1} = \frac{1}{\alpha+\beta} \begin{pmatrix} \beta & \alpha \\ 1 & -1 \end{pmatrix}$.

Using these results, we can calculate the transition matrix $\mathbf{P}_t$,

$$\begin{aligned} \mathbf{P}(t) = e^{\mathbf{Q}t} &= \sum_{n=0}^{\inf} \frac{t^n}{n!} \mathbf{B} \begin{pmatrix} -0 & 0 \\ 0 & (-\alpha-\beta)^n \end{pmatrix} \mathbf{B}^{-1} = \mathbf{B} \begin{pmatrix} 1 & 0 \\ 0 & e^{(-\alpha-\beta)t} \end{pmatrix} \mathbf{B}^{-1} \\ &= \frac{1}{\alpha+\beta} \begin{pmatrix} \beta + \alpha e^{(-\alpha-\beta)t} & \alpha - \alpha e^{(-\alpha-\beta)t} \\ \beta - \beta e^{(-\alpha-\beta)t} & \alpha + \beta e^{(-\alpha-\beta)t} \end{pmatrix}. \end{aligned}$$

Then, the expected trajectory of U_t when the process is in transient state is

equal to

$$\begin{aligned} E[U_t] &= \boldsymbol{\nu}_0' \, \mathbf{P}(t)\mathbf{s} \\ &= \boldsymbol{\nu}_0' \, \frac{1}{\alpha+\beta} \begin{pmatrix} \beta + \alpha e^{(-\alpha-\beta)t} & \alpha - \alpha e^{(-\alpha-\beta)t} \\ \beta - \beta e^{(-\alpha-\beta)t} & \alpha + \beta e^{(-\alpha-\beta)t} \end{pmatrix} \mathbf{s}. \end{aligned}$$

Let $\lambda = (-\alpha - \beta)$. The expected trajectory of V_t is

$$\begin{aligned} E[V_t] &= \int_0^t E[U_s]\, ds \\ &= \int_0^t \boldsymbol{\nu}_0' \, \frac{1}{\alpha+\beta} \begin{pmatrix} \beta + \alpha e^{\lambda t} & \alpha - \alpha e^{\lambda t} \\ \beta - \beta e^{\lambda t} & \alpha + \beta e^{\lambda t} \end{pmatrix} \mathbf{s}\, ds \\ &= \boldsymbol{\nu}_0' \, \frac{1}{\alpha+\beta} \begin{pmatrix} \int_0^t \beta + \alpha e^{\lambda t}\, ds & \int_0^t \alpha - \alpha e^{\lambda t}\, ds \\ \int_0^t \beta - \beta e^{\lambda t}\, ds & \int_0^t \alpha + \beta e^{\lambda t}\, ds \end{pmatrix} \mathbf{s} \\ &= \boldsymbol{\nu}_0' \, \frac{1}{\alpha+\beta} \begin{pmatrix} \beta t + \alpha e^{\lambda t}\lambda^{-1} - \alpha\lambda^{-1} & \alpha t - \alpha e^{\lambda t}\lambda^{-1} - \alpha\lambda^{-1} \\ \beta t - \beta e^{\lambda t}\lambda^{-1} - \beta\lambda^{-1} & \alpha t + \beta e^{\lambda t}\lambda^{-1} - \beta\lambda^{-1} \end{pmatrix} \mathbf{s}. \quad (4.6) \end{aligned}$$

Finally, we can apply the time change to (4.6):

$$E[Y_t] = \boldsymbol{\nu}_0' \, \frac{1}{\alpha+\beta} \begin{pmatrix} \beta G(t) + \alpha e^{\lambda G(t)}\lambda^{-1} - \alpha\lambda^{-1} & \alpha G(t) - \alpha e^{\lambda G(t)}\lambda^{-1} - \alpha\lambda^{-1} \\ \beta G(t) - \beta e^{\lambda G(t)}\lambda^{-1} - \beta\lambda^{-1} & \alpha G(t) + \beta e^{\lambda G(t)}\lambda^{-1} - \beta\lambda^{-1} \end{pmatrix} \mathbf{s}.$$

Therefore, we have obtained a closed form solution for the transient mean function, which is a non-linear function with 5 parameters: the intensity rates α and β, and the Gompertz parameters D, λ and μ.

4.3.2 Stationary state

If U_t is irreducible and all the states are positive recurrent, then the Markov chain has a stationary distribution given by

$$\boldsymbol{\pi}_i = \frac{(\frac{\alpha}{\beta})^i}{\sum_{i=0}^{k}(\frac{\alpha}{\beta})^i)}$$

for $i = 0, \ldots, k$. Then, $E[U_t] = \mu = \sum_{i=0}^{k} \pi_i \, s_i$ and

$$\begin{aligned} E[V_t] &= \int_0^t E[U_s]ds \\ &= E[U_t]t \\ &= \mu t. \end{aligned}$$

Finally, the mean trajectory is

$$E[Y_t] = \mu G(t) \tag{4.7}$$

that is a proportion of the Gompertz function. Note that if, instead of using $G(t)$ as in 2.6, we use:

$$F(t) = \exp\left(-\exp\left(1 + \frac{\mu e(\lambda - t)}{D}\right)\right), \tag{4.8}$$

then the mean trajectory is exactly the Gompertz function, where μ plays the role of D, the difference between the maximum and the initial population size. Again, we have obtained a closed form solution for the mean function, in this case, for the stationary state.

In the following graph we have plot the stationary and transient state mean functions. The solid line is the mean function in the stationary state, and the

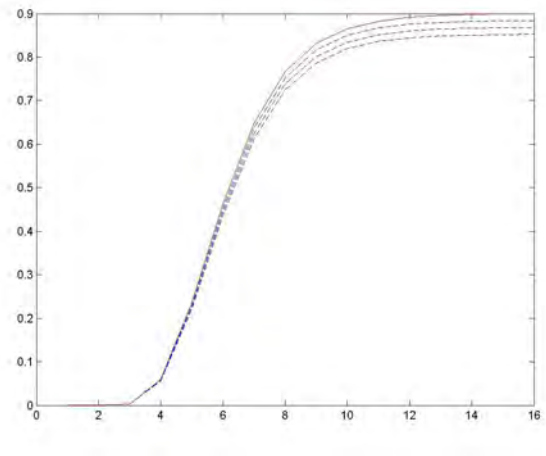

Figure 4.8: Mean trajectories in stationary sate (red line) and transient state (dashed lines). Gompertz parameters:$\mu = 0.26$, $D = 1$ and lag= 4

dashed lines represent mean trajectories in transient state with different initial distribution. When the initial distribution is closer to the stationary distribution, the curve is closer to the solid line.

4.4 Bayesian Inference

In this section, we examine two approaches to Bayesian inference for growth curve data generated from the model described previously. The first approach is applied to the case of a model where the underlying Markov chain has only two states, and is based on Gibbs sampling. The second approach can be applied to the more general case of multiple states and is based on approximate Bayesian computation or ABC techniques.

4.4.1 Gibbs Sampling approach for the two state model with equal rates

Suppose that we observe single or multiple growth curve data at a series of time points. Then in our model defined by (4.1) and (4.2), the likelihood function is analytically unavailable, but for the case of two state in the Markov process U_t, we can find an explicit expression for the likelihood when conditioning on the initial state and the number of jumps in successive time intervals. This allows for the implementation of a Gibbs sampling algorithm.

Formally, consider a continuous, time homogeneous Markov process with state space $\mathcal{S} = \{0, 1\}$, where state transitions occur according to a Poisson process with rate α. Suppose that bacterial population data are observed after fixed, successive time points $0 < T_1 < \cdots < T_n$. Then, the unknown parameters are the Gompertz parameters and the rate parameter, α.

4.4.1.1 Estimation of the Gompertz parameters

Various approaches to estimation of the Gompertz parameters could be considered. A fully Bayesian approach would imply setting prior distributions to these parameters as described in the previous chapters and then sampling from the posterior conditional distributions within the MCMC algorithm. However, here, for simplicity, we prefer to use a classical approximation. Recall firstly that under the assumption that the process is in equilibrium initially, then from (4.7), the mean trajectory is $E[Y_t] = \frac{1}{2}G(t)$. Therefore, we propose to use standard, classical weighted mean squares techniques to estimate these parameters by fitting the scaled Gompertz curve to the mean trajectory at the sample data time points.

The Gompertz parameters are assumed known for the remainder of the anal-

ysis. This implies that the overall approach to inference in this case is a form of empirical Bayes analysis combining both classical and Bayesian estimation techniques, see e.g Cassella (1985).

4.4.1.2 Estimation of α

Suppose now that the Gompertz parameters are known. Then, the time transformation is carried out the Gompertz function with known parameters as in (4.2). From (4.1), the observed data are $\mathbf{y} = (y_1, \ldots, y_n)$ where $y_i = t_{i1}$ is the total (transformed) time spent in state 1 in interval i, so that $G(T_i) - G(T_{i-1}) = t_{0i} + t_{i1}$ where t_{i0} is the corresponding (transformed) time in interval i spent in state 0.

To compute the conditional likelihood function we will use the concept of random division of an interval which we briefly present below following David and Nagaraja (2003).

Random division of an interval

Suppose that n points are dropped at random on the unit interval $(0, 1)$. The ordered distances of these points from the origin are denoted by $u_{(i)}$ $(i = 1, 2, ..., n)$ and let $w_i = u_{(i)} - u_{(i-1)}$ $(u_{(0)} = 0)$ be the interval of time between them. Then the random variables $U_{(1)}, U_{(2)}, ..., U_{(n)}$ are distributed as n order statistics from a uniform $\mathcal{U}(0, 1)$ parent, that is, with joint pdf equal to $n!$ over the simplex $0 \leq u_{(1)}, \leq u_{(2)}, \leq ..., u_{(n)} \leq 1$. Correspondingly, the pdf of the w_i is

$$f(w_1, w_2, \ldots, w_n) = n! \quad w_i \geq 0, \sum_{j=1}^{n} w_j = 1. \tag{4.9}$$

The distribution is completely symmetrical in the w_i. Indeed, if we define

$$w_{n+1} = 1 - \sum_{j=1}^{n} w_j, \tag{4.10}$$

we have the (degenerate) joint probability density function ($j = 1, 2, ..., n, n+1$)

$$f(w_1, w_2, ..., w_n, w_{n+1}) = n! \quad w_i \geq 0, \sum_{j=1}^{n+1} w_j = 1, \tag{4.11}$$

which is still symmetrical in all s_j. It follows that the joint distribution of any k of the $W_j (k = 1, 2, ..., n)$ is the same as that of the first k, and in particular that the distribution of the sum of any k of the W_j is that of

$$U_{(k)} = W_1 + W_2 + ... + W_k, \tag{4.12}$$

namely

$$f_{U_k}(u) = \frac{1}{B(k, n+1-k)} u^{k-1}(1-u)^{n-k} \quad 0 \leq u \leq 1. \tag{4.13}$$

The W_js are commonly referred to as *spacings*.

The random division of the interval may in fact originate from a Poisson process, such as our problem, with events occurring in some interval of time. Then, the distribution of the k'th order statistic, U_k, in the interval $[0, T]$ is a scaled beta distribution, $\mathcal{B}(k, n+1-k)$:

$$f_{U_k}(u) = \frac{1}{B(k, n+1-k)} \frac{u^{k-1}(T-u)^{n-k}}{T^n} \quad 0 \leq u \leq T. \tag{4.14}$$

Calculating the likelihood function

Suppose that we know the initial state, say s_1, at the start of the first time interval, and the number of state changes that occur in each time interval, say N_i for $i = 1, \ldots, n$. Then, the likelihood function is:

$$f(\mathbf{y}|\alpha, s_1, N_1, \ldots, N_n) = \prod_{i=1}^{n} f(y_i|\alpha, s_i = \text{mod}(s_{i-1} + N_{i-1}, 2), N_i) \tag{4.15}$$

where $\text{mod}(a, b)$ represents a modulo b, that is the densities of each y_i are conditionally independent given the state at the start of interval i and the number of state transitions in the interval.

Now consider two cases: when N_i is odd and when N_i is even. Consider now the different time intervals in each state.

- If N_i is odd, the process spends half of the time intervals in state 1 and the remainder in state 0 and therefore, the distribution of the sum of $(N_i+1)/2$ intervals is equal to the distribution of the order statistic $U_{((\tilde{N}_i+1)/2)}$ as defined in (4.14), that is:

$$f(y_i|N_i, \alpha) = \frac{1}{B(\frac{N_i+1}{2}, \frac{N_i+1}{2})} \frac{y_i^{(N_i+1)/2-1}(T_i - y_i)^{(N_i+1)/2-1}}{T_i^{N_i}} \tag{4.16}$$

- N_i even

  As the number of time intervals in period i is odd, the process spends $N_i/2 + 1$ time intervals in state 1 if the initial state is 1, or $N_i/2$ if the initial state is 0. Therefore, from (4.14),

$$f(y_i|s_i, N_i, \alpha) = \frac{1}{B(\frac{N_i}{2} + s_i, \frac{N_i}{2} + (1 - s_i)} \frac{y_i^{N_i/2+s_i-1}(T_i - y_i)^{N_i/2-s_i}}{T_i^{N_i}} \tag{4.17}$$

4.4.1.3 Conditional posterior distributions

Assume that α has a gamma prior distribution, say $\alpha \sim \mathcal{G}(a, b)$. Then we have:

$$\begin{aligned} f(\alpha|\mathbf{y}, s_1, N_1, \ldots, N_n) &\propto f(\mathbf{y}|\alpha, s_1, N_1, \ldots, N_n) f(\alpha|s_1, N_1, \ldots, N_n) \\ &\propto f(\alpha|N_1, \ldots, N_n) \\ &\propto f(N_1, \ldots, N_n|\alpha) f(\alpha) \\ &\propto \prod_{i=1}^{n} \alpha^{N_i} e^{-\alpha(G(T_i)-G(T_{i-1}))} \alpha^{a-1} e^{-b\alpha} \\ \alpha|\mathbf{y}, s_1, N_1, \ldots, N_n &\sim \mathcal{G}(a + n\overline{N}, b + n\overline{T}) \end{aligned}$$

where $\overline{N} = (1/n)\Sigma_{i=1}^{n} N_i$ and $\overline{T} = (1/n)\sum_{i=1}^{n}(G(T_i) - G(T_{i-1}))$ is the average length of the transformed time intervals.

Latent variables N_i

$$\begin{aligned} f(N_i|\mathbf{y}, s_1, \mathbf{N}_{-i}, \alpha) &\propto f(\mathbf{y}|\alpha, s_1, N_1, \ldots, N_n) f(N_i|\mathbf{N}_{-i}, \alpha) \\ &\propto f(\mathbf{y}|\alpha, s_1, N_1, \ldots, N_n) \frac{(\alpha(G(t_i) - G(t_{i-1})))^{N_i}}{N_i!} \end{aligned}$$

The posterior distributions of the N_is do not have a simple closed form and we use a Metropolis-Hastings algorithm to sample from these distributions based on generating candidate values from a Poisson distribution centred at the current value plus 0.5.

Latent variable s_1

Assume that s_1 has a Bernoulli prior distribution, say $P(s_1 = 1|p) = p$. Then,

$$\begin{aligned} f(s_1|\mathbf{y}, N_1, \ldots, N_n, \alpha) &\propto P(s_1) f(\mathbf{y}|\alpha, s_1, N_1, \ldots, N_n) \\ &\propto \prod_1^{\overline{n}} \frac{1}{B(\frac{\tilde{N}_i}{2} + s_1, \frac{\tilde{N}_i}{2} + (1 - s_1))} \frac{y_i^{\tilde{N}_i/2+s_1-1}(T_i - y_i)^{\tilde{N}_i/2-s_1}}{T_i^{\tilde{N}_i}} P(s_1) \\ &\propto \prod_1^{\overline{n}} \frac{1}{B(\frac{\tilde{N}_i}{2} + s_1, \frac{\tilde{N}_i}{2} + (1 - s_1))} y_i^{s_1}(T_i - y_i)^{-s_1} p^{s_1}(1-p)^{1-s_1} \\ &\sim Bernoulli(p') \end{aligned}$$

where $\overline{n}$ is how many times the number of jumps in an interval was even, $\tilde{N}_i = \sum_{j=1}^{i} N_j$ and $p' = \frac{p^{\overline{n}} \prod(y_i/(T_i - y_i))}{(1-p)^{\overline{n}} + p^{\overline{n}} \prod(y_i/(T_i - y_i))}$.

Gibbs sampler

Given the posterior conditional distributions calculated previously, a Metropolis Hastings within Gibbs sampler can be defined to sample the posterior distribution of α as follows:

1. Initialize counter k=1 and set the initial values: $\alpha^{(0)}$, $s_1^{(0)}$ and $\mathbb{N}^{(0)}$

2. Generate $\alpha^{(k)} \sim \mathcal{G}(a + n\overline{N}^{(k-1)}, b + n\overline{T})$

3. Generate $s_1^{(k)} \sim \mathcal{B}(p')$

4. Generate $N_1^{(k)}$:

4.1 For all N_i, generate a candidate from the proposal distribution $Q(N_i^{(k-1)}|N_i^{(*)})$: $N_i^{(*)} \sim \mathcal{P}(N_i^{(k-1)} + 0.5)$

4.2 Generate $U \sim \mathcal{U}_{[0,1]}$ If $U \leq \min\{1, \frac{P(N_i^*)Q(N_i^{(k-1)}|N_i^{(*)})}{P(N_i^{(k-1)})Q(N_i^*|N_i^{(k-1)})}\}$, then $N_i^{(k)} =$

N_i^*. If not, $N_i^{(k)} = N_i^{(k-1)}$.

5. Change $k = k+1$ and return to step 2 until convergence is reached.

4.4.1.4 Example

Assuming that the intensity rate of the jumps is $\alpha = 10$, we generated a five sets of growth curve data with twenty observations, equally spaced over time. Assuming that the process is in stationary state, Gompertz parameters were estimated by non-linear least squares and fixed when implementing the Gibbs sampling to estimate α. We generated a sample of 20000 iterations, after a burn in period of equal size. Looking at the plot of the cumulative mean of the sampled values of α, on the left hand side of Figure 4.9, we see that the chain has converged convergence. On the right hand side, we see the posterior distribution of α which is centred on the true value. The posterior mean of α is equal to 9.791 and the median is 9.705. A 95% credible interval is equal to $(7.36, 12.85)$.

4.4.2 Approximate Bayesian Computation

When considering the general case of our model, with more than two states in the U_t process, it is not clear that a similar expression for the likelihood can be found as in the two state case. Therefore, the Gibbs sampling algorithm described previously cannot be implemented and instead, we suggest applying approximate Bayesian computation (ABC).

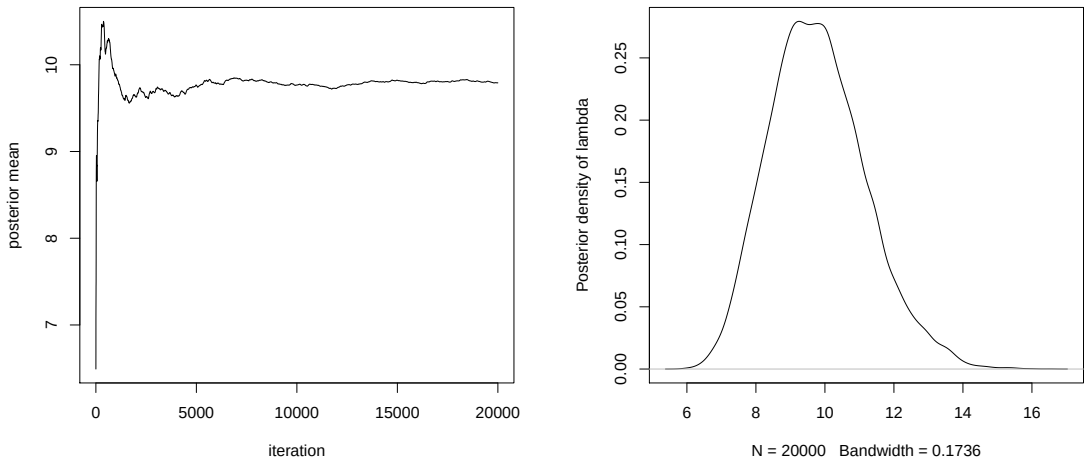

(a) Cumulative mean (b) Posterior density

Figure 4.9: Trace plot and posterior density of α

4.4.2.1 A brief review of ABC

In many complex models, the likelihood function is unknown or intractable which makes the implementation of standard Bayesian algorithms such as MCMC impossible. However, in some of these cases, it may be much more straightforward to simulate data from the model. In these cases, ABC can be used to provide an approximation of the posterior distribution. In a nutshell, in this approach, parameter values are simulated from the prior distribution and then data are simulated from the model conditional on these parameters. Then a similarity criterion between the simulated and observed data is defined as an appropriate distance between some summary statistics computed on both data sets. Parameters which generate data sufficiently similar to the sample data are accepted. For fuller reviews in the ecological and genetic contexts see Beaumont (2010) and Lopes and Boessenkool (2010).

ABC was originally developed to perform population genetics analysis (Tavare

et al. (1997) and Pritchard et al. (1999)), but recently it is being applied in a wide range of fields, such as ecology, epidemiology, molecular evolution, conservation genetics, etc. The increasing popularity on this method is due mainly to its capability to deal with very complex models and high dimensional data via the use of Monte Carlo simulations that avoid the need to use explicit likelihood functions.

Assume that we have a model parameterized by $\boldsymbol{\theta}$. Then the basic algorithm can be written as follow:

1. `Sample a value of the model parameter from the prior distribution:` $\theta^{(i)} \sim f(\theta)$
2. `Simulate data from the model, given` $\theta^{(i)}$`:` $\mathbf{D}^{(i)} \sim f(\mathbf{D}|\theta^{(i)})$
3. `Summarize` $\mathbf{D}^{(i)}$ `with a set of chosen summary statistics` $\mathbf{S}(\mathbf{D}^{(i)})$
4. `Reject` $\boldsymbol{\theta}^{(i)}$ `if` $d(\mathbf{S}(\mathbf{D}^{(i)}), \mathbf{S}(\boldsymbol{y})) \geq \epsilon$
5. `Repeat until required number of candidates accepted.`

where $\mathbf{D}$ are the simulated data, $\mathbf{y}$ is the observed data, d is a measure of distance, $\mathbf{S}$ is some summary statistic and $\epsilon > 0$ is a tolerance level. When ϵ tends to zero, the algorithm provides a sample from the distribution $f(\boldsymbol{\theta}|\mathbf{S}(\boldsymbol{y})$ which is an approximation of the desired distribution. If the summary statistic $\mathbf{S}$ is sufficient, the $f(\boldsymbol{\theta}|\mathbf{S}(\boldsymbol{y})) = f(\boldsymbol{\theta}|\boldsymbol{y})$.

Recently, in the literature a number of modifications have been proposed to improve the basic ABC algorithm. Firstly, Beaumont et al. (2002), propose a regression method to improve the sampling of the posterior density. Their algorithm introduces two innovations: weighting the parameters, $\boldsymbol{\theta}_i$, according to

their distance from the real data and adjusting the $\boldsymbol{\theta}_i$ using local-linear regression to weaken the effects of that discrepancy.

Secondly, in the absence of of prior information flat distribution should be used. However, if the prior distribution is diffuse then many improbable parameter values can be generated so that the acceptance rate of the algorithm will be very low and the algorithm becomes very inefficient. One possibility to overcome the problem of inefficiency in that cases is to use a sequential algorithm as proposed by S.A. et al. (2007) and Toni et al. (2009). The idea is to run the ABC method using a rough estimate of the ith posterior as the $(i+1)$th prior. As the number of iterations increases the posterior distribution becomes sharper and located closer to the true value.

The third main modified version of the ABC method is MCMC-ABC, proposed in Marjoram et al. (2003). This algorithm starts by sampling from the prior $f(\theta)$ and then a new value of the parameter is proposed using a proposal distribution which depends on the current value of the parameter, $K(\boldsymbol{\theta}|\boldsymbol{\theta}_{i-1})$. If the parameter value holds the ABC rejection step ($d(\mathbf{S}(\mathbf{D}^{(i)}), \mathbf{S}(\mathbf{y})) \leq \epsilon$) and then, the Metropolis rejection step, the proposed value is accepted.

4.4.2.2 Implementation of ABC

Consider now the general model with state space $\mathcal{S} = \{s_1, \ldots, s_k\}$ and rates α, β and known Gompertz parameters for simplicity. Assume gamma prior distributions for the intensity rate parameters, α, β. Assume that we observe data, $\boldsymbol{y}$.

Then the ABC algorithm proceeds by simulating parameter values and then simulating growth curve data at the same time points as the observed data given

these parameter values as follows.

1. Sample from the prior: $\alpha^{(i)}, \beta^{(i)} \sim \mathcal{G}(a, b)$

2. Simulate data given $\alpha^{(i)}, \beta^{(i)}$: $\boldsymbol{y}^{(i)} \sim f(\boldsymbol{y}|\lambda^{(i)})$

3. Reject $\alpha^{(i)}, \beta^{(i)}$ if $d(\boldsymbol{y}^{(i)}, \boldsymbol{y}) \geq \epsilon$, where $d(\boldsymbol{y}^{(i)}, \boldsymbol{y}) = \sum_{j=1}^{n} w_i |y_j^{(i)} - y_j|$

4. Repeat until required number of candidates accepted.

In the case where a single curve is observed, the weights are set to be equal. When the observed data consist of several replications of the same process, simulated data is evaluated by taking into account its distance with respect to the mean curve. The weights then aim to account for the variability of the process at different point of times. For instance, as was said previously, replications of the growth curve show less variability at the beginning of the observation period and more variability as time evolves. Thus, our weights are computed to be inversely proportional to the maximum distance observed at each point of time. After that, we accept the 1% of the generated values of α, β, with the lowest distance between the observed and simulated data.

Note that although we do not detail this here, the implementation of the algorithm in the case of unknown Gompertz parameters does not present any extra difficulties. These parameters can also be simulated from the prior and the same distance measures as above can also be used.

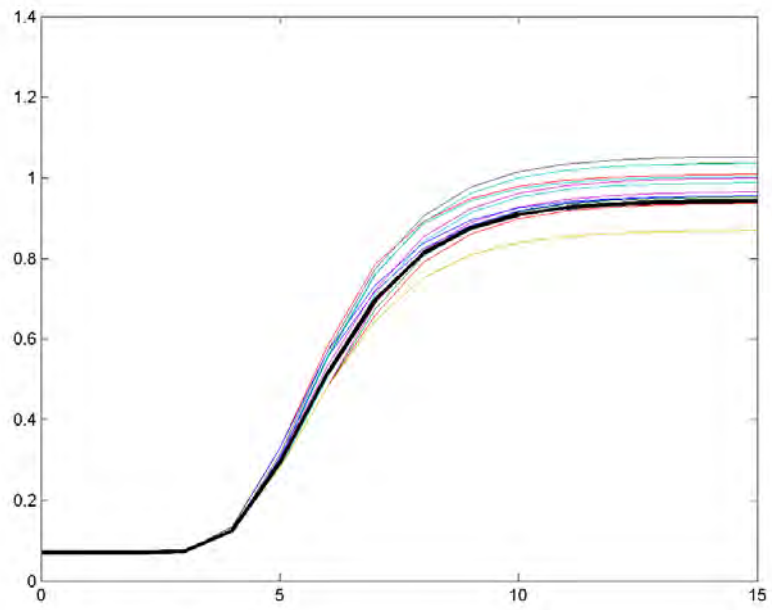

Figure 4.10: Simulated data

4.4.2.3 Example I

We simulated a set of 20 curves, each with 16 observations at equal point of times. Data was generated by assuming that the intensity rate is $\alpha = \beta = 1$, the growth rate of the Gompertz function is 0.26, the lag parameters is 4 and the maximum population growth is 1. The Markov chain has only two states, $\mathcal{S} = \{0.8, 1\}$. The simulated data are shown in Figure 4.4.2.3. The thick black line is the mean curve that we will use to compute the distance in the rejection step of the algorithm.

We assume gamma prior distributions for all the parameters due to their are non-negative. The prior distribution for the intensity rate is $\alpha \sim \mathcal{G}(1, 1)$, and for the Gompertz parameters the gamma prior distributions have means equal to the least squares estimated values and variance 1. Finally, we compute the relative mean integrate square error (RMISE) to set the number of iterations needed:

Table 4.1: Parameter estimates and RMISE

Numer of iterations	Lambda	Mu	Lag	D	RMISE
10000	0.99953	0.29589	4.18890	0.97269	0.00223
50000	0.99704	0.27122	3.98730	1.01920	0.00055
100000	1.00230	0.25849	4.00960	1.01730	0.00098
500000	1.00170	0.26529	4.00120	1.01460	0.00097
True value	1	0.26	4	1	

$$RMISE = \frac{1}{N}\sum_{i=1}^{N}(\frac{(\theta_i - \theta)^2}{\theta^2}) \tag{4.18}$$

where N is the number of sampled points from the posterior distribution, θ_i is the ith sampled point from the posterior distribution of the parameter and θ is the true value of the parameter. Results are shown in Table 4.1.

We see that RMISE seems to have stabilized after around 100000 iterations. We can see also that estimations are very closed to the true values of the parameters.

4.4.2.4 Example II

Now, we will apply the ABC method to the *Listeria monocytogenes* data described previously. In this case, we consider twenty growth curves, with sixteen equally spaced observations in each case shown on the right hand side of Figure 4.5. Given the previous simulated example, we think that 100000 points are enough to perform the analysis and we keep the 1‰ best. The left hand side of Figure 4.11 shows the total curves that ABC method generates, and on the right the the curves kept after the rejection step, that is the curves which have less distance to the mean observed curve (central thick black line). The right hand side of Figure 4.11, the plot also shows the maximum and the minimum observed

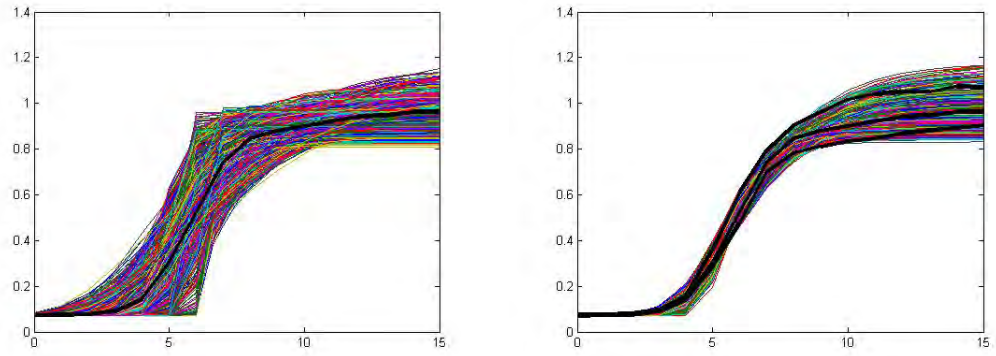

(a) All curves generated with ABC (b) The best 1‰ of the curves.

Figure 4.11: All and the best 1% of the generated curves

Table 4.2: Parameter estimates given different state spaces

	$\mathcal{S} = \{0.8, 1\}$	$\mathcal{S} = \{0.8, 1, 1.2\}$	$\mathcal{S} = \{0.8, 1, 1.2, 1.4\}$	$\mathcal{S} = \{0.8, 0.9\}$	$\mathcal{S} = \{0.8, 0.9, 1\}$	$\mathcal{S} = \{0.8, 0.9, 1, 1.1\}$
α	0.96	1.00	0.99	1.00	1.00	0.99
μ	0.28	0.28	0.27	0.28	0.26	0.29
lag	3.88	3.90	3.87	3.89	3.80	3.93
D	1.07	1.03	1.04	1.09	1.10	1.08

curves (thick black lines) to see that the simulated curves obtained from the ABC show a variability similar to that observed with the real data.

The posterior means of the Gompertz function are equal to $\mu = 0.27616$, lag= 3.8859 y $D = 1.0734$ and posterior mean of the intensity rate is equal to $\lambda = 0.96261$. Posterior densities are shown in Figure 4.12

Finally, we repeat the analysis but considering different state spaces for the underlying Markov process. Results are presented in table 4.2. The results do not change significantly among the different cases. Therefore, based on the Occam's razor principle we prefer the simpler model.

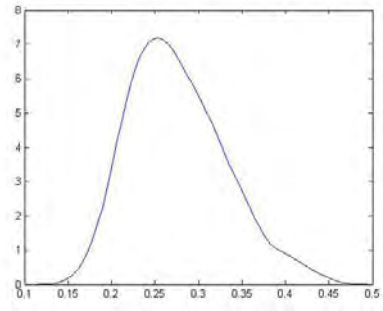

(a) Growth rate parameter

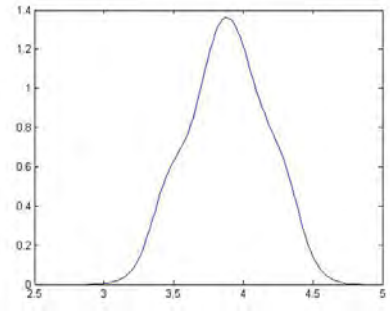

(b) Lag parameter

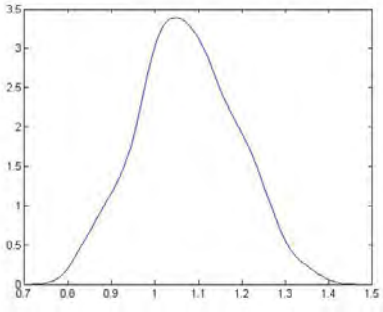

(c) Maximum population growth

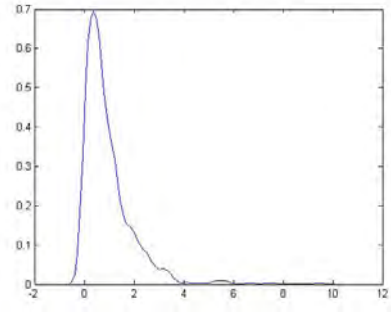

(d) Intensity rate of jumps

Figure 4.12: Posterior means

4.5 Conclusions

In this chapter, we have presented a new, continuous time model for bacteria growth based on a stochastic generalization of the Gompertz curve. We have shown that our model can simulate data that show similar characteristics to real bacteria growth data and have also developed two approaches to Bayesian inference for our model based on both exact and likelihood free approaches.

Chapter 5

Extensions

Here we present various extensions of the ideas proposed in this thesis and some further avenues for future research. In Section 1, we consider extensions of the ideas introduced in Chapter 3 to the case of interacting populations. Secondly, in Section 2, we briefly comment on an application of these ideas outside of the area of bacterial growth to the development of a neural network based software reliability model. Finally, in Section 3, we present some further extensions of our work.

5.1 Predator prey modeling

The models proposed in this dissertation study the case of populations growing in isolation. Nevertheless, in reality, populations interact with other species. In particular, in the context of microorganisms, **??** introduce a general model for interactions between prey and predator populations based on the Lotka-Volterra

model of (1.9) and (1.10).

$$\begin{aligned} \frac{dN}{dt} &= N(t)f(N(t-\delta)) - g(N(t),P(t))P(t) \\ \frac{dP}{dt} &= eg(N(t-\tau),P(t-\tau))P(t) - \mu P(t) \end{aligned}$$

where $N(t)$ and $P(t)$ are the prey and predator population concentrations at time t, f is the prey growth function, g represents the functional response relating the reduction in prey population to current predator and prey population sizes, e is a multiplicative constant reflecting the efficiency of the predator population in reproduction, τ and δ are time lags and μ represents the death rate of predators.

Although in the literature there is agreement about the dynamical framework of a predator-prey system, the explicit forms of the functional responses can be highly controversial. **??** propose using splines to estimate the functions f and g. Continuing the line of investigation of these authors, we propose using neural networks, as in Chapter 3, to estimate the functional responses, f and g. To illustrate, we have made a preliminary study applied to data on a protozoan predator-prey interaction. Figure 5.1 shows the observed and estimated phase trajectories of the predator-prey system in this case.

Further work is currently underway in this area.

5.2 Software reliability modeling

The non-parametric models proposed in Chapter 3, can be applied to many different fields, where the parameters of a primary model can be fitted as a function of some given covariates using some form of non-parametric regression approach. In particular, we have used these techniques in Wiper et al. (2012), to introduce a simple parametric model for software failure where the failure rate depends on

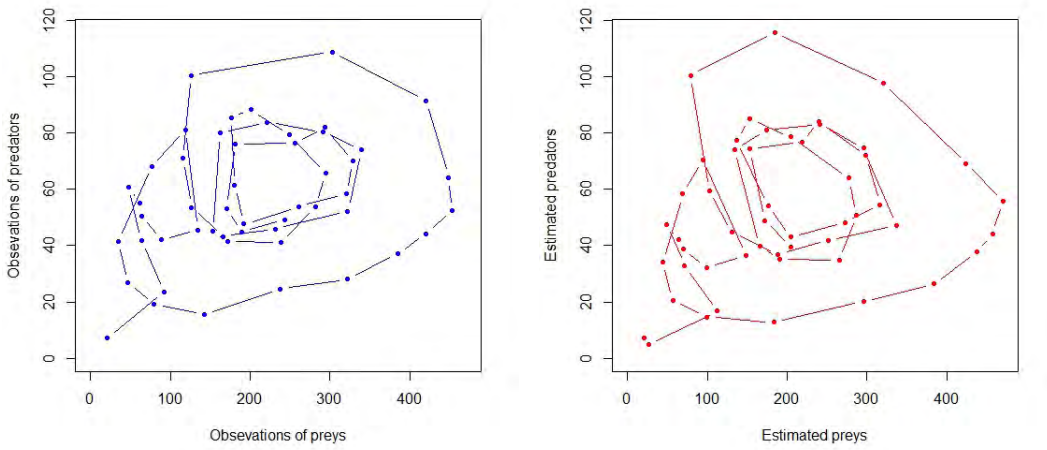

(a) Observed prey and predator evolution (b) Estimated prey and predator evolution

Figure 5.1: Estimated and observed phase trajectories

software metrics information and is modeled via neural networks. This is briefly summarized below.

Consider the case where the times between successive software failures, say $T_1, T_2, \ldots$ are observed and where it is presumed that the software is corrected, possibly imperfectly, after each failure. Then, it is natural to assume a nonhomogeneous Poisson process for failures so that we model

$$T_i|\lambda_i \sim \text{Ex}(\lambda_i) \tag{5.1}$$

for $i = 1, 2, \ldots$. Many standard software reliability models assume this basic exponential form. For instance, the Jelinski Moranda model (Jelinski and Moranda (1972)) sets

$$\lambda_i = (N - i + 1)\mu$$

where N represents the number of faults in the original code, μ is the fault discovery rate and perfect fault correction is assumed.

Suppose that after each software failure is observed, the code is modified and software metrics such as lines of code or other complexity measures reflecting the state of the code are evaluated. Then, we relate the failure rate of the software to the software metrics as follows:

$$\log \lambda_i = g(\mathbf{x}_i)$$

where $\mathbf{x}_i = (x_{i1}, \ldots, x_{ip})^T$ are the metrics available after $i-1$ failures have been observed. Typically, the relation between the log failure rate and the metrics is highly non linear and therefore, we proposed the use of a feed forward neural network, that is:

$$\begin{aligned} g(\mathbf{x}) &= \beta_0 + \sum_{j=1}^{k} \beta_j \Upsilon\left(\boldsymbol{\gamma}_j^T \mathbf{x}\right) \quad \text{where} \\ \Upsilon(c) &= (1+\exp(-c))^{-1} \end{aligned}$$

and $\boldsymbol{\gamma}_j = (\gamma_{j1}, \ldots, \gamma_{jp})^T$.

The same prior structures as used in Chapter 3 are applied to the neural network model and inference is again carried out using `WinBUGS`. Figure 5.2 taken from Wiper et al. (2012) shows a set of Bayesian predictive intervals for numbers of weekly software failures for a real data set consisting of the numbers of failures in fourteen weeks where a similar, previous time period has been used as training data. More details are available in this paper.

5.3 General extensions

In Chapter 2, we studied the case when various growth curves are observed under the same identical conditions. The hierarchical model proposed was based on a

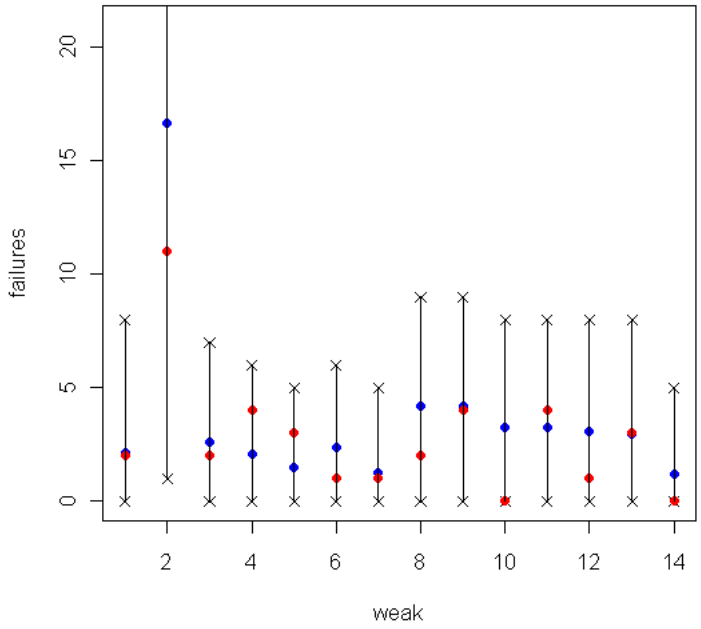

Figure 5.2: Observations (red circles), predictive mean values (blue circles) and 95% credible intervals.

Gompertz curve, as this is one of the most widely applied primary models. A natural extension is to apply the same ideas to alternative, parametric, growth curve models such as the logistic or Baranyi models discussed in Chapter 1. In particular, it would then be interesting to consider the problem of selection between models using for instance the deviance information criterion. Equally, the extension to varying environmental conditions via the neural network based approach of Chapter 3 would also be interesting to explore for these alternative models.

Secondly, outside of the laboratory, in real life, environmental factors such as temperature may vary considerably throughout the storage and distribution time of perishable foods. Therefore, another natural extension of our proposed models of Chapter 3, is to consider the possibility that the environmental factors change over time. Incorporating time-varying factors will lead to dynamical system.

The model we proposed in Chapter 4 should prove to be useful for other applications where deterministic models are too restrictive and can not capture the various sources of variations that exist in real life. Implementation for this model was carried out using an empirical Bayes approach via a Gibbs sampler for the case of a two state model and it is natural to see if a fully Bayes algorithm which also fits the Gompertz parameters in a Bayesian way could be developed. Secondly, for the general model, it is clear that many improvements to the simple ABC algorithm we propose here could be possible. It would also be interesting to incorporate the techniques of Chapter 3 in this model to allow us to simultaneously study bacterial populations under different conditions. Finally, the extension of our model to interacting populations should be of great interest in several biological applications.

Bibliography

Andrieu, C., N. Freitas, and A. Doucet (2001). Robust full Bayesian learning for radial basis networks. *Neural Computation 13*(10), 2359–2407.

Augustin, J. and V. Carlier (2000). Modelling the growth rate of Listeria monocytogenes with a multiplicative type model including interactions between environmental factors. *International Journal of Food Microbiology 56*(1), 53–70.

Baranyi, J. (1998). Comparison of stochastic and deterministic concepts of bacterial lag. *Journal of Theoretical Biology 192*(3), 403–408.

Baranyi, J., C. Pin, and T. Ross (1999). Validating and comparing predictive models. *International Journal of Food Microbiology 48*(3), 159–166.

Baranyi, J. and T. Roberts (1994). A dynamic approach to predicting bacterial growth in food. *International Journal of Food Microbiology 23*(3-4), 277–294.

Baranyi, J. and T. Roberts (1995). Mathematics of predictive food microbiology. *International Journal of Food Microbiology 26*(2), 199–218.

Beaumont, M. (2010). Approximate bayesian computation in evolution and ecology. *Annual Review of Ecology, Evolution, and Systematics 41*, 379–406.

Beaumont, M., W. Zhang, and D. Balding (2002). Approximate bayesian computation in population genetics. *Genetics 162*, 2025–2035.

Brooks, S. and A. Gelman (1998). General methods for monitoring convergence of iterative simulations. *Journal of Computational and Graphical Statistics 7*(4), 434–455.

Buchanan, R., R. Whiting, and W. Damert (1997). When is simple good enough: a comparison of the Gompertz, Baranyi, and three-phase linear models for fitting bacterial growth curves. *Food Microbiology 14*(4), 313–326.

Cassella, G. (1985). An introduction to empirical bayes data analysis. *The American Statistician 39*, 83–87.

Celeux, G., F. Forbes, C. Robert, and D. Titterington (2006). Deviance information criteria for missing data models. *Bayesian Analysis 1*(4), 651–674.

Congdon, P. (2010). *Applied Bayesian Hierarchical Methods*. Chapman and Hall.

Cowles, M. and B. Carlin (1996). Markov Chain Monte Carlo convergence diagnostics: A comparative review. *Journal of the American Statistical Association 91*(434), 883–904.

David, H. and H. Nagaraja (2003). *Order statistics* (third ed.). Wiley.

Delignette-Muller, M., M. Cornu, R. Pouillot, and J. Denis (2006). Use of Bayesian modelling in risk assessment: Application to growth of Listeria monocytogenes and food flora in cold-smoked salmon. *International journal of food microbiology 106*(2), 195–208.

Donnet, S., J. Foulley, and A. Samson (2010). Bayesian analysis of growth curves using mixed models defined by stochastic differential equations. *Biometrics 66*(3), 733–741.

Efron, B. and R. J. Tibshirani (1993). *An introduction to the Bootstrap*. New York: Chapman & Hall.

Fine, T. (1999). *Feedforward neural network methodology*. Springer Verlag.

Fitzmaurice, G., M. Davidian, G. Verbeke, and G. Mohlenbergs (2008). *Longitudinal Data Analysis*. Chapman and Hall.

García-Gimeno, R., C. Hervás-Martínez, et al. (2002). Improving artificial neural networks with a pruning methodology and genetic algorithms for their application in microbial growth prediction in food. *International Journal of Food Microbiology 72*(1-2), 19.

Geeraerd, A., C. Herremans, C. Cenens, and J. Van Impe (1998). Application of artificial neural networks as a non-linear modular modeling technique to describe bacterial growth in chilled food products. *International journal of food microbiology 44*(1-2), 49–68.

Gelfand, A. (1996). Model determination using sampling-based methods. in w. gilks, s. richardson, d. spiegelhalter (eds.). *, Markov Chain Monte Carlo in Practice*, 145–161.

Gelfand, A. and S. Ghosh (1998). Model choice: a minimum posterior predictive loss approach. *Biometrika 85*, 1.

Gelman, A. and D. Rubin (1992). Inference from iterative simulation using multiple sequences. *Statistical Science 7*, 457–511.

Geweke, J. (1992). *Bayesian Statistics 4*, Chapter Evaluating the accuracy of sampling-based approaches to calculating posterior moments. Clarendon Press.

Gilioli, G., S. Pasquali, and F. Ruggeri (2008). Bayesian inference for functional response in a stochastic predator-prey system. *Bulletin of Mathematical Biology 70*(2), 358–81.

Gilks, W., S. Richardson, and D. J. Spiegelhalter (1996). *Markov chain Monte Carlo in practice*. London: Chapman and Hall.

Gompertz, B. (1825). On the nature of the function expressive of the law of human mortality, and on a new mode of determining the value of life contingencies. *Philosophical Transactions of the Royal Society of London 115*, 513–583.

Grijspeerdt, K. and P. Vanrolleghem (1999). Estimating the parameters of the Baranyi model for bacterial growth. *Food Microbiology 16*(6), 593–605.

Hajmeer, M., I. Basheer, and Y. Najjar (1997). Computational neural networks for predictive microbiology II. Application to microbial growth. *International journal of food microbiology 34*(1), 51–66.

Jelinski, Z. and P. Moranda (1972). *Software reliability research*. Academic Press.

Kéry, M. (2010). *Introduction to WinBUGS for Ecologists: Bayesian approach to regression, ANOVA, mixed models and related analyses*. Academic Press.

King, R., B. Morgan, O. Gimenez, and S. Brooks (2009). *Bayesian Analysis for Population Ecology*. Chapman and Hall/CRC.

Lande, R., S. Engen, and B. E. Saether (2003). *Stochastic populated dynamics in ecology and conservation*. Oxford University Press.

Lavine, M. and M. West (1992). A Bayesian method for classification and discrimination. *Canadian Journal of Statistics 20*(4), 451–461.

Lee, H. (2004). *Bayesian nonparametrics via neural networks*. Society for Industrial Mathematics.

Levenberg, K. (1944). A method for the solution of certain non-linear problems in least squares. *Quarterly of Applied Mathematics 2*, 164–168.

Lopes, J. and S. Boessenkool (2010). The use of approximate bayesian computation in conservation genetics and its application in a case study on yellow-eyed penguins. *Conservation Genetics 11*(2), 421–433.

Lotka, A. J. (1925). *Elements of Physical Biology*. Baltimore: Williams and Wilkins.

Lunn, D., A. Thomas, N. Best, and D. Spiegelhalter (2000). WinBUGS-a Bayesian modelling framework: concepts, structure, and extensibility. *Statistics and Computing 10*, 325–337.

MacKay, D. (1995a). Bayesian methods for neural networks: Theory and applications. Technical report, Cambridge: Cavendish Laboratory, Cambridge University.

MacKay, D. (1995b). A practical bayesian framework for backpropagation networks. *Neural Computing 4*, 448–472.

Malthus, T. R. (1798). *An Essay on the Principle of Population*. Reprint (1998). Amherst, NY: Prometheus Books.

Marjoram, P., J. Molitor, V. Plagnol, and S. Tavaré (2003). Markov chain monte carlo without likelihoods. *Proceedings of the National Academy of Science of the USA 100*, 15324–15328.

Marquardt, D. (1963). An algorithm for least-squares estimation of nonlinear parameters. *SIAM Journal on Applied Mathematics 11*, 431–441.

McCarthy, M. (2007). *Bayesian Methods for Ecology*. Cambridge University Press.

McKellar, R. (2001). Development of a dynamic continuous-discrete-continuous model describing the lag phase of individual bacterial cells. *Journal of Applied Microbiology 90*, 407–413.

McKellar, R. and X. Lu (2004). *Modeling microbial responses in food*. CRC Press.

Müller, P. and D. R. Insua (1998). Issues in Bayesian analysis of neural network models. *Neural Computation 10*(3), 749–770.

Muller, P. and D. Rios Insua (1998). Issues in Bayesian analysis of neural network models. *Neural Computation 10*, 749–770.

Murray, J. D. (2003). *Mathematical Biology*. Berlin: Springer .

Neal, R. (1996). *Bayesian learning for neural networks*. Springer Verlag.

Pouillot, R., I. Albert, M. Cornu, and J. Denis (2003). Estimation of uncertainty and variability in bacterial growth using Bayesian inference. Application to Listeria monocytogenes. *International journal of food microbiology 81*(2), 87–104.

Powell, M., M. Tamplin, B. Marks, and D. Campos (2006). Bayesian synthesis of a pathogen growth model: Listeria monocytogenes under competition. *International journal of food microbiology 109*(1-2), 34–46.

Pritchard, J., M. Seielstad, A. Perez-Lezaun, and M. Feldman (1999). Population growth of human y chromosomes: a study of y chromosome microsatellites. *Molecular Biology and Evolution 16*(12), 1791–1798.

Ratkowsky, D., J. Olley, T. McMeekin, and A. Ball (1982). Relationship between temperature and growth rate of bacterial cultures. *Journal of Bacteriology 149*(1), 1.

Renshaw, E. (2011). *Stochastic Population processes: Analysis, Approximations, Simulations*. Oxford University Press.

Robert, C. and K. Mengersen (1999). Reparameterisation issues in mixture modelling and their bearing on MCMC algorithms. *Computational Statistics and Data Analysis 29*(3), 325–344.

Roeder, K. and L. Wasserman (1997). Practical Bayesian density estimation using mixtures of normals. *Journal of the American Statistical Association 92*(439), 894–902.

Rosso, L., J. Lobry, and J. Flandrois (1993). An unexpected correlation between cardinal temperatures of microbial growth highlighted by a new model. *Journal of Theoretical Biology 162*(4), 447–463.

Russo, T., P. Baldi, A. Parisi, G. Magnifico, S. Mariani, and S. Cataudella (2009). Lévy processes and stochastic von bertalanffy models of growth, with application to fish population analysis. *Journal of theoretical biology 258*(4), 521–529.

S.A., S., Y. Fan, and M. Tanaka (2007). Sequential monte carlo without likelihoods. *Proceedings of the National Academy of Science 104*, 1760–1765.

Seber, G. and C. Wild (1989). *Nonlinear regression*. Wiley.

Spiegelhalter, D., N. Best, B. Carlin, and A. van der Linde (2002). Bayesian measures of model complexity and fit. *Journal of the Royal Statistical Society. Series B, Statistical Methodology 64*(4), 583–639.

Stern, H. (1996). Neural networks in applied statistics. *Technometrics 38*(3), 205–214.

Tavare, S., D. Balding, R. Griffiths, and P. Donnelly (1997). Inferring coalescence times from dna sequence data. *Genetics 145*(2), 505.

Taylor, H. and S. Karlin (1998). *An Introduction to Stochastic Modeling: 3rd edition*. Academic Press.

Toni, T., D. Welch, N. Strelkowa, A. Ipsen, and M. Stumpf (2009). Approximate bayesian computation scheme for parameter inference and model selection in dynamical systems. *Journal of the Royal Society Interface 6*, 187–202.

Turchin, P. (2003). *Complex Population Dynamics: A Theoretical/empirical Synthesis*. Princeton University Press.

Vehtari, A. and J. Lampinen (2003). Expected utility estimation via cross-validation. *Bayesian statistics 7*, 701–710.

Verhulst, P. F. (1838). Notice sur la loi que la population suit dans son accroissement. *Correspondance Mathématique et Physique 10*, 113–121.

Volterra, V. (1926). Fluctuations in the abundance of a species considered mathematically. *Nature 118*(558-60).

Wijtzes, T., J. De Wit, I. Huis, R. Van't, and M. Zwietering (1995). Modelling bacterial growth of Lactobacillus curvatus as a function of acidity and temperature. *Applied and environmental microbiology 61*(7), 2533.

Wiper, M., A. Palacios, and J. Marín (2012). Bayesian software reliability prediction using software metrics information. *Quality Technology & Quantitative Management 9*, 35–44.

Zwietering, M., T. Wijtzes, J. De Wit, and V. R. K. (1992). A decision support system for prediction of the microbial spoilage in foods. *Journal of Food Protection 55*, 973–979.